Genetic variation of innate immune receptor genes in Systemic Lupus Erythematosus

Roberts, Amy Louise

Awarding institution:
King's College London

Genetic variation of innate immune receptor genes in Systemic Lupus Erythematosus

Amy Roberts

Submitted for the degree of Doctor of Philosophy (PhD)

Department of Genetics and Molecular Medicine,

King's College London, 2014

For Megan ‘Mam’ Roberts

Abstract

Genetic variations within loci encoding cell surface receptors of the innate immune system, such as Complement Receptor 3 (CR3) and Fc gamma Receptors (FcγRs), are strongly associated with Systemic Lupus Erythematosus (SLE). Such genetic associations implicate the functional importance of these receptors in disease pathogenesis.

CR3 (also known as CD18/CD11b) is an integrin receptor found on multiple immune cell types, including monocytes/macrophages, neutrophils, and Natural Killer (NK) cells. CR3 is a promiscuous receptor with many natural ligands, including complement fraction iC3b, ICAM-1, and β-glucan, and functions as a phagocytic receptor, leukocyte adhesion molecule, and immune regulator. *ITGAM* encodes the α-chain (CD11b) of CR3, and a common polymorphism (rs1143679) within *ITGAM*, which results in a non-synonymous amino acid substitution (R77H) in CD11b, is robustly associated with SLE (OR=1.76).

In this thesis I demonstrate that the SLE-associated R77H common polymorphism does not affect the cell surface expression of CR3 on *ex vivo* monocytes and neutrophils in a healthy cohort of European ancestry. Additionally, a collaborative resequencing project identified two case-specific non-synonymous coding variants in *ITGAM*, which I demonstrate result in the under-functioning of CR3-mediated phagocytosis using an *in vitro* model. Finally, using a CR3-specific small molecule drug, which has therapeutic potential in inflammatory disease, I observed a CR3-dependent significant reduction in STAT5 phosphorylation following NK cell activation with cytokines.

There are two genetic variants found within the *FCGR* locus on chromosome 1 which are robustly associated with SLE; homozygosity of the I232T (rs1050501) polymorphism within FcγRIIb (*FCGR2B*), and decreased gene copy number of *FCGR3B*. Recent work demonstrated that a consequence of a deletion at the *FCGR* locus, spanning the entire *FCGR3B* gene and parts of the upstream *FCGR2C* and downstream *FCGR2B* genes, results in ectopic expression of FcγRIIb on NK cells. In this thesis I explored the possibility of a genetic interaction between the two – copy number variation (*FCGR3B*) and rs1050501 (*FCGR2B*) - SLE-associated variants, but failed to detect such an effect within the European cohort used.

Acknowledgements

Needless to say, the work towards this thesis would not have been possible without the support of my two supervisors, Professor Tim Vyse and Dr Ben Rhodes. I am indebted to Prof. Tim Vyse, whom I have had the pleasure of working with for many years, and whose ongoing encouragement has helped me to develop confidence as a scientist. I owe my sincere gratitude to Dr Ben Rhodes for being an extremely supportive and inspiring supervisor throughout my PhD. My research skills have improved immensely under his guidance. I am also grateful to Arthritis Research UK for funding this PhD studentship (19317).

I am fortunate to be part of an incredibly friendly and supportive group in Tim Vyse's laboratory. In addition to their contribution to my work, I have also made many long-lasting friendships and my colleagues have made my PhD an enjoyable experience on a daily basis. I would like to give particular thanks to Dr David Morris, who is a fantastic colleague and a great friend.

My family are nothing short of amazing. Despite being far away, not a day goes by where I am not fully aware of my parents' ongoing support, and I cannot express how much I appreciate all that they have done for me. Likewise, my brother Matthew and sister-in-law Lindsay have always given me help and encouragement whenever I have needed it. In acknowledgment of this I look forward to being equally supportive to my wonderful nephew and niece, Ethan and Isabelle, in whichever paths they choose. My grandmother and friend, Gwen, whom I adore, never fails to make me smile. I wish I could have shared this with my grandfather, Bill, and grandmother, Megan, who are no longer with us. However, their encouragement and love echoes on, and their smiles are always in my thoughts.

And, of course, my friends: I honestly couldn't have written this thesis without their encouragement, in all its forms. They listened when I needed to talk; made me laugh when I needed to forget; gave me a hug when the end was in sight. But above all this, they make me happy, always.

Hoffwn hefyd diolch o galon i athrawon Ysgol Gyfun y Cymer Rhondda am roi'r ysbrydoliaeth i mi barhau gydag addysg.

Statement of Contribution

This thesis is the result of my own work. However, some of the data collection and analysis was performed in collaboration with colleagues, and I wish to acknowledge their contribution as follows:

Ellen Thomas (Imperial College London) designed and performed the resequencing of *ITGAM* on the 454 platform, and Shriram Bhosle (Imperial College London) conducted the analysis, which lead to the discovery of the two novel *ITGAM* rare variants discussed in Chapter 4. The follow-up genotyping of these rare variants, also presented in Chapter 4, was performed by Thomas Axelsson and Ann-Christine Syvänen (Uppsala University, Sweden) using Illumina Custom 384 Chip genotyping, and the genotype calling was performed by James Bentham (King's College London).

The cytokine secretion assays following NK cell activation (Figure 5.1) is the work of Ben Rhodes (King's College London) and is presented and discussed as such in Chapter 5. The results of this work enabled my intracellular signalling studies.

Elena Sanchez (King's College London) contributed to the *FCGR2B*-I232T genotyping of the Twins UK Bioresource samples, as reported in Chapter 6. The interaction analysis for the two *FCGR* variants using R, also in Chapter 6, was performed by David Morris (King's College London).

Additionally, the work in this thesis would not have been possible without the King's College London Genomic Centre and the National Institute for Health Research Biomedical Research Centre at Guy's and St Thomas' NHS Foundation Trust.

Table of Contents

List of Figures

List of Tables

List of Abbreviations

A	Alanine
Ab	Antibody
ACR	American College of Rheumatology
ANA	Anti-nucluer antibodies
APC	Antigen presenting cell
Bp	Base pairs
BSA	Bovine serum albumin
CDCV	Common disease-common variant
CN	Copy number
CNV	Copy number variation
CR3	Complement receptor 3
DC	Dendritic cell
DMEM	Dulbecco's Modified Eagle Medium
DMSO	Dimethyl sulfoxide
DNA	Deoxyribonucleic Acid
dsDNA	Double-stranted DNA
DZ	Dizygotic
EBV	Epstein-Barr virus
F	Phenylalanine
FACS	Fluorecence-Activated Cell Sorting
FBS	Feotal bovine serum
FSC	Forward scatter
G	Glycine
GPI	Glycosylphosphatidylinositol
GVB	Gelatin veronal buffer
GWAS	Genome-wide association study
H	Histidine
HBSS	Hank's Balanced Salt Solution
I	Isoleucine
IC	Immune complexes
ICAM	Intracellular adhesion molecule
IFN	Interferon

Ig	Immunoglobulin
IGV	Integrative genomics viewer
IL	Interleukin
IFN	Interferon
JAK	Janus kinase
Kb	Kilobase
KDa	Kilodalton
LA1	Leukadherin-1
LAD	Leukocyte adhesion-molecule deficiency
LD	Linkage disequilibrium
LGM	Lymphocyte growth medium
LPS	Lipopolysaccharides
mAb	Monoclonal antibody
MAF	Minor allele frequency
Mb	Megabase
MFI	Mean fluorescence intensity
mRNA	Messenger RNA
MZ	Monozygotic
NIHR	National Institute of Health Research
NK	Natural killer
OR	Odds ratio
ORF	Open reading frame
P	Proline
PAMP	Pathogen-associated molecular patterns
PBS	Phospahte balanced solution
PCR	Polymerase Chain Reaction
PFA	Paraformaldehyde
PMA	Phorbol myristate acetate
PRT	Paralogue ratio test
PTS	Parallel tagged sequencing
R	Arginine
RBC	Red blood cell
REDVR	Restriction enzyme digest variant ratio
RNA	Ribonucleic acid

S	Serine
SLE	Systemic lupus erythematosus
SNP	Single nucelotide polymorphism
SSC	Side scatter
SSP	Site-specific primers
STAT	Signal transducer and activator of transcription
T	Threonine
TLR	Toll-like receptor
TNF	Tumour necrosis factor
UK	United Kingdom
UV	Ultraviolet
V	Valine
WT	Wild-type
WTCCC	Wellcome Trust Case Control Consortium
Y	Tyrosine

Chapter 1: Introduction

1.1 Systemic Lupus Erythematosus

1.1.1 Overview

Systemic lupus erythematosus (SLE) is a chronic autoimmune disease with a broad spectrum of symptoms and wide range of severity resulting from the breakdown of immune tolerance. It can affect any organ system of the body due to its characteristic presence of autoantibodies to nuclear components (antinuclear antibodies (ANA)), including anti-double-stranded DNA (dsDNA) (Borg et al. 1990). However, there is no single clinical or immunological feature required for diagnosis: disease diagnosis is dependent on the presence of at least four of the diverse range of pathologies listed in the American College of Rheumatology (ACR) 1982 classification criteria (Tan et al. 1982), in any combination, making SLE a very heterogeneous disorder. Clinical features include fatigue, skin rashes, neurological complications, arthritis, and glomerulonephritis, as a result of tissue damage following immune complex deposition and subsequent local inflammation. Despite significant improvements in recent decades, SLE is still associated with increased morbidity and decreased life expectancy (O'Neill and Cervera 2010).

Two of the cellular characteristics of SLE are impaired clearance of apoptotic cells by phagocytes (Herrmann et al. 1998; Gaipl et al. 2007), and B cell auto-reactivity (Rahman 2004), highlighting the involvement of both innate and adaptive immune systems, respectively, in disease pathology. The work in this thesis focuses on the role of the innate immune system in SLE, and the effects of genetic variants in genes encoding receptors on the surface of innate immune cells.

1.1.2 Innate Immune dysfunction in SLE: The 'waste disposal' hypothesis

In addition to recognising and destroying invading pathogens during the inflammatory response, the phagocytic cells of the innate immune system – neutrophils, macrophages – recognise apoptotic cells and rapidly dispose of them to avoid an inflammatory response (Abbas, Lichtmann 2012; Hochreiter-Hufford and Ravichandran 2013). Apoptosis is the programmed cell death triggered by multiple stimuli, including infection and damage due to cytotoxic environmental exposure (such as

UV radiation). Apoptotic cells are opsonised with soluble ligands of phagocytic receptors, such as complement factors, enabling their effective recognition (Pittoni and Valesini 2002). The 'waste disposal' hypothesis is a central paradigm of SLE disease biology, and refers to the under-functioning of apoptotic clearance by phagocytes (Gaipl et al. 2007; Pittoni and Valesini 2002; Herrmann et al. 1998). Defective clearance of apoptotic cells leads to their accumulation and subsequent release of nuclear components. Through presentation by antigen-presenting cells (APCs), such as dendritic cells (DCs), and exposure to cells of the adaptive immune system, this leads to the production of the characteristic autoantibodies to nuclear components (Kelley et al. 2010). Genetic variants in genes encoding phagocytic receptors, such as *ITGAM*, which encodes the α-chain of complement receptor 3 (CR3), are among the strongest risk factors for SLE, adding further support to this paradigm of disrupted 'waste disposal' (Fagerholm et al. 2013).

Interferon (IFN) is a potent anti-viral defence mechanism of the innate immune system, primarily produced by plasmacytoid dendritic cells (pDC) in response to viral antigens. However, there is a known 'IFN signature' in SLE patients, where serum levels of IFN-α – part of the type I interferon family - are elevated and IFN-responsive genes are upregulated, and this is further correlated with disease severity (Baechler et al. 2003). Type I interferon can stimulate the maturation of monocytes into activated DCs, and also the differentiation of B cells into antibody-producing plasma cells (Jego et al. 2003). It is thought that autoantigens and autoantibody-containing immune complexes (ICs) in SLE patients stimulate the production of IFN, which in turn drives autoantigen presentation and autoantibody production, in a positive feedback loop that propagates disease (Baechler, Gregersen, and Behrens 2004).

Several studies have revealed substantial amounts of DNA fragments circulating in the plasma of SLE patients, which is furthermore associated with disease activity, and the circulating DNA fragments have lower methylation levels (Sato et al. 1999; Lövgren et al. 2004). Apoptotic DNA, but not necrotic DNA, has been shown to induce anti-dsDNA antibodies (Abs) in BALB/c non-SLE prone mice, which lead to severe glomerular deposits of immunoglobulin G (IgG) antibodies (Wen et al. 2007). The methylation of apoptotic DNA is lower than necrotic DNA, and the hypomethylated status of apoptotic DNA was demonstrated to be a key, but not exclusive, factor in the induction of the SLE-like symptoms in healthy mice: up-methylation of apoptotic DNA impairs, but does not abolish, its ability to induce auto-Abs; de-methylation of necrotic or normal DNA enabled it to induce auto-Abs

(Wen et al. 2007). Indeed, the contribution of epigenetic changes to autoimmunity is actively being explored (Ballestar 2011) and DNA methylation state has been shown to contribute to SLE discordance in monozygotic twins (discussed below 1.1.3) (Javierre et al. 2010).

Additionally, increased rates of apoptosis have been observed in lymphocytes of SLE patients. Such apoptotic dysfunction could also increase the exposure of nuclear antigens leading to ANAs. However, the presence of autoantibodies is not sufficient for disease onset, as these are found in ~5 of healthy individuals and are associated with ageing (Niederer et al. 2010a). It is the presence of autoantibodies, particularly ANAs, together with reduced ability to clear autoantibody-containing ICs by phagocytes, followed by inappropriate inflammatory response to deposited ICs that contribute to SLE pathogenesis (Gaipl et al. 2007). Low-affinity Fcγ receptors (FcγRs), which bind the Fc domain of IgG molecules, are encoded within the *FCGR* locus on chromosome 1q23.3. Multiple genetic associations across this locus implicate the under-functioning of FcγRs in SLE pathogenesis, adding further support to defective autoantibody IC clearance in disease biology (Niederer et al. 2010a).

1.1.3 Epidemiology and the evidence for a genetic contribution

There is a striking sex difference in SLE prevalence; 90% of cases are female. Furthermore, the child-bearing years between puberty and menopause harbour the greatest risk of disease onset, strongly suggesting an important hormonal role in SLE (O'Neill and Cervera 2010). However, an X chromosome gene-dose effect may also contribute to the observed sex imbalance. Indeed, the prevalence of SLE in males with Klinefelter's syndrome (47, XXY) is significantly greater than in 46, XY males, and approaches that of (46, XX) females (Scofield et al. 2008).

There are also population differences in SLE risk. The disease is distributed unevenly across the globe, and there are known variations in prevalence across ancestral populations (Shapira, Agmon-Levin, and Shoenfeld 2010). Such population-specific variance is observed within the same geographical area, suggesting these differences are attributable to genetic factors as opposed to environmental differences. For instance, Amerindians and African-Americans have greater disease susceptibility compared with European Americans (Shapira, Agmon-Levin, and Shoenfeld 2010). The population-specific differences are quite remarkable; a study in Birmingham, UK, reported a prevalence of 1:500 in Afro-Caribbean females, 1:1000 for South East Asian females, and 1:2500 for

White British females (Smith and Gordon 2010). Furthermore, ancestral groups with increased prevalence also exhibit younger median age of disease onset and increased disease severity (Shapira, Agmon-Levin, and Shoenfeld 2010). However, in addition to genetic ancestry, socio-economic factors have also been shown to influence SLE outcome, although their contribution to disease onset has yet to be explored (Sutcliffe et al. 1999).

The contribution of genetic factors to SLE susceptibility is further supported by familial aggregation of disease and increased concordance rate between monozygotic (MZ) twins compared with dizygotic (DZ) twins and full siblings: 24-57% and 2-5%, respectively (Deapen et al. 1992; Bogdanos et al. 2012; Alarcón-Segovia et al. 2005). SLE discordance between monozygotic twins suggests that factors aside from variation of genetic sequence contribute to disease susceptibility; it is important to differentiate sequence variation from epigenetic changes here as there is growing evidence that epigenetic factors contribute to twin discordance (Javierre et al. 2010). Despite this, the study of the inherited 'fixed' genetic variants contributing to SLE risk will ultimately aid our understanding of the immunological mechanisms contributing to disease onset (Rhodes and Vyse 2008). Immunological dysfunction pre-dates the clinical manifestations of SLE, which presents a problem of establishing phenotypic disease paradigms of cause and effect (Arbuckle et al. 2003). Genetic variations that are associated with disease risk, on the other hand, are not affected by disease progression. Furthermore, their effects on cellular functions can be studied in isolation of disease using *ex vivo* cells from healthy individuals or *in vitro* models, aiding the understanding of immune dysfunction leading to disease onset. Ultimately, understanding these underlying mechanisms will hopefully aid the development of targeted therapeutics.

In addition to the role of hormones in SLE risk, as discussed above, a number of known environmental factors have been shown to contribute to SLE susceptibility, such as infectious agents (e.g. Epstein-Barr Virus (EBV)), diet, and chemicals (Gourley and Miller 2007). Environmental conditions interact with DNA by means of epigenetic modifications, which are cell- and tissue-type specific, in both normal and pathological individuals. Epigenetic changes, although reversible, are not necessarily altered/lost during mitosis, or even meiosis (Bird 2007). Both methylation and histone post-transcriptional modifications affect gene expression, which in turn affect protein expression and the functioning of the immune system.

1.2 The Genetics of complex diseases

The past 10 years has seen great technological advancements, which have aided the identification of genetic variants contributing to complex disease onset (Rhodes and Vyse 2008). These variants range in size from single nucleotide polymorphisms (SNPs) to copy number variations (CNV) of large segments of DNA, and typically contribute modest effect size on disease risk (Moser et al. 2009).

1.2.1 GWAS and the Common Disease-Common Variant hypothesis

Under the common disease-common variant (CDCV) hypothesis, genetic variants, which are not disease-specific but present throughout the population, confer modest contribution to disease risk. However, given their contribution to disease onset, these variants will be present at significantly higher frequencies in disease cohorts. It is the accumulation of such variants, perhaps in concert with environmental triggers, which may ultimately lead to diseased onset in the 'threshold liability model' (Becker 2004; Wandstrat and Wakeland 2001). Genome-wide association studies (GWAS), a 'hypothesis-free' approach where the frequencies of hundreds of thousands of SNPs across the genome are compared between large cohorts of cases and controls, has uncovered a plethora of common alleles with modest effect sizes (odds ratios (OR)<2) associated with complex diseases, under the CDCV hypothesis. There are currently 52 genetic loci known to be independently associated with SLE - the vast majority of which are products of the genome-wide technological advancements of recent years – and the genetic variation within these loci is estimated to account for 15-20% of the total additive genetic variance (Harley et al. 2008; Moser et al. 2009), [J. Bentham, D. L. Morris, et al. 2014, manuscript in submission].

Under the CDCV hypothesis, the majority of the heritability of common diseases was predicted to be attributable to common genetic variants. Therefore, GWA studies were expected to explain the majority of the genetic variance (Reich and Lander 2001). This certainly isn't the case for most complex diseases, as with SLE, and the amount of remaining unexplained genetic variance (the so called 'missing heritability', discussed below) following very large GWA studies is higher than initially anticipated (Manolio et al. 2009; Eichler et al. 2010; So et al. 2011). However, GWAS has been successful in highlighting the involvement of previously unknown genes/pathways in disease

susceptibility and has provided the foundation for future work, such as resequencing projects searching for rare variants within known disease-associated loci (discussed in 1.2.2).

1.2.2 Rare variants

Rare variants with larger effect sizes (OR≥2), but present at frequencies that fall below the detectable threshold of most GWA studies (<5%), have been hypothesised to explain part of the 'missing' genetic effect of complex diseases (Pritchard 2001; Pritchard and Cox 2002). Although these variants are individually rare, they are collectively common, therefore may make a significant contribution to disease risk on the population level.

However, due to their low minor allele frequency (MAF) and incomplete penetrance, individual rare variants may never reach statistically significant levels of association, irrespective of very large sample sizes (Heinzen et al. 2012). Furthermore the relatively high *de novo* mutation rate in humans means chromosomes of unaffected individuals will also harbour rare, or even private, mutations that may or may not influence disease risk (Keinan and Clark 2012). Coupled with the expansion of the human population growth in recent history, this has resulted in an excess of rare variants within our genomes (Keinan and Clark 2012). Genome- or exome-wide sequencing may therefore uncover many new variants, but determining which of these are functionally relevant to disease is not easy by genetic analysis alone (Cooper and Shendure 2011).

One approach is to use the notable common variant discoveries of GWAS to focus on resequencing candidate genes that are already known to contain common disease risk variants. Indeed, many studies have now successfully identified additional rare variants in GWAS-associated loci (Torgerson et al. 2012; Rivas et al. 2011). However, the largest of such studies focused on the coding exons of 25 autoimmune GWAS-associated loci and concluded that there was a negligible affect from rare variants in these loci (Hunt et al. 2013).

The optimal analysis of rare variants is still an area of high debate, and various methodologies have been suggested (Madsen and Browning 2009; B. Li and Leal 2008; D.-Y. Lin and Tang 2011). Some methods involve weighting which rely on computational predictions of functional effects (Price et al.

2010). As of yet, there has been no unified agreement on the best genetic methodology for rare variant analysis, and issues regarding the robustness of case-control approaches – which are often used for common variant associations - are being addressed (Cheng and Chen 2013).

Ultimately, it is functional analyses of individual rare variants that will best enable us to understand their importance in disease pathogenesis. Furthermore, by resequencing disease-associated loci, the functional analysis of rare variants will add confirmatory evidence to disease biology paradigms established by the functional effect of common variants. Chapter 4 of this thesis explores the contribution of rare variants within the SLE susceptibility gene *ITGAM* to disease pathogenesis.

1.2.3 Copy Number Variation

Copy number variation (CNV) is the name given to the phenomenon that segments of DNA, ranging from kilobases (Kb) to megabases (Mb), can diverge from a diploid number of two copies present in an individual genome. CNV is not a rare occurrence in the human genome and is thought to make a substantial contribution to phenotypic variation (Schaschl, Aitman, and Vyse 2009). There is a great deal of inter-population variation in the frequency of CNV, and indeed the range of observed copies (Hardwick et al. 2011; Molokhia et al. 2011).

Some copy number variable loci have been associated with disease susceptibility (Olsson and Holmdahl 2012), including low copy number (CN) of *FCGR3B* with SLE susceptibility (discussed in 1.7.2) and increased CN of *DEFB* genes with Psoriasis susceptibility (Willcocks et al. 2008; Hollox et al. 2008). This type of variation is often missed in genome-wide association studies due to low linkage disequilibrium (LD) between CNV and common SNPs, or regions of such complexity are excluded from such studies, and it has been postulated that CNV could contribute to the unexplained genetic risk of complex diseases (Eichler et al. 2010). However, a large genome-wide survey concluded that it was unlikely for common CNV alone to explain much of the 'missing heritability' (Conrad et al. 2010). Interestingly this study also suggested that, in the presence of high LD, CNV could be the causal variation underlying some observed GWAS signals (Conrad et al. 2010).

1.2.4 Genetic Interactions

The paradigm of 'missing heritability' in recent years has focused on as-of-yet unidentified genetic variants that, once identified, are expected to increase the amount of narrow-sense (additive) heritability of complex diseases. However, this paradigm assumes an additive model of contribution for each genetic variant, both known and unknown (Zuk et al. 2012). Without fully exploring the possibility of epistasis between associated genetic variants, whereby the combined effect of two risk factors is greater than the sum of the effects of the individual variants, we may be underestimating the amount of heritability currently explained (Eichler et al. 2010). In which case, at least part of what is currently considered as 'missing heritability' could in fact be 'phantom heritability' due to the assumption that heritability of complex diseases is largely additive (Zuk et al. 2012). Therefore, exploring the possibility of genetic interactions is of key and current importance within complex disease genetics.

Indeed, gene-gene interactions between associated SNPs in SLE have been successfully identified in recent years (X. Zhou et al. 2012; Hughes et al. 2012; Leng et al. 2012; Zuo et al. 2014). In one study, a candidate gene approach was employed; five genes – *BLK*, *TNFSF4*, *TRAF1*, *TNFAIP3*, and *REL* – all known to be involved in B cell and T cell signalling, were chosen for interaction analyses in Chinese and European populations. The study was successful in providing evidence for gene-gene interactions, in particular between *BLK* and *TNFSF4* (X. Zhou et al. 2012). Similarly, another study chose two SLE-associated genes, *BLK* and *BANK1*, involved in B cell signalling and successfully demonstrated a gene-gene interaction between them, and, furthermore, demonstrated a functional interaction between the two protein products, BLK and BANK1 (Castillejo-López et al. 2012). With evidence supporting complex disease associations across an increasing number of loci, hypothesis-free searches for genetic interactions are unlikely to be fruitful due to multiple-testing restrictions. Thus, hypotheses derived from common pathways and/or protein-protein interactions can aid the discovery of gene-gene interactions (Sun and Kardia 2010).

I explore the possibility of a hypothesis-based genetic interaction between the *FCGR2B*-I232T SNP and *FCGR3B* CNV (discussed in section 1.7) in Chapter 6 of this thesis.

1.2.5 Sub-phenotype analyses

As discussed above, SLE is a very heterogeneous disorder. Recently, efforts have been made to dissect the genetic associations contributing to various sub-phenotypes, such as the presence of anti-dsDNA autoantibodies, and lupus nephritis (Bolin et al. 2013; Kim-Howard et al. 2010; Chung et al. 2011). In such analyses, some variants known to be associated with SLE no longer pass significance thresholds, suggesting they may contribute to specific clinical features. Although, reduced sample sizes following sub-phenotype stratification perhaps presents a problem for significant associations; particularly with less common subphenotypes (e.g. only ~5% of SLE cases are ANA negative). However, phenotypic homogeneity within the case cohort will be beneficial to delineating genetic variants contributing to specific immunological abnormalities.

1.2.6 Overlap with other autoimmune diseases

The comparison of GWA studies between autoimmune diseases has revealed some overlap in the loci conferring genetic susceptibility (e.g. *BLK, TNIP1, TNFAIP3*), suggesting variants within these loci contribute to general immune dysfunction as opposed to disease-specific phenotypes (Zenewicz et al. 2010). Although, there is growing evidence that this overlap in genetic susceptibility is limited (Ramos et al. 2011). The paradigm that specific genetic variants cause particular dysfunctions and collections of such variants lead to SLE onset is interesting, and support for such notions can sometimes be drawn from other diseases. As discussed above in section 1.1.2, there is a known 'IFN signature' in SLE patients (Baechler, Gregersen, and Behrens 2004). Gain-of-function variants of the SLE-susceptibility gene *IFIH1* are associated with elevated IFN responses in interferonopathies, such as Aicardi-Goutières syndrome (Rice et al. 2014; Robinson et al. 2011).

1.3 *ITGAM*

1.3.1 Association with SLE

Following a genome-wide linkage study, suggesting chromosomal position 16p12.3-q12.2 harboured SLE risk (Lee and Nath 2005), a candidate-gene approach then identified variation in *ITGAM* (16p11.2), as the causative association in a European population (Nath et al. 2008). Furthermore, by using two cohorts of African ancestry, in which the linkage disequilibrium (LD) across *ITGAM*, as with

all other genomic regions, is weaker, the minor allele (A) of the non-synonymous single nucleotide polymorphism (SNP) rs1143679 was isolated as the causal variant (Nath et al. 2008). Additionally, the association between SLE and 16p11.22 was independently identified in a GWA study (Hom et al. 2008). The association with the minor allele of rs1143679 was further validated in independent cohorts of European and Hispanic ancestry ($P_{meta} = 7.1 \times 10^{-50}$, OR = 1.83) but the SNP was found to be largely monomorphic (ancestral 'G' allele only) in Korean and Japanese cohorts (S. Han et al. 2009). A study in Hong Kong Chinese and Thai populations however, confirmed the same risk allele with disease association and furthermore with renal nephritis in SLE cases (W. Yang et al. 2009). This study also suggested a secondary independent association with rs1143683 (A858V) within *ITGAM*; the potential contribution of this polymorphism to SLE is addressed in Chapter 4. Recently a meta-analysis of 12,155 cases and 14,300 controls from ethnically diverse populations including European, African American, Latin American, East Asian, and South Asian, demonstrated a robust association between rs1143679 and SLE (OR=1.76; 3.6×10^{-90}; Maiti et al. 2014). The MAF of rs1143679 is estimated to be ≈0.15-0.2 in SLE cases across multiple ethnicities (S. Han et al. 2009).

ITGAM encodes the CD11b polypeptide, which non-covalently pairs with CD18 (encoded by *ITGB2*) to form complement receptor 3 (CR3; discussed in detail in section 1.4). The rs1143679 polymorphism results in an arginine (R) to histidine (H) substitution at codon 77 (R77H) of CD11b. The R77H variant is located in the β-propeller domain of CD11b, which is not thought to be a direct binding site for any of the known CR3 ligands. However, as this transmembrane protein carries cell signals and, in doing so, alters its conformation, the R77H variation could affect the protein's cell signalling leading to impaired function. In light of SLE pathologies, several CR3 functions could contribute to disease onset, in particular the diminished processing of iC3b-opsonised apoptotic cells.

1.3.2 Association with SLE sub-phenotypes

Clinical sub-phenotype analyses in a European cohort identified a strong correlation between rs1143679 and renal disease, discoid rash and immunological manifestations (Kim-Howard et al. 2010). Also, a genome-wide association study with SLE cases stratified for anti-dsDNA autoantibody production – a clinically important sub-phenotype - found *ITGAM* to be more strongly associated

with anti-dsDNA positive SLE (OR=1.8; p=1.1 $x10^{-15}$) than anti-dsDNA negative SLE (OR=1.3; p=2.1 $x10^{-4}$) (Chung et al. 2011).

1.3.3 Association with other autoimmune diseases

There is some overlap between the genetic associations of SLE and other autoimmune diseases, such as variations in *BLK, TNIP1* and *PRDM* (Zenewicz et al. 2010; Ramos et al. 2011). Large case-control studies have reported associations between rs1143679 and Sjogren's syndrome (OR=1.12; P_{meta}= 0.008), and systemic sclerosis (OR=1.12; P_{meta}= 0.019), although these are very modest in comparison to the association seen with SLE (Anaya et al. 2011; Carmona et al. 2011). No association was found with multiple sclerosis, rheumatoid arthritis, juvenile idiopathic arthritis, celiac disease, and type-1 diabetes (Anaya et al. 2011; Phipps-Green et al. 2009). Variation within *ITGAM* does not appear to confer susceptibility to general autoimmunity, but instead is thought to be largely SLE-specific.

1.4 Complement Receptor 3

1.4.1 Overview

ITGAM encodes CD11b/α_m (165KDa), which binds non-covalently with CD18/β_2 (95KDa) to form the heterodimeric cell surface receptor known as complement receptor 3 (CR3), also known as CD18/CD11b, $\alpha_m\beta_2$, and macrophage receptor-1 (Mac-1). CR3 is one of four members of the B_2-integrin family, which are possessed by all vertebrates and exclusively expressed on leukocytes (Hynes 2002). In addition to CD11b, CD18 can pair with CD11a (forming LFA-1; $\alpha_L\beta_2$), CD11c (forming CR4; $\alpha_X\beta_2$), and CD11d (forming $\alpha_D\beta_2$). Complete CD18 (β_2) deficiency results in a rare and often fatal inherited disease known as Leukocyte adhesion-molecule deficiency disorder (LAD) (Shaw et al. 2001). This life-threatening disorder highlights the importance of the β_2-integrin family to the innate immune system.

1.4.2 Expression profile and conformational states

CR3 is mainly expressed on cells of the innate immune system - phagocytic cells (neutrophils, monocytes/macrophages), myeloid dendritic cells, and Natural Killer (NK) cells - but can also be

found on $CD27^+$ memory B cells (Ross and Větvicka 1993; Kawai et al. 2005). Its cell surface expression is not maintained at a consistent level, but instead is up-regulated from the messenger (m)RNA level in response to inflammatory signals. Leukocytes yet to undergo activating stimuli have low densities of cell surface receptors that are involved in inflammatory processes, such as CR3 (Ley 2002). Large intracellular pools of such receptors are stored in secretory vesicles and are available for immediate up-regulation of cell surface expression following appropriate activating signals. When a neutrophil undergoes this so-called 'priming' process, the intracellular vesicles fuse with the plasma membrane, releasing the store of receptors, and rapidly increasing their cell-surface density (Edwards 1995). Such changes in the expression levels of receptors on leukocytes, in addition to the upregulation of their ligands on endothelial cells in response to tissue damage or infection, triggers extravasation from the blood, though progression of slow rolling, firm adhesion, and, finally, transmigration (Springer 1995).

In addition to the regulation of its cell surface expression, the conformational state of CR3 is also modifiable. CR3, and indeed other integrins, undergo conformational changes in response to allosteric activation, attributed to the "switchblade" mechanism of activation through receptor straightening (Hynes 2002; Kinashi 2006). This mechanism can result from direct interaction of the CR3 extracellular domain to a stimulus, resulting in 'outside-in' signalling. Additionally, CR3 can respond to signals originating from other cell-surface receptors in what is known as 'inside-out' signalling (Lefort et al. 2009). The same conformational changes occur under both mechanisms, with the extension and straightening of the extracellular domain, and separation of the CD11b and CD18 cytoplasmic tails; ultimately these conformational changes enable high-affinity ligand-binding (Luo, Carman, and Springer 2007).

1.4.3 Ligand binding

The ligand-promiscuity of CR3 permits it to carry out many immune functions, and these are summarised in Table 1.1 (Ross and Větvicka 1993; Z. Li 1999; van Lookeren Campagne, Wiesmann, and Brown 2007; Walzog et al. 1999). The diversity of CR3 ligands ranges from molecules of the immune system, including complement factor iC3b and intracellular adhesion molecule (ICAM)-1, to pathogen-associated molecular patterns (PAMPs), such as lipopolysaccharides (LPS) from gram-negative bacteria, dsRNA of viruses, and β-glucan from yeast.

There are two well-established ligand binding sites on CD11b: the inserted (I)-domain, located near the N-terminal headpiece of the polypeptide, and the lectin-like domain, located proximal to the transmembrane domain at the C-terminal end of the polypeptide (Diamond et al. 1993; Thornton et al. 1996). The I-domain is ~200 amino acids in length and has specificity for ICAM-1, iC3b, and fibrinogen (Ross and Větvicka 1993). It is only fully exposed when CR3 occupies an activated state following conformation changes. The development of an antibody (clone CBRM1/5) with epitope specificity for the I-domain allows CR3 activation to be measured (Diamond and Springer 1993).

Ligation of the lectin-like site, which is constitutively exposed on CR3, induces an intermediate 'primed' conformational state of the integrin receptor (O'Brien et al. 2012). This has been shown to enhance I-domain-dependent functions. For instance, the presence of polysaccharides on microbial membranes, such as β-glucan on the cell surface of *Saccharomyces cerevisiae*, recognised by the lectin-like site, increases the CR3-dependent cytotoxic activities of neutrophil and NK cell to iC3b-coated targets (Xia et al. 1999; Vetvicka, Thornton, and Ross 1996; Větvicka et al. 1999). Likewise, the interaction of CR3 with glycosylphosphatidylinositol (GPI)-linked receptors, such as CD16b on the cell surface of neutrophils (discussed below in 1.4.4.2), is thought to occur via the lectin-like domain and increase CR3 binding to iC3b.

Table 1.1 Summary of CR3 ligands and their origin

CR3 carries out multiple immune functions due to its specificity for a diverse range of ligands

Ligand	Origin	Binding Site	Function
iC3b	Opsonised target cells	I-domain	Phagocytosis; cytotoxixity
ICAM-1	Endothelial cells	I-domain	Adherence
Fibrinogen	Extracellular matrix	I-domain	Adherence
β-glucan	*Saccharomyces cerevisiae*	Lectin-like	Receptor priming
dsRNA	Virus	? I-domain	Endocytosis
GPI-linked receptors (CD16B, CD14)	Neutrophils; monocytes	Lectin-like	Cooperative phagocytosis

ICAM-1 = Intracellular Adhesion Molecule 1; GPI = glycosylphosphatidylinositol

1.4.4 Functions

1.4.4.1 Intercellular Adhesion

CR3 acts as an intercellular adhesion molecule during leukocyte extravasation. It engages with its ligand ICAM-1, which is upregulated on the surface of endothelial cells in response to tumour necrosis factor (TNF) and Interleukin (IL)-1 following tissue damage or infection. The paradigm of leukocytes extravasation from the blood involves slow rolling, firm adhesion, and transmigration (Springer 1995). During weak adhesion and slow rolling, neutrophils may respond to other inflammatory signals and, if an activation threshold is reached, β2 integrins switch to the high-affinity conformational state and result in neutrophil firm adhesion and subsequent transmigration (Ley 2002; Ma, Plow, and Geng 2004). The binding of CR3 with ICAM-1 has been shown to regulate the velocity of the cells following P-selectin-mediated slow-rolling (Moore et al. 1995; Jessica L Dunne et al. 2003), and CD18-, CR3-, or LFA-1 (CD11a/CD18)-deficient mice, were all shown to have elevated leukocyte rolling velocities (J. L. Dunne 2002). However, another study using LFA-1-deficient mice, together with β2-integrin blocking monoclonal antibodies, suggests CR3 has a minimal role to play in firm adhesion and instead mediates the eventual emigration of neutrophils (Henderson et al. 2001).

1.4.4.2 Phagocytosis

The complement system is a mechanism of opsonising microbes and apoptotic cells for effective clearance by phagocytosis. CR3 acts as a phagocytic receptor through its complement factor ligand iC3b. This is a product of complement activation, whereby the complement protein C3 is cleaved by C3 convertase producing C3a and C3b. Whereas C3a stimulates inflammation by acting as a chemoattractant for neutrophils, the larger C3b fragment becomes covalently attached to the surface of the target cell where the complement system was activated, acting as an opsonin to promote phagocytosis (Abbas, Lichtmann 2012). Indeed ligation of this complement factor to CR3 alone is sufficient to induce phagocytosis of opsonised targets without the need for synergistic activation (Murphy 2012).

CR3 has also been shown to interact with membrane-bound FcγRIIIb (CD16b), which is a GPI-linked protein, on the cell surface of neutrophils. CD16b binds IgG but, given the absence of a

transmembrane domain, is thought to be unable to transduce cell signals. Strong evidence exists for the cooperation of CR3 with CD16b to mediate phagocytosis of IgG-opsonized targets (Krauss et al. 1994). CR3 is also a receptor for neutrophil-derived soluble (s)CD16 (Galon et al. 1996). Such FcγR-CR3 interaction is thought to be a reciprocal relationship leading to the activation of CR3 via the lectin-like domain located in the C-terminal region of CD11b (discussed above in 1.4.3) thereby increasing iC3b binding by CR3 (Stockl et al. 1995). Likewise, on human monocytes, the GPI-linked receptor CD14 cooperates with CR3 to phagocytose *Borrelia burgdorferi* (Hawley et al. 2011). CD14 is also implicated in the phagocytosis of apoptotic cells, which could further implicate CR3 in apoptotic clearance and SLE (Pittoni and Valesini 2002).

1.4.4.3 Immune regulation

CD11b-deficiency has been shown to enhance both Toll-like receptor (TLR)4- (C. Han et al. 2010) and TLR9-triggered (Bai et al. 2012) immune responses on murine dendritic cells (DCs). Reports on the regulatory role of CR3 following receptor engagement have been somewhat contradictory; engagement of monocyte CR3 with anti-CD11b antibodies or soluble CD23 has been shown to increase the production of pro-inflammatory cytokines, such as TNF, IL-1β, Macrophage inflammatory protein (MIP)-1α, and MIP-1β (Fan and Edgington 1993; Roger Rezzonico et al. 2000; R. Rezzonico 2001), and engagement of neutrophil CR3 with an anti-CD18 antibodies has been shown to upregulate IL-8 production during the inflammatory response (Walzog et al. 1999); yet monocyte CR3 engagement down-regulate the pro-inflammatory cytokine IL-12 and induces IL-10 secretion (Marth and Kelsall 1997; Yoshida et al. 1998). However, these seemingly paradoxical results are explained in light of ligand-avidity; natural ligands induce high-avidity CR3 engagement leading to anti-inflammatory responses, whereas low-avidity engagement results in pro-inflammatory responses (Wang et al. 2010). Furthermore, a recent study demonstrated the differential function of CR3 on macrophage and myeloid dendritic cell LPS engagment (Ling et al. 2014), suggesting cell type, as well as ligand avidity, may also contribute to some paradoxical results in the literature.

Very little is known about CR3 function on NK cells, and, despite the growing evidence of CR3 as an immune regulator, it is often listed as an activating receptor in the binary categorisation of NK cell receptors in review articles (Vivier et al. 2008). NK cells, in particular the $CD56^{bright}$ subset, are

prominent producers of cytokines, therefore CR3 may also play an important regulatory role in the cytokine production of NK cells. This is discussed further in section 1.5.

1.5 Natural Killer cells

1.5.1 NK cells in SLE

Natural Killer (NK) cells are characterised by the presence of CD56 and the absence of CD3, and can be divided into two subsets depending on the level of CD56 expression: $CD56^{dim}$ and $CD56^{bright}$ (Abbas, Lichtmann 2012). The former, which comprise ~90% of the total NK cells are efficient cytotoxic cells and secrete lower levels of cytokines, whereas the $CD56^{bright}$ sub-population secrete greater levels of cytokines but only acquire cytotoxicity after prolonged activation (Cooper, Fehniger, and Caligiuri 2001; Cooper 2001). NK cells play a regulatory role within the immune system, which is of particular interest to inflammatory diseases such as SLE. Following priming by monocyte-derived cytokines (monokines) IL-12, IL-15, and IL-18, NK cells secrete pro-inflammatory cytokines, such as IFN-γ, which aid the activation of macrophages and dendritic cells (DCs), providing a positive feedback loop (Fehniger et al. 1999). Additionally, NK cells have the ability to kill immature DCs, hyperactive macrophages, and activated $CD4^+$ T cells through cytotoxicity (Vivier et al. 2008).

Excess IFN-γ production by NK cells has been observed in SLE (Hervier et al. 2011). Historically, however, the role of NK cells in SLE has been rather overlooked. However, studies have suggested that the NK cells in the peripheral blood of SLE patients are reduced in numbers and function (Park et al. 2009; Yabuhara et al. 1996; Schleinitz et al. 2010). A recent study adds further support to these findings, with the difference in NK cell number between cases and controls being more pronounced in patients with active disease (Henriques et al. 2013).

Genetic studies are also beginning to redirecting our attention towards the involvement of NK cells. For instance, as discussed below in section 1.7.4, a consequence of the SLE-associated *FCGR3B* gene deletion also results in the ectopic expression of the inhibitory CD32b on NK cells (Mueller et al. 2013; van der Heijden et al. 2012). Additionally, polymorphisms in *STAT4* – a key mediator of NK cell signalling - are among the strongest risk factors for SLE susceptibility (Harley et al. 2008; Bolin et al. 2013). It has been demonstrated that expression of CD11b and CD27, the TNF-receptor family

member, are markers for NK cell maturity, in both mice and humans (Hayakawa and Smyth 2006; Silva et al. 2008). However, aside from being a marker of maturity, the role of CR3 on NK cells is incompletely understood, and the consequences of the R77H polymorphism on NK cell function have yet to be fully explored. In chapter 5 of this thesis I explore the effects of LA1 on the intracellular signalling of NK cells, following cytokine activation, as discussed below.

1.5.2 JAK-STAT Signalling

Cytokine signalling through type I and II family cytokine receptors, such as those expressed on NK cells, is dependent on the Janus kinase (JAK) and Signal Transducers and Activators of Transcription (STAT) pathways. There are four JAKs – JAK1-3 and Tyk-2, and seven STATs – STAT1-4, 5a, 5b, and 6. In resting cells, JAKs are non-covalently associated with the cytoplasmic domains of the cytokine receptors, and monomeric, non-phosphorylated STAT proteins are present in the cytoplasm. Upon ligand-binding, cytokine receptor chains are brought together and associated JAKs are activated, which in turn phosphorylate the tyrosine residues in the cytoplasmic receptor domains (Abbas, Lichtmann 2012). These phosphotyrosines are recognized by specific STATs; it is this level on which cytokine signalling specificity is controlled. Interleukins can activate common JAKs yet their downstream signalling can diverge at the STAT level; it is the tyrosine-based motifs in the receptor components that dictate their STAT specificity (Stahl et al. 1995; Johnston et al. 1995). For instance, IL-12 and IL-13 both utilise Jak-2 and Tyk-2, yet IL-13, unlike IL-12, does not phosphorylate STAT4 (Yakubenko et al. 2013). Once the Src homology 2 (SH2) domains of the STATs have bound to the cytokine receptor chains, they are themselves tyrosine (and serine) phosphorylated by JAKs. Phosphorylated STATs can dimerise, enabling their translocation to the nucleus and subsequent sequence-specific DNA binding to activate transcription. STATs may form homo- or heterodimers, which adds to the level of signalling diversity. Additionally, the roles of STAT5 tetradimers in signalling are currently being recognised (Levy and Marié 2012; J.-X. Lin et al. 2012).

1.7 *FCGR* locus

1.7.1 Architecture of the FCGR locus

The *FCGR* locus on chromosome 1q23.3 encodes five low-affinity IgG receptors; four of which are activating - FcγRIIa (CD32a), FcγRIIc (CD32c), FcγRIIIa (CD16a), and FcγRIIIb (CD16b), encoded by *FCGR2A, FCGR2C, FCGR3A,* and *FCGR3B*, respectively - and FcγRIIb (CD32b) alone, encoded by *FCGR2B*, is an inhibitory receptor. Each gene has a unique cell expression profile, as summarised in Table 1.2.

Table 1.2 Expression profiles of the human Fcγ receptors and their association with SLE.

Receptors are listed in the order of their encoding genes, from centromere to telomere, along chromosome 1q23., The number of cases and controls used plus the p-values obtained for associations are given, and references to meta-analyses are used, where appropriate.

Gene Name	Protein Name	Expression	Variants associated with SLE (cases/controls, p-value; reference)
FCGR2A	CD32a, FcγRIIa	Neutrophils, monocytes, macrophages, DCs	R131H (720/2337 $p=6.8x10^{-7}$; Harley et al. 2008)
FCGR3A	CD16a, FcγRIIIa	Macrophages, monocyte subsets, NK cells	F158V (3493/2426, $p_{meta}=0.0001$; L.-H. Li et al. 2010)
FCGR2C	CD32c, FcγRIIc	NK cells, B cells	n/a
FCGR3B	CD16b, FcγRIIIb	Neutrophils	Reduced CN (1808/3565, $p_{meta}=9.1x10^{-7}$; McKinney and Merriman 2012)
FCGR2B	CD32b, FcγRIIb	B cells, monocytes, macrophages, DCs	232T-homozygosity (2287/3596, $p_{meta}=8x10^{-6}$; Willcocks et al. 2010)

Due to evolutionary segmental duplication, the locus is split into two ~85Kb paralogous blocks that share an estimated overall homology of 93.7% (Mueller et al. 2013). The centromeric block contains *FCGR2A*, *FCGR3A* and the 5' end of *FCGR2C*; the telomeric block includes the 3' end of *FCGR2C*, *FCGR3B* and *FCGR2B* (Figure 1.1). As with other regions displaying CNV, this segment homology is thought to account for the CNV seen at both *FCGR3A* and *FCGR3B* (Mueller et al. 2013). There is a higher frequency and broader range of CNV at the *FCGR3B* gene compared with *FCGR3A* (Breunis et al. 2009). *FCGR2C* arose from the same segmental duplication: its 5' end is 99.2% homologous to that of *FCGR2B*, and its 3' end is homologous to that of *FCGR2A* (Figure 1.1A). It is often thought of a pseudo-gene as only ~18% of Europeans possess a variant in exon 3 of *FCGR2C* which alters the stop codon to an open reading frame (ORF). In the presence of this ORF, CD32c is expressed on B cells and NK cells (Metes et al. 1998; Xinrui Li et al. 2013).

This locus has long been known for its influence on autoimmunity. There are multiple SLE associations with polymorphisms spanning the locus, including *FCGR2A*-R131H (rs1801274), *FCGR3A*-F158V (rs396991), *FCGR3B* copy number variation (CNV), and *FCGR2B*-I232T (rs1050501), as summarised in Table 1.2, implicating under-functioning of these receptors in IC clearance and disease biology (Yuan et al. 2009; L.-H. Li et al. 2010; McKinney and Merriman 2012; Willcocks et al. 2010).

Figure 1.1 The *FCGR* locus on chromosome 1q23.3

A) shows the genomic composition of the five *FCGR2/3* genes in the absence of a gene deletion. Red and blue shaded boxes represent the region involved in the 85Kb segmental duplication, with the darker shades highlighting the 24.5Kb containing the breakpoint. B) shows the genomic composition in the presence of an 85Kb deletion, resulting in complete absence of *FCGR3B* and the amalgamation of *FCGR2C/FCGR2B* forming the chimeric *FCGR2B'* gene. The purple segment is representative of the 24.5Kb segment of complete sequence homology of *FCGR2C* and *FCGR2B*.

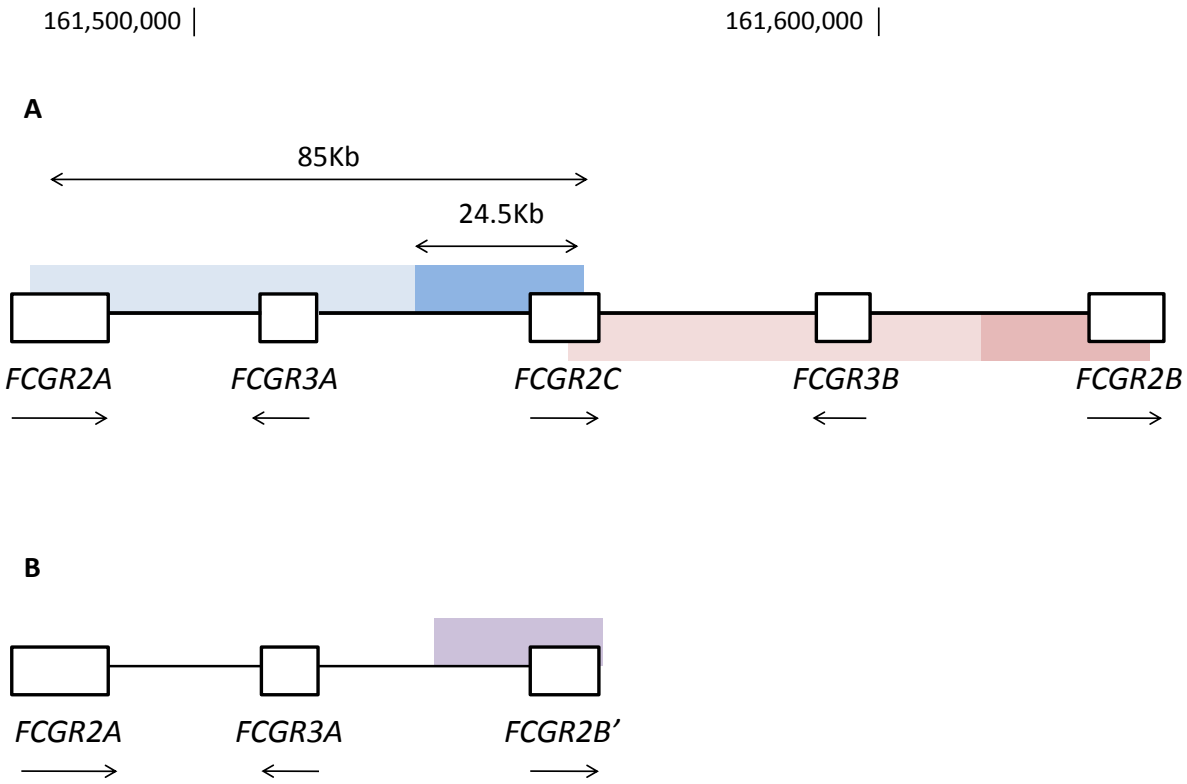

1.7.2 Reduced copy number of FCGR3B

Evidence of a contribution to SLE risk from the copy number variation within this locus came from the rat *Fcgr3* and human orthologous *FCGR3B* genes, whereby a reduced copy number (<2) was found to be associated with glomerulonephritis (Aitman et al. 2006). Using a quantitative (q)PCR assay, low copy number of *FCGR3B* was later confirmed to be associated with systemic autoimmunity in two independent cohorts of European ancestry (Fanciulli et al. 2007). However, the

accuracy of using qPCR to measure CNV has since been questioned. A novel PCR-based assay called the Paralogue Ratio Test (PRT; described in section 2.11) was developed for high-throughput copy number calling (Armour et al. 2007), and the technology has been successfully employed for the study of CNV at multiple loci across the human genome, aiding the understanding of this structural variation in human disease (Walker, Janyakhantikul, and Armour 2009). Applying the PRT to the *FCGR3* locus allowed more accurate copy number calling, and replicated the association with SLE in European (P=0.018; OR=1.57) and Chinese ($P=4 \times 10^{-4}$; P=1.65) cohorts (Niederer et al. 2010b). Meta-analyses have confirmed this robust association between reduced copy number of *FCGR3B* and SLE ($P_{meta}=9.1x10^{-7}$, OR=1.59; McKinney & Merriman, 2012). *FCGR3B* CNV has since been shown to be correlated with both CD16b protein expression on neutrophils and soluble serum levels of CD16b. Furthermore, the reduced expression was shown to impair immune complex binding and clearance by neutrophils, thus adding a functional perspective to the genetic association (Willcocks et al. 2008).

The NA1 and NA2 allotypes of CD16b differ by five amino acids and are encoded by two alleles which differ by six single nucleotide variations, one of which encodes a synonymous codon, within *FCGR3B*. NA1 has been shown to be the allotype with the highest affinity for IgG (Salmon, Edberg, and Kimberly 1990). The association within *FCGR3B* was further extended to a biallelic-CNV model, whereby disease risk associated with gene deletion being greater for the higher-affinity NA1 allotype than the lower-affinity NA2 (Morris et al. 2010). Despite conflicting results regarding the LD between *FCGR3B* copy number and surrounding *FCGR* SNPs in the studies by Morris et al. and Niederer et al., both studies concluded that reduced copy number of *FCGR3B* was an independent risk factor for SLE (Morris et al. 2010; Niederer et al. 2010b).

1.7.3 FCGR2B-I232T and SLE

The rs1050501 non-synonymous polymorphism (Chr1:161643798), located in exon 5 of *FCGR2B* gene, was initially identified in a Japanese cohort. The SNP encodes an isoleucine (I) to threonine (T) amino acid change at codon 232 of the CD32b polypeptide - the only inhibitory receptor in the FcγR family – and 232T-homozygosity was found to be associated with SLE (Kyogoku et al. 2002). This association has since been replicated in other East Asian populations (Chen et al. 2006; Chu et al. 2004; Siriboonrit et al. 2003).

There have been some inconsistencies regarding the association of *FCGR2B*-I232T with SLE in European cohorts, with some studies reporting no association (V. Magnusson 2004; Xiaoli Li et al. 2003). However, these studies had relatively small sample sizes, particularly given the low MAF (0.1) in Europeans (Clatworthy et al. 2007), compared with that in East Asians (0.22-0.25) (Chen et al. 2006; Chu et al. 2004; Siriboonrit et al. 2003). However, a larger case-control study using UK cohorts found a significant association (p=0.014; OR=2.8) between 232T-homozygosity and SLE (Willcocks et al. 2010). Furthermore, a meta-analysis of the published European studies showed an OR of 2.06 (p=0.022) for 232T-homozygosity, providing strong evidence of association (Willcocks et al. 2010).

Amino acid 232 forms part of the transmembrane domain of CD32b and the I232T variant has been show to affect the formation of lipid rafts, thus reducing the regulatory function of CD32b on B cells and macrophages (Floto et al. 2005; Kono et al. 2005). Interestingly, the minor allele of the I232T variant has also been shown to be protective against progress to severe malaria following infection, as the under-functioning minor allele enhanced phagocytosis of infected erythrocytes through a mechanism of reduced inhibition (Willcocks et al. 2010; Clatworthy et al. 2007). The relatively high frequency of the minor alleles of some complex disease-associated polymorphisms does suggest positive selection pressure under particular environmental conditions, and given that severe malaria infection is strongly associated with childhood mortality, the I232T variant could be an example of such a phenomenon (Clatworthy et al. 2007). SLE has a higher prevalence, and is more severe, in South-East Asian and African populations, which are areas historically troubled by malaria infections (Clatworthy et al. 2007). This is reflected in the increased MAF of some associated variants in these populations, compared with European population (Willcocks et al. 2010).

1.7.4 Ectopic Expression of CD32b

Recently the effect of the *FCGR3B* gene deletion has been explored in the broader context of the locus. The ~85Kb deletion extends across the entire *FCGR3B* gene, upstream into the 5' end of *FCGR2C* and downstream into the 5' end of *FCGR2B*. The breakpoint has been mapped to within a 24.5Kb region of complete sequence homology in the 5' region of *FCGR2C* and *FCGR2B* (Figure 1.1). The absence of sequence duplication surrounding the deletion suggests the breakpoint creates a seamless amalgamation of the *FCGR2C* and *FCGR2B* genes (Mueller, 2013). Furthermore, this chimeric *FCGR2C/FCGR2B* gene, termed *FCGR2B*', has the 3' coding region deriving from *FCGR2B* yet

is under the regulatory control of that of *FCGR2C*, which results in the ectopic expression of the inhibitory CD32b receptor on NK cells (van der Heijden et al. 2012; Mueller et al. 2013). The functionality of CD32b on NK cells has yet to be demonstrated. However, effector functions of NK cells are controlled by the fine balance of many activating and inhibitory receptors, therefore the ectopic expression of this uniquely inhibitory Fc receptor is very intriguing. In Chapter 6 of this thesis, I explore the possibility of a genetic interaction between *FCGR3B* CNV and the *FCGR2B*-I232T polymorphisms. It is possible that part of the genetic association seen with reduced CNV is due to the ectopic expression of CD32b; it is also possible that the effect size of the *FCGR2B*-I232T association is underestimated without the consideration of *FCGR3B* CNV. That is, the under-functioning CD32b-232T variant may also contribute to SLE risk when ectopically expressed on NK cells, as has been demonstrated with B cells and macrophages (Kono et al. 2005; Clatworthy et al. 2007).

1.8 Summary and project aims

The 'waste disposal' hypothesis is a central paradigm of SLE disease biology, and refers to the under-functioning of apoptotic clearance by phagocytes. In support of this notion, genetic variants in genes encoding phagocytic receptors, such as *ITGAM* and the *FCGR* genes, are among the strongest risk factors contributing to SLE susceptibility. The study of the genetic variations associated with disease risk will ultimately aid our understanding of the immunological mechanisms contributing to disease onset, as they are not affected by disease progression, and will hopefully aid the development of targeted therapeutics.

The work presented in this thesis aims to:

- Determine the impact of the *ITGAM* common polymorphism rs1143679 (CD11b-R77H) on cell surface expression of CR3
- Investigate the contribution of rare variants within *ITGAM* to SLE
- Explore the underlying NK cell signalling effects of a potential CR3-targetted therapeutic
- Test for the potential genetic interaction between two SLE-associated variants within the *FCGR* locus – *FCGR3B* CNV and *FCGR2B*-I232T

Chapter 2: Methods

2.1 Samples

2.1.1 Ex vivo cells

Whole blood was obtained with consent from healthy volunteers, with no history of autoimmunity, from the Twins UK National Institute for Health Research (NIHR) Bioresource. Heparin was used an anti-coagulant and samples were processed on the same day as blood collection.

2.1.2 DNA

2.1.2.1 UK SLE cohort

The genomic DNA from SLE patients of European ancestry used in the following studies were collected by Professor Tim Vyse (ethical approval MREC/98/2/6 and 06/MRE02/9) prior to the start of this project. Each proband met the American College of Rheumatology (ACR) 1982 revised criteria for diagnosis (Tan et al. 1982).

2.1.2.2 Control Cohorts

Genomic DNA from healthy controls of European ancestry from the Wellcome Trust Case Control Consortium (WTCCC) 1958 birth cohort and TwinsUK National Institute for Health Research (NIHR) Bioresource were used as stated below.

2.2 Cell surface expression of CD11b on *ex vivo* cells by flow cytometry

Whole blood was used to measure cell surface expression of CD11b, and percentage of activated CD11b, on neutrophils and monocytes, under both resting and activated conditions, by Fluorescence-Activated Cell Sorting (FACS). Healthy volunteers (2.1.1) were used in pairs of opposing homozygous genotypes for the SLE-associated polymorphism rs1143679: R77-homozygous (WT) and 77H-homozygous. 20ml whole blood was enriched for leukocytes by sedimentation in 3% dextran-500, which removes erythrocytes. Samples were resuspended in Hank's balanced salt solution (HBSS) with 20 mM HEPES, 1 mM calcium chloride and 1 mM magnesium chloride. Cell activation

was achieved by incubation with 200nM phorbol myristate acetate (PMA, Sigma) for 10 minutes at 37°C.

Four leukocyte-enriched whole blood aliquots of 2.5 x10^5 cells were stained for 45minutes at 4°C with PerCyP-conjugated anti-CD14 and one of the following monoclonal antibodies:

1. PE-conjugated anti-CD11b (clone: ICRF44)
2. PE-conjugated IC
3. APC-conjugated anti-CD11b (clone: CMBR1/5)
4. APC-conjugated IC

Following cell surface staining, red blood cells were lysed using Lysis Sloution© (BD Bioscience) and cells were fixed using BD FACS Fixative Solution© (BD Bioscience). Samples were run on a BD FACS CANTO II flow cytometer using BD FACS Diva software. 30,000 events were collected. Forward-scatter (FSC) and side-scatter (SSC) area were used to identify the neutrophil population based on their cell size and granularity, respectively. The anti-CD14-PerCyP mAb was used to identify the $CD14^+$ monocytes. The anti-CD11b (clone: ICRF44) antibody and PE conjugated isotype control were used to measure total cell surface expression of CD11b. The anti-CD11b (clone: CMBR1/5), which recognizes an epitope on activated CD11b molecules (Diamond and Springer 1993), and APC-conjugated isotype control were used to measure the percentage of activated CD11b. FlowJo Software (version 7.6.4) was used to analyse the FACS data, and GraphPad Prism v.5 was used to compare mean fluorescent intensities (MFI) between genotype groups with a paired t-test.

2.3 Amplification of 500bp upstream of *ITGAM* start codon

I Polymerase Chain Reaction (PCR) amplified 40ng of genomic DNA by with 0.5U Hot Star *Taq* polymerase (Qiagen) and 0.5µM of each of forward (5'-CACCATGCCCAGCTAATTAAA) and reverse (5'-CTCCTCCCCACCCAGAGT) primers (Sigma Aldrich) in a total volume of 10µl (See Appendix A1 for full details). The primers were designed using Primer3 (v.0.4.0) software (http://frodo.wi.mit.edu/) and gave a product size of 587bp. The reverse primer is located in exon 1 to ensure I could sequence upstream of the start codon. Amplification was carried out on a G-Storm T4 thermocycler (see Appendix B1 for thermocycler conditions).

2.4 Capillary Sequencing

2.4.1 PCR confirmation and EXO-SAP clean-up

I ran 7µl of PCR product on a 2% agarose gel with 0.00025% (v/v) ethdium bromide, and observed the stained gels with a UV-transilluminator. I cleaned 1µl of the PCR products by adding 5.75µl ddH_20 and 0.25µl EXO-SAP (VWR), and incubating the samples at 37°C for 30 minutes, followed by an enzyme-inactivating step at 80°C for 15 minutes, to remove excess primers and dNTPs.

2.4.2 Big Dye© reaction

3.5µl of the EXO-SAP product (clean, amplified DNA) was labelled with 0.25µl Big Dye© v3.1 (Life Technologies), with 5 pmoles primer (same as used for PCR, unless otherwise stated), in a total volume of 5.25µl. The samples were incubated at 96°C for 30 seconds, 50°C for 15 seconds, and 60°C for 60 seconds, for a total of 30 cycles in a G-Storm T4 thermocycler.

I added 5.25µl of an ethanol-based precipitation solution (Appendix C1) to clean the DNA product following the Big Dye© reaction. This was incubated at room temperature for 15 minutes followed by a 30 minutes centrifugation at 3000rpm. The solution was removed from the pelleted DNA with a short 10 second centrifugation of the inverted plate at 400rpm. I added 100µl of 70% ethanol, to clean the DNA, and centrifuged for 10 minutes at 3000rpm. Once more, a short centrifugation at 400rpm was used to remove the ethanol and the DNA pellet was further dried for 5 minutes at 60°C on a thermocycler. I added 10µl of Hi-Di formamide (Applied Biosystems) to each well of the 96-well plate and the DNA was then denatured at 95°C for 2 minute.

2.4.3 ABI 3730xl DNA Analyser and Analysis

The samples were processed on an ABI 3730xl DNA analyser (Applied Biosystems) in the King's College Genomics Centre. Electropherograms were visually analysed using the BioEdit Alignment Editor Software.

2.5 Discovery of rare coding variants within *ITGAM*

2.5.1 454 sequencing and analysis

This work was performed by Ellen Thomas and Shriram Bhosle, Imperial College London.

Genomic DNA from 73 SLE patients meeting American College of Rheumatology criteria underwent whole genome amplification (Qiagen Repli-G). Ethical approval was given by London Multicentre Research Ethics Committee and participants gave written consent. Standard (KOD polymerase, Merck) and long-range (Sequalprep, Invitrogen) PCR reactions were carried out in 13 amplicons, giving products between 600 base pairs and 4 kb in length, covering 24 kb of the *ITGAM* gene including all thirty exons. The PCR products were run on an agarose gel and purified using the Qiagen MinElute 96 UF PCR Purification Kit. Seven amplicons greater than 1.5kb were pooled and sheared to fragments of 500-800bp on the Covaris E210. The six short PCR products were added to the sheared products and each pool was tagged with a unique DNA barcode using the Parallel Tagged Sequencing (PTS) protocol (Meyer, Stenzel, and Hofreiter 2008), starting at the blunt end repair step. The barcoded PCR products were quantified using the Invitrogen Quant-iT Picogreen dsDNA kit and combined into a single pool using 10ng of each tagged sample. Dephosphorylation and restriction digestion was carried out according to the PTS protocol and the pool of sheared and indexed PCR products was taken through 454 Titanium library preparation according to the manufacturer's protocol (GS FLX Titanium General Library Preparation Method Manual v5.3.2), starting at step 3.5. Library quality was checked using an RNA Pico 6000 assay on the Agilent Bioanalyser and quantified using a RiboGreen assay (Thermo Fisher Scientific) using the Nanodrop 3300 fluorospectrometer. The library was diluted to 1 x 10^8 molecules/µl, amplified and sequenced according to the manufacturer's protocol for 454 GS FLX sequencing. With 896,206 reads which passed filters, an average coverage of 105x was achieved. 88% of the samples were covered at a level sufficient for variant calling (more than 10 reads) in at least 80% of the target region. Additional PCRs (KOD polymerase, Merck) were generated covering exons 8, 13 and 14 due to low coverage in the 454 data. Capillary sequencing of these amplicons used the 3730xl platform (Applied Biosystems).

454 sequence read demultiplexing used 'untag' software (Meyer, Stenzel, and Hofreiter 2008), base calling used Pyrobayes (Quinlan, Stewart, and Marth 2008), and alignment to the reference genome used BWA (H. Li and Durbin 2009). Variant calling was carried out using GATK (McKenna et al. 2010) without duplicate read removal, using hard filters: coverage at least 10-fold, genotype quality threshold 50, SNP quality threshold 30, and allele balance threshold 0.75.

2.5.2 Confirmation of rare variants by capillary sequencing

Table 2.1 summarises the 17 potential novel variants observed in the 454 sequencing of *ITGAM*; 16 of which are non-synonymous coding variants (named conventionally by the codon number and change in amino acid), and one splice site variant. Primer pairs (Sigma Aldrich) were designed using the Primer3 (v.0.4.0) software (http://frodo.wi.mit.edu/) to produce amplicons <400bp of *ITGAM* regions containing the putative variants. The small sizes of the amplicons enabled easy amplification and sequencing.

I amplified 30ng of genomic DNA from the appropriate SLE samples in a total volume of 20µl (reaction conditions are summarised in Appendix A). Amplification was carried out on a G-Storm T4 thermocycler, as summarised in Appendix B. Capillary Sequencing was carried out as above (Methods 2.4), and electropherograms were visually analysed for the presence of the novel variants.

Table 2.1 Summary of primers used for PCR amplification of *ITGAM* regions containing putative rare variants

Variants are named in the conventional format: amino acid change and the codon numbers. A stop codon is designated by *. Splice variant is named by the genomic location and 'SS' prefix. Purple shading indicates the novel variants confirmed by capillary sequencing.

Forward Primer	Reverse Primer	Tm(°C)	CD11b Variant
5' CTCCCCACATGTCGAAGTTT	5' ACACAGGAGTGCCTGGAAAG	56.8	Q79*
5' TTGTCCCTCCTGTTTCCTGC	5' CTGTCTGCCTCAGGGATGAC	56.8	R246Q
5' TTGCTAGCCTCACACCATGA	5' CAGATGCCTGACTCACCCTC	53	K295E
5' TGCCTTCCGCAGTGAGAAAT	5' CAGATGCCTGACTCACCCTC	56.8	A320T N326D
5' CCCCCATTACTACGAGCAGA	5' AAACAGTATCAGGCCCCAAC	56.8	R498G
5' CACAGCTGAGAAGCAGAGGA	5' GGGTCCTCGATGCAATTCTA	56.8	S672G L680Q
5' CACAGCTGAGAAGCAGAGGA	5' GACCCCAACTCTGGACTCAC	53	F735S
5' GTCTCTGTTCTGCTGGAGCA	5'ACAGGTCAAGCGGGAAGAAG	56.8	L792P
5' TGTCTGCGTCTCTGTTCTGC	5' TTCCGGTAGGACAGGTCAAG	56.8	SS31336581
5' ACCCATTACCCATGTGCCTG	5' ATCGATTTTCCTCCCCAGCC	56.8	F941V
5' AACCCCCAGAAATCCAGAGT	5'AGAGACTGAGGCGCAGAGAG	56.8	V1019L V1019A
5' ACATCAAGGTGTGTGGGGTC	5' ATAGTTCCTCAGCGCCCAAG	56.8	S1068R
5' GGCTTCTTCAAGCGGCAATA	5' GTCCTGTCGGGGATACTTCG	56.8	G1145S

2.6 Genotyping novel rare variant in larger cohorts

2.6.1 Site-specific primer (SSP) PCR

2.6.1.1 Theory

The site-specific primer polymerase chain reaction (SSP-PCR) is a multiplex PCR with four primers; a pair of non-allele-specific 'outer' primers, and a pair of allele-specific 'inner' primers (Figure 2.1). It is essential that the final 3' nucleotide of a primer aligns perfectly with the DNA template for 5'-3' DNA extension within a PCR reaction. It is therefore possible to utilise this for allele-specific amplification. The final 3' nucleotide of the two inner primers – forward and reverse - of an SSP are designed to overlap at the polymorphic nucleotide of interest, and each primer is specific for one allele. Therefore, each inner primer will only be capable of mediating DNA extension from one of two possible alleles.

There are three possible PCR products from the various combinations of 'outer' and 'inner' primers, and if designed to yield amplicons of various sizes, they can be easily visualised under UV light following ethidium bromide gel electrophoresis to give high-throughput genotyping (Figure 2.1).

2.6.1.2 Genotyping F941V by SSP-PCR

Using the Primer3 (v.0.4.0) software (http://frodo.wi.mit.edu/), I designed four primers to give three possible PCR amplicons as summarised in Table 2.2 and 2.3.

The DNA from 345 SLE cases was genotyped using 96-well plates including a positive heterozygous control (88:2.1) and a ddH_2O negative control on each. Amplification of 10ng of genomic DNA was carried out in a total volume of 10µl, and the reaction and thermocycler conditions are summarised in Appendix 1. Following amplification on a G-storm T4 thermocycler, 7µl of PCR product was run on a 2% agarose gel with 0.0025% (v/v) ethidium bromide and visualised with a UV-transilluminator. Genotypes were called by the presence/absence of allele-specific bands.

Figure 2.1 Schematic representations of the F941V SSP-PCR primer combinations and the resulting gel electrophoresis banding pattern

Arrows of matched colours signify paired forward and reverse primers and their resultant amplicon sizes. The final 3' nucleotides of the inner primers have allele-specificity for the polymorphism of interest (shown in bold). Lanes 1 and 2 show samples homozygous for the wild-type 'T' allele. Lanes 3 and 4 show samples heterozygous for the rare variant; both 'T' (265bp) and 'G' (151bp) alleles have been amplified. All four DNA samples contain the non-allele-specific 372bp control amplicon. Water negative control (Lane 5) and Hyper Ladder IV (Lane 6) are also shown.

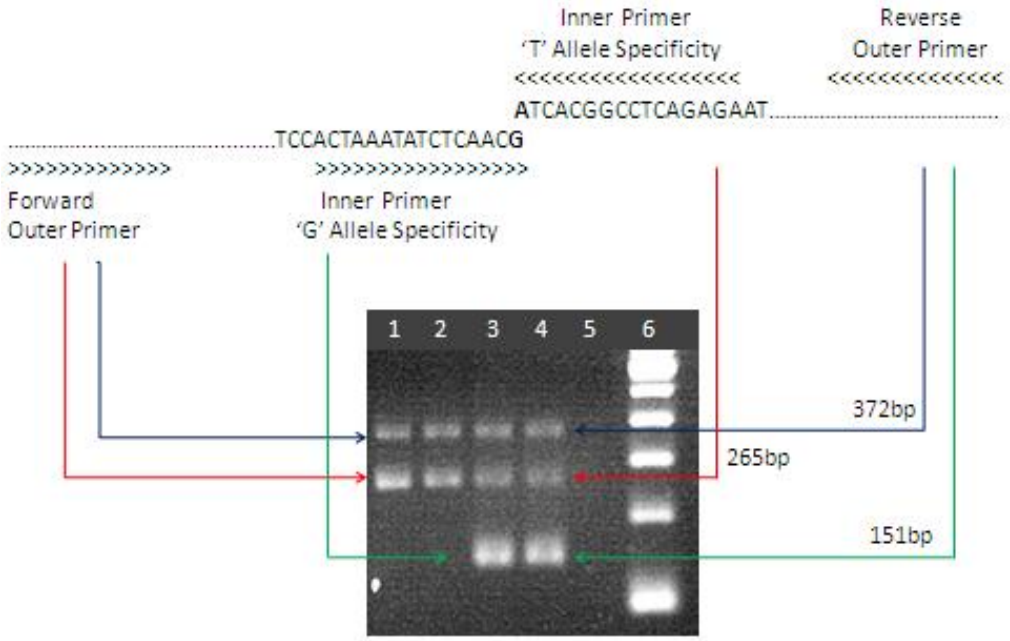

Table 2.2 SSP-PCR primer sequences and specificities

Allele-specific nucleotides at the 3' end of the inner primers are indicated in bold

Primer Name	Primer Sequence	Allele specificity	Amino Acid Specificity
Outer Forward	5' TTGTGACGTGTGTGTGAGT	-	-
Outer Reverse	5' CCATCCCTGTTTCTGCATTT	-	-
Inner Forward	5'GGGTCTCCACTAAATATCTCAAC**G**	G	Valine
Inner Reverse	5' GGTATTCTCTGAGGCCGTGA**A**	T	Phenylalanine

Table 2.3 SSP-Primer possible combinations

The three possible PCR amplicons produced by the forward and reverse primer combinations

Forward Primer	Reverse Primer	Allele-Specificity	Amplicon size (bp)
Outer Forward	Outer Reverse	-	372
Outer Forward	Inner Reverse	T	265
Inner Forward	Outer Reverse	G	151

2.6.2 Genotyping F941V and G1145S on the Illumina Custom 384 Chip

An Illumina Custom 384 Chip was designed to genotype 384 SNPs in 1,772 SLE samples of European ancestry (2.1.2) to validate the findings of the recent SLE GWAS conducted in the laboratory of Prof. Tim Vyse. Both F941V and G1145S rare variants were included on this chip in order to estimate the frequency of both novel rare variants in a large SLE cohort. This work was carried out at UPPSALA, Sweden. Heterozygous samples 88:2.1 and 50:2.2 were included in the samples as positive controls for genotype calling. I provided the surrounding sequences (150b upstream and downstream), and nucleotide changes, to Thomas Axelsson (UPPSALA, Sweden) and James Bentham (King's College London) performed the genotype calling.

2.6.3 Genotyping G1145S by capillary sequencing

The G1145S variant failed Quality Control for genotype calling for the Illumina Custom 384 Chip (2.6.2), possibly due to its proximity (3bp) to the P1146S common polymorphism. For the same reason, I was not confident that an SSP-PCR assay for G1145S would be robust. Therefore I used capillary sequencing and Big Dye technology, as described above in section 2.4, to genotype G1145S in 949 additional SLE cases. I used the same primers, PCR reaction composition, and thermocycler conditions for G1145S amplification as previously described in section 2.5.2. Samples were amplified in 96-well plates, with each plate containing a positive heterozygous control (50:2.2) and a ddH_2O negative control.

2.6.4 Rare variants in online datasets

I utilised a large-scale publicly-available sequencing project dataset to screen *ITGAM* for the confirmed rare variants in healthy controls of European ancestry. The National Heart Lung and Blood Institute's (NHLBI) Exome Variant Server (http://evs.gs.washington.edu/EVS/) documents exome sequencing of 8600 European-American chromosomes.

2.7 *In silico* analyses of F941V and G1145S

2.7.1 Comparisons of human CD11 amino acid sequences

I used the MultAlin software (Corpet, Cellulaire, Toulouse, & Tolosan, 1988; http://multalin.toulouse.inra.fr/multalin/) to compare the protein sequences of the four human CD11 molecules that pair with CD18 as part of the β2 integrin family. The four proteins CD11a, CD11b, CD11c and CD11d are encoded by *ITGAX, ITGAM, ITGAL,* and *ITGAD,* respectively.

2.7.2 Functional Prediction tools

I used two online algorithms, PolyPhen (Adzhubei et al. 2010) and SIFT (Kumar, Henikoff, and Ng 2009), to predict the functional consequences of the non-synonymous coding variants F941V and G1145S.

2.8 *In vitro* studies of function

2.8.1 Site-directed mutagenesis

10ng of a pcDNA3.1-CD11b vector (Life Technologies) was mutated to contain one of four *ITGAM* variants – F941V, G1145S, M441T, and A858V - using the PCR-based QuikChange II XL Site-Directed Mutagenesis kit (Agilent). The primer sequences and PCR reaction composition is summarised in Apppendix A, and the thermocycler conditions are summarised in Appendix B. Following the mutagenesis, 1µl *Dpn*I enzyme was added directly to the 50µl PCR reaction and incubated at 37°C for one hour to digest the parental plasmid DNA.

2.8.2 Bacterial transformation and colony selection

45µl of XL-10 Gold Ultra-competent cells were incubated with 2µl of β-mercaptoethanol and 2µl *Dpn-I* digested plasmid DNA on ice for 30 minutes followed by 30 seconds at 42°C in a water bath, and a further 2 minutes on ice. 0.5ml pre-warmed S.O.C. medium was added to the transformed XL-10 Gold Ultra-competent cells and placed in a shaking incubator for one hour at 37°C.

Agar plates containing 0.1mg/ml carbenicillin were coated with 200µl of the bacterial culture and incubated over-night at 37°C. Ten colonies per variant were then individually picked and placed into 5ml LB Broth (plus 0.1mg/ml carbenicilin) in 50ml falcon tubes, and inoculated at 37°C in a shaking incubator over-night.

2.8.3 Mutation screening

A Qiagen mini-prep kit, as per the manufacturer's instructions, was used to isolate a small amount of DNA from the over-night inoculations. I used capillary sequencing, as described in section 2.4.2 above, to sequence the plasmids in forward orientation for mutation screening. Table 2.4 lists the primers used. These primers were designed using the *ITGAM* cDNA sequence and Primer3 (v.0.4.0) software (http://frodo.wi.mit.edu/) and purchased from Sigma Aldrich. Glycerol stocks were also made for each of the cultures and stored at -80°C. Once the mutagenesis was confirmed to be successful, the corresponding glycerol stocks were thawed slightly and plated by dilution method on agar plates (plus carbenecillin) and incubated at 37°C overnight to produce single colonies. A single colony was picked and inoculated in 100ml LB Broth for 12-16 hours at 37°C for use with a Maxi-prep kit (Qiagen), as per the manufacturer's instructions.

Table 2.4 Primers used for mutation screening by capillary sequencing

Variant	Forward Primer (5'-3')
F941V	GCCGGTGAAATATGCTGTCT
G1145S	AGACGGAGACCAAAGTGGAG
M441T	GGGCTGGTGGAGTCTTTCTA
A858V	GGGAGTTCAACGTGACAGTG

2.8.4 Maintenance of COS-7 cells

The simian fibroblast cell line, COS-7 (ATCC), were maintained in Dulbecco's Modified Eagle Medium (DMEM; Life Technologies), supplemented with 10% foetal bovine serum (FBS) and 1% Penicilin/Streptomycin, in a cell culture incubator at 37°C and 5% CO_2. These adherent cells were typically grown in T75 flasks (Nunco) in a total volume of 10ml. Media were removed from flasks with an aspirator and the cells were washed twice with 10ml phosphate buffered solution (PBS) to remove any residual serum. 1ml of trypsin solution (Sigma) was then added to the cell layer and incubated for ~3 minutes at 37°C to loosen the cells from the flask.

2.8.5 Transient Transfections

Following trypsinisation, I estimated the number of COS-7 with Trypan Blue and a Countess™ (Invitrogen) automated cell counter and then pelleted $1x10^6$ cells at 300g for 10 minutes per transfection. The cells were resuspended in 100µl Nucleofector Solution R (Lonza). To co-transfect the cells, I added 1.25µg of one of five pcDNA3.1-CD11b vectors (WT, M441T, A858V, F841V or G1145S) together with 1.25 µg pcDNA3.1-CD18 and used COS-7 (ATCC) programme on a Nucleofector II (Lonza) machine. In duplicate, 40×10^4 cells were added to an acid-cleaned coverslip in a 24-well plate. The remaining transfected cells were cultured overnight in a T25 flask for expression screening by flow cytometry.

2.8.6 Measuring CR3 expression on transfected COS-7 cells

One day after transfection, cell-surface expression of CR3 was measured using a PE-conjugated anti-CD11b (clone ICRF44; eBioscience). Transfected cells were stained in the dark for 30mins on ice and

processed on a BD FACS Canto II flow cytometer. Live COS-7 cells were identified by plotting FSC-area against SSC-area using FACS DIVA software (BD Bioscience). 10,000 events were collected within this gate.

I used FlowJo software v.7.6.4 to estimate the percentage of CR3 positive cells and the mean fluorescence intensity (MFI) of the positive population. I compared expression levels of CR3 in the WT, M441T, A858V, F941V and G1145S transfected cells by using the MFI values and a paired two-tailed t-test on Prism5 software (GraphPad).

2.8.7 Phagocytic Assay

This was carried out on the same day as the flow cytometry expression analysis. 5µl (=2.5x10^6) sheep red blood cells (sRBCs) in Alsevier (TCS Biosciences) were incubated with 10µl goat anti-sheep IgG (Sigma) in 500µl Gelatin veronal buffer (GVB; Sigma) and rotated on a daisy wheel at room temperature for one hour. Following this, the IgG opsonized red cells were pelleted 4000rpm for one minute and resuspended in 90µl GVB plus 10µl C5-depleted human serum (Sigma), and incubated at 37°C for 20 minutes in a water bath. The iC3b-opsonized sRBC ($sRBC_{iC3b}$) were pelleted at 4000rpm for one minute and resuspended in 500µl serum-free DMEM. I then further diluted the $sRBC_{iC3b}$ 1:50 in serum-free DMEM, to obtain a final concentration of 1x10^5cells/ml.

Transfected COS-7 cells were incubated with 500µl (=50,000 cells) of the $sRBC_{iC3b}$ mixture for 30 minutes at 37°C, 5% CO_2 in a tissue culture incubator. In order to stop phagocytosis, the 24-well plate was placed on ice before the $sRBC_{iC3b}$–containing DMEM was removed. Externally bound $sRBC_{iC3b}$ were stained with 200µl of a 1:300 dilution in 5% Bovine Serum Albumin (BSA)/PBS of an Alexa-488 conjugated mouse anti-goat IgG antibody (Invitrogen) in the dark and on ice for 8 minutes. Following this, the cells were fixed with 200µl 4% paraformaldehyde (PFA; VWR) for 10 minutes at room temperature and then permeabilised with 200µl of 0.2% Triton-X (Sigma) for 3 minutes. The cells were washed twice with 0.5ml 0.5% BSA/PBS before the internal and external $sRBC_{iC3b}$ were stained with 200µl of a 1:300 dilution (in 5% BSA/PBS) of an Alexa-555 conjugated mouse anti-goat IgG antibody (Invitrogen), and the COS-7 nuclei were stained with 0.5µl DAPI, protected from light at room temperature for 40 minutes. The cells were washed with 0.5% BSA/PBS, followed by PBS, and finally 1ml ddH_2O, before being removed from the 24-well plate with

fine-pointed curved forceps and mounted individually onto 4µl Mowiol (Calbiochem) on microscope coverslips (VWR). They were left to dry overnight, protected from the light.

2.8.8 Fluorescent Microscopy

I used a Zeiss Axiophot fluorescent microscope, with x20 lens, and attached camera to photograph the coverslips for further analysis. A UV-light, green fluorescent, and blue fluorescent filter was used to excite the DAPI-stained nuclei, the Alexa-555 labeled $sRBC_{iC3b}$ (external and internal of the COS-7 cells), and Alexa-488 labeled $sRBC_{iC3b}$ (external), respectively, and three JPEG images were created for each COS-7 cell to be analysed.

2.8.9 Analysis

I visually analysed the photographs using Microsoft Picture Viewer. For each COS-7 cell, I counted the Alexa-555 labeled $sRBC_{iC3b}$, which represent all associated $sRBC_{iC3b}$ (internal and external), and calculated the Association Index (AI) using the following equation:

$$\text{Association Index} = \frac{\text{mean number of engaged } sRBC_{iC3b}}{100 \text{ COS-7 cells}}$$

Because the Alexa-488 is used to stain $sRBC_{iC3b}$ before COS-7 cell permeabalisation, only $sRBC_{iC3b}$ engaged with CR3 on the outside of the COS-7 cell are labeled. Therefore, in this assay, a phagocytic event is represented by a $sRBC_{iC3b}$ which is labelled with Alexa-555 but has no equivalent Alexa-488 stain. By counting the number of $sRBC_{iC3b}$ stained only by Alexa-555, I calculated the Phagocytic Index (PI) and Percentage Phagocytosis (PP) using the following equations:

$$\text{Phagocytic Index} = \frac{\text{mean number of phagocytosed } sRBC_{iC3b}}{100 \text{ COS-7 cells}}$$

$$\text{Percentage Phagocytosis} = \frac{\text{mean percentage phagocytosis}}{\text{COS-7 cell}}$$

I used two-tailed paired t-tests to compare the AI, PI and PP between CD11b-WT and each of the four variants on Prism5 software (GraphPad).

2.9 Effects of LA1 on NK cell viability and signalling

2.9.1 Peripheral Blood Mononuclear Cell (PBMC) Isolation

Peripheral blood mononuclear cells (PBMCs) were isolated from 50ml of whole blood from healthy volunteers (2.1.1), plus 100µl heparin, by density gradient separation. Whole blood diluted 1:3 with phosphate balanced solution (Invitrogen) was layered onto 15ml of Histopaque (Sigma) in 50ml falcon tubes (Becton Dickson) and centrifuged for 20 minutes at 800g with no brake. The PBMC rings were removed and washed twice – once with PBS and once with 1%BSA/PBS - to remove any contaminating platelets. The number of live cells was calculated using Trypan Blue and a Countess™ (Invitrogen) automated cell counter.

2.9.2 Isolation of NK Cells

I used a MACS NK cell negative isolation kit (Miltenyi Biotech) to separate untouched NK cells from other mononuclear cells. This is achieved by firstly incubating the PBMCs with a Biotin-Antibody Cocktail for 5 minutes at 4°C to label the T cells, B cells, dendritic cells, and monocytes, followed by 10 minute incubation at 4°C with a MicroBead Cocktail. The sample is then passed through a magnetic LS MACS column attached to a MACS separator (Miltenyi Biotech), as per the manufacturer's instructions, to deplete the sample of the labelled cell types. Once again, the number of NK cells was determined using Trypan Blue and a Countess™ (Invitrogen).

2.9.3 Estimation of cell population purity by flow cytometry

2 x 10^5 cells were stained for 45 minutes on ice with the following mouse anti-human monoclonal antibodies (eBioscience): anti-CD56 (APC), anti-CD16 (FITC), anti-CD14 (PerCP-Cy5.5), anti-CD3 (Pacific Blue), and anti-CD19 (PE). An unstained sample was also included. Samples were washed with 1ml PBS and resuspended in 250µl PBS before processing on a BD Canto II Flow cytometer. Forward-scatter and side-scatter area were used to plot live cells by size and granularity, respectively. 10,000 events were counted by BD FACS DIVA software and analysed by FlowJo (v.7.6.4).

2.9.4 Compensation

I used compensation beads (BD Biosciences) to compensate for spectral overflows during the flow cytometry. These were prepared as per the manufacturer's instructions, with 1µl of an antibody – for each fluorochrome to be used - being incubated with one drop of both positive and negative compensation beads at room temperature for 10 minutes in 100µ 1%BSA/PBS. These compensation controls were processed first and the compensation between fluorochromes was automatically calculated by the BD FACS DIVA software before experimental samples were processed.

2.9.5 Cell Viability Assay

I used the CellTiter-Glo® Luminescent Cell Viability Assay (Promega) to measure whether the Leukadherin-1 (dissolved in DMSO; LA1) drug had a detrimental effect on NK cell survival, compared with the DMSO control. Isolated NK cells were resuspended in Lymphocyte Growth Medium (LGM) at a concentration of 0.5 $x10^6$ cells/ml. The cells were split into two aliquots in a 12-well cell culture plate, and incubated with either 1:2000 (v/v) DMSO (Sigma) or LA1 (15mM; Merck Millipore) for 30 minutes at 37°C. These samples were then further split into 100µl (=50,000 cells) aliquots in a 96-well plate and incubated overnight at 37°C with one of three conditions:

- no further stimulus
- 1µl of IL-12 (10µg/ml) and 1µl of IL-15 (30µg/ml)
- 1µl of IL-12 (10µg/ml) and 1µl of IL-18 (10µg/ml).

Each condition was run in quadruplicate. At 24 hours, the 96-well plate was removed from the incubator and equilibrated to room temperature before adding 50µl of the CellTiter-Glo® Reagent to the medium containing cells. Cell lysis was induced with an orbital shaker for three minutes, and an Orion II luminometer (Berthold) was used to read the luminescence of the samples with a one second measurement time. A two-tailed unpaired t-test was used to compare the luminescence levels using Prism5 software (GraphPad).

2.9.6 Monokine activation of NK cells

NK cells were plated at a concentration of 1 x 10^6/ml in Lymphocyte Growth Medium (LGM) in 12-well plates and incubated for 30 minutes with 0.5µl/ml of either LA1 (15mM) or DMSO (vector control). Following this, 2 x 10^5 cells (=200µl) were plated in wells of a 96-well plate for cytokine stimulation. Combinations of either IL-12 (10µg/ml) and IL-15 (30µg/ml), or IL-12 and IL-18 (10µg/ml) were used, with 2µl of each (=1:100 v/v) added to the cell suspension. Two samples (one with DMSO and the other with LA1 pre-treatment) had no cytokines added and were used as non-activated controls (see 2.10.3 and 2.10.4.2). Cells were incubated at 37°C for various time points (see Chapter 5). Cells were fixed with 200µl 4% PFA for 10 minutes at room temperature and then washed with 2ml 1% BSA/PBS and spun at 800g for 5 minutes; this was repeated three times.

2.9.7 Cell surface and intracellular staining

In order to differentiate between the NK cell subsets, the fixed cells were resuspended in 100µl 1% BSA/PBS and stained with 1µl of a Pacific Blue conjugated anti-CD56 monoclonal antibody (Biolegend) for 45 minutes, protected from light, at room temperature. Following this, cells were permeablised with ice-cold methanol-based PermBuffer III (BD Biosciences) on ice for 30 minutes. To remove any residual methanol, cells were washed with 2ml 1% BSA/PBS, and centrifuged at 800g for 5 minutes; this was repeated three times. The NK cells were resuspended in 100µl 1%BSA/PBS and stained with 5µl of PhosFlow antibodies (BD Biosciences) – specific for phosphorylated intracellular signalling molecules (Table 2.5) - for one hour, protected from light, at room temperature. No isotype controls were used in this experimental design; instead, the non-activated cells (see 2.10.2) stained with the anti-phospho antibodies (Table 2.5) were used as negative controls for the levels of aspecific antibody binding (Hulspas et al. 2009).

Table 2.5 Summary of monoclonal antibodies used in the PhosFlow assays to measure NK cell signalling.

Antibody	Epitope	Mouse Isotype
Alexa488 anti-pSTAT3	pY705	IgG2, k
Alexa647 anti-pSTAT4	pY693	IgG2b, k
Alexa647 anti-pSTAT5	STAT5A pY694 and STAT5B pY699*	IgG1, k
Alexa488 anti p-p38	pT180/pY182	IgG1, k

*see Table 5.1

2.9.8 Flow Cytometry and Analysis

Samples were processed on a BDCanto II Flow cytometer with FACS DIVA software (BD Bioscience). The population of live NK cells were identified and gated by size and granularity using the forward- and side-scatter area voltages. A total of 30,000 events were recorded within this gate. I later used FlowJo (v.7.6.4) for the quantitative analysis. Firstly, by plotting forward-scatter area against forward-scatter width, I was able to isolate singlet cells and discount events that appeared to be doublet cells (Figure 2.2B). I used a side-scatter area/Pacific Blue scatter plot to identify the $CD56^{brught}$ population (Figure 2.2C). I recorded the median fluorescence of each of the fluorochromes used for both total NK cells and the $CD56^{brught}$ population. The fold-change was calculated with the following equation, where MFI is the median fluorescence intensity.

$$\text{Fold-change} = \frac{\text{MFI at time point}}{\text{MFI at T=0}}$$

I used GraphPad (Prism) to test the difference in median fold-change, using a Willcoxon's matched paired test, between LA1 and DMSO pre-treated cells at T=10 and T=2 hours.

Figure 2.2 Identification of NK cell subsets by flow cytometry

Isolated NK cells as viewed using FlowJo following analysis on a BD CANTO II. A) The NK cell population is clustered using forward- and side-scatter area plot. B) Singlet NK cells are isolated by plotting forward-scatter area against forward-sctater width. Recorded events with a large width:area ratio are likey to be doublet cells and are therefore excluded. C) NK cells can be further separated into two subsets based on their CD56 expression. A Pacific Blue-conjugated anti-CD56 antibody was used for the extracellular staining. I created two gates for subsequent analysis: total NK and CD56^{bright} cells.

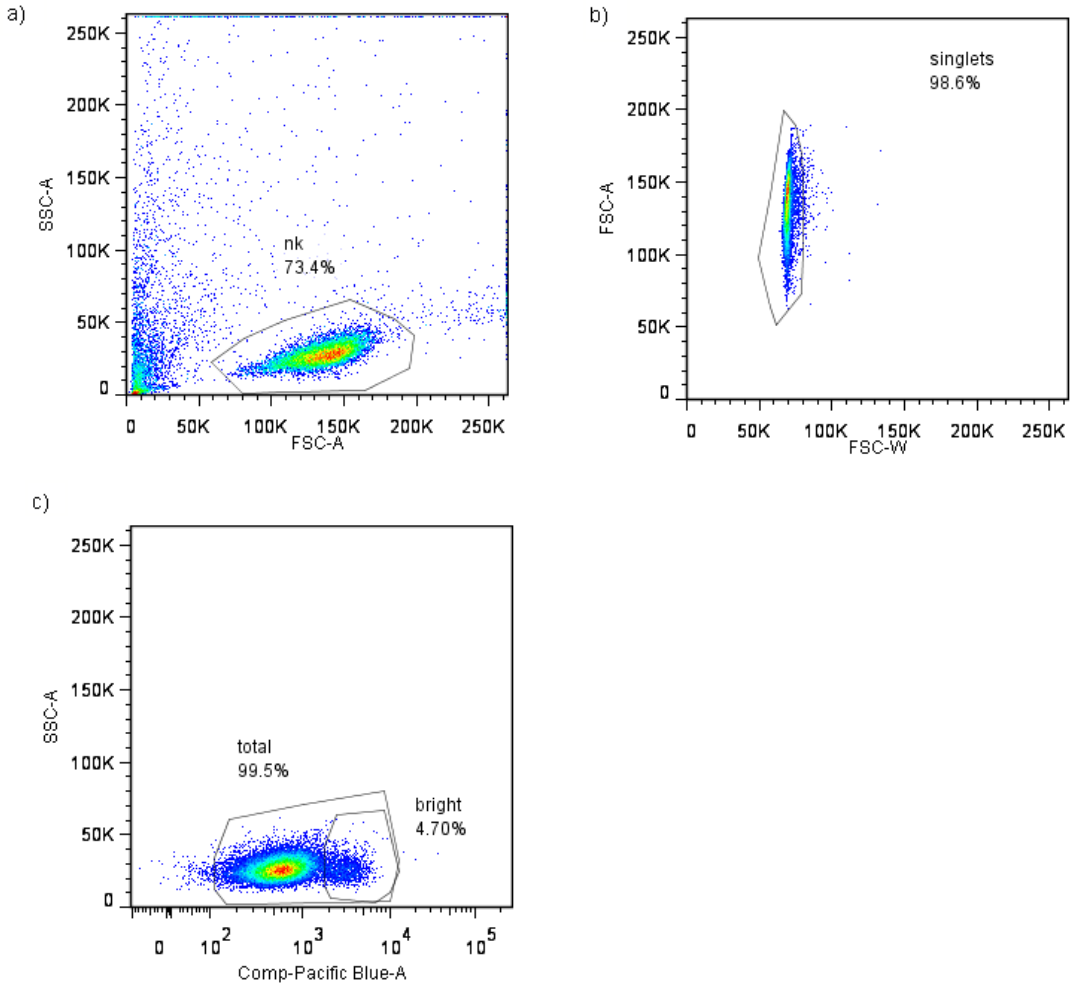

2.10 *FCGR2B*-I232T genotyping

Due the high degree of genomic identity between *FCGR2B* and *FCGR2C*, it was necessary for the reverse primer to be situated in intron 6, in order to ensure *FCGR2B* specificity. The PCR product was therefore 3Kb in length. I amplified 20ng of DNA using the SequalPrep™ Long-range PCR kit (Invitrogen) with 1unit of Hot Star *Taq* and 5pmoles of forward and reverse primers, as specified in Appendix A, in a total volume of 10µl. I used a nested forward primer (5'-CTGCAGAAGTGAGTGACTCA -3') for the sequencing reaction, which is located 170bp upstream of the I232T variant (Chr1:161643798; hg19) and allowed reliable genotyping. Aside from this difference, the sequencing was carried out as stated in section 2.4.

2.11 Paralogue Ratio Test (PRT)

2.11.1 Theory

This PCR-based technique relies upon small sequences of genetic homology between a region of the copy number variability (region of interest) and an independent non-copy number variable region of the genome (Armour et al. 2007). PCR primers are designed to give two products of slightly different sizes – one from the variable region and one from the independent control region – and are labelled on the 5' end with a fluorescence dye. This design allows the PCR products to be size-separated by electrophoresis on an Applied Biosystems genetic analyzer, and visualised by Genemapper software (Applied Biosystems). The areas under the two peaks –which are relative to the amount of PCR product obtained - are compared within each sample to estimate the copy number of the variable region of interest. This technique has been applied to multiple genomic loci to measure CNV (Machado et al. 2013; X.-J. Zhou et al. 2012; Fernando et al. 2010).

2.11.2 FCGR3B CNV

Due to the high degree of sequence identity between *FCGR3A* and *FCGR3B* (see Introduction), the PRT primer pair amplify products of the same size (67bp) from both *FCGR3A* and *FCGR3B*; therefore the ratio between the variable (chromosome 1) and control (chromosome 18) region is representative of the total *FCGR3* copy number. A second PCR-based assay is needed, called the Restriction Enzyme Digest Variable Region (REDVR), in order to differentiate between the two copy number variable *FCGR3* genes.

The PCR primers, the reverse of which is labelled with a VIC fluorescent tag (Appendix A6.2), amplify 182bp regions of both *FCGR3A* and *FCGR3B*, containing a sequence variation between the two genes. The *FCGR3A* fragment contains a *Taqα*1 restriction enzyme cut site, giving products of 134bp (and 48bp), whereas *FCGR3B* does not. This enables differentiation between the two genes, and the absence of the larger, uncut product indicates the complete absence of *FCGR3B* (Figure 2.3). Thus the combination of the ratio between *FCGR3*: control (PRT), together with the *FCGR3A:FCGR3B* (REDVR) ratio enables accurate copy number calling of both *FCGR3* genes (Hollox, Detering, and Dehnugara 2013).

2.11.3 Measuring FCGR3A and FCGR3B copy number

10ng of DNA was amplified with 0.5µM forward and reverse (FAM or HEX labelled) primers and 0.5units of *Taq* polymerase (Qiagen), in a total volume of 10µl, as specified in Appendix A. The assay was run in duplicate on 96-well plates, one with a reverse primer fluorescently labelled with FAM and the other with HEX. This differential fluorescent labelling of the PCR primers enabled the pooling of the PRT products, and for mean values to be used in further analysis. 1µl of each FAM and HEX labelled PRT PCR product, plus 0.15µl 400HD ROX™ size standard, was added to 10µl of formamide (Sigma) and denatured at 95°C for 3 minutes. The PRT assay yields products of 67 and 72bp from chromosome 1 and chromosome 18, respectively. Peak area ratios were used to estimate a total CN for *FCGR3A* plus *FCGR3B* against the non-CNV region on chromosome 18.

10ng of DNA was amplified with 0.5µM of each of the primer and 0.5U of *Taq* polymerase (Qiagen), in a total volume of 10µl (Appendix A). 2µl of the PCR product was digested with 2.5U *Taqα*1, in a total volume of 10µl, for 4 hours at 65°C. 1.4µl of the *Taqα1*-digested REDVR product, plus 0.15µl 400HD ROX™ size standard, was added to 10µl of formamide and denatured at 95°C for 3 minutes.

2.11.4 Genemapper Analysis

Each 96-well plate contained seven positive controls of varying copy numbers, and a water negative control. Plates were repeated if the positive controls gave unexpected results. Samples were analysed by electrophoresis on an Applied Biosystems genetic analyser and Genemapper (Applied Biosystems) software was used to visually analyse the results (Figure 2.3).

The VIC-labelled REDVR products gave peak areas at 134 (digested – *FCGR3A*) and 182 bp (undigested – *FCGR3B*) and were used to generate *FCGR3A:FCGR3B* ratios. *FCGR3A* CN was not used in further analysis.

2.12 Statistical Analyses

FCGR2B-I232T genotype and allele frequencies were compared between cases and controls by Chi-squared tests or Fisher's exact tests, where appropriate, using GraphPad Prism 5. An interaction between *FCGR2B*-I232T and *FCGR3B*-CNV was tested for by fitting an additive logistic regression model (SLE status as the outcome) using the statistical computing language R. David Morris (King's College London) ran the analysis in R.

Figure 2.3 Measuring *FCGR3B* copy number using the PRT assay

Images are representative of data as visualised using Genemapper software**.** A) FAM-labelled PRT products from *FCGR3* (67bp; left histogram) and non-copy number variable (CN in diploid genome=2) reference locus on chromosome 18 (72bp; right histogram). The ratio of the areas under the histograms are used to calculate the number of *FCGR3* copies, per genome, compared with the non-copy number variable region (CN=2). B) VIC-labelled REDVR products following *Taqα1* digestion. Digested *FCGR3A* products (134bp; left histogram) and undigested *FCGR3B* (182bp; right histogram) products are seen. The ratio of the areas under the histograms are used to calculate the copy number of *FCGR3A* and *FCGR3B* per genome.

A)

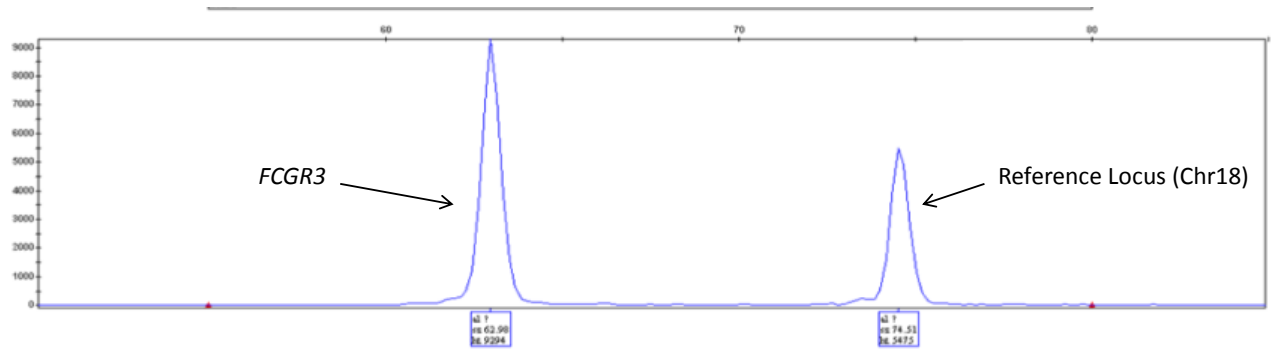

B)

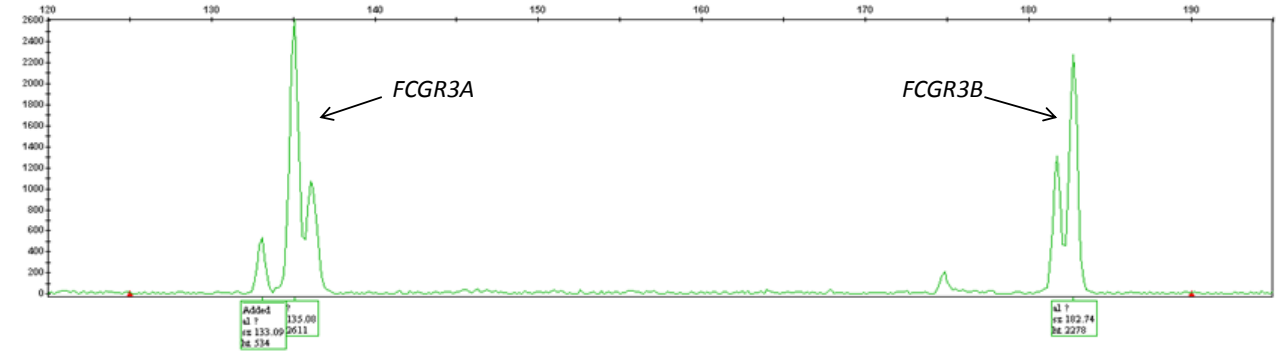

Chapter 3: Cell surface expression of CR3 on *ex vivo* monocytes and neutrophils

3.1 Introduction

Altered protein expression has been shown to be the underlying mechanism through which disease-associated variations manifest their effect, the extreme examples of which being gene-dosage effects of copy number variable loci resulting in altered mRNA and protein levels (Groth et al. 2010; Willcocks et al. 2008). Additionally, showing that a polymorphism does not affect protein expression is invaluable in further establishing the functional effects of a non-synonymous variation, allowing a comprehensive interpretation of functional assays.

The cell surface expression of CR3 requires the non-covalent binding of CD11b and CD18. It is therefore possible that a missense variant within CD11b - such as the SLE-associated R77H - could affect the coupling of these two polypeptides resulting in reduced expression. Protein-coding mutations in CD18, which cause Leukocyte Adhesion Deficiency (LAD) diseases, have been shown to affect the ability of CD18 to pair with CD11 polypeptides (Shaw et al. 2001). Therefore, by measuring the cell surface expression of CR3 between genotypic groups, the R77H effects on the CD11b-CD18 polypeptide partnership can be interpreted.

In addition, by investigating CR3 expression dependent on R77H genotype, it is possible to determine whether or not the 77H variant (rs1143679) is in tight LD with a variant in the regulatory region of *ITGAM* which may affect gene expression. For instance, if the 77H variant was found on a haplotype that reduced *ITGAM* gene expression resulting in lower cell-surface expression of CR3, this could lead to the overestimation of the magnitude of detected functional effects directly attributed to the missense polymorphism. Likewise, elevated cell-surface expression could result in an underestimation of any detectable functional impairment. It is therefore essential to delineate potential effects of expression alterations before interpreting functional assays with confidence.

As discussed in section 1.4.2, CR3 undergoes conformational changes in response to allosteric activation (Hynes 2002). The same conformational changes occur under both mechanisms, with the

extension and straightening of the extracellular domain, and separation of the CD11b and CD18 cytoplasmic tails; ultimately these conformational changes enable high-affinity ligand-binding (Luo, Carman, and Springer 2007). It is plausible that a missense variant could alter the 3D structure of a protein such that conformational changes are impaired. Therefore, in addition to absolute protein levels, it is possible that a histidine residue at position 77 of CD11b could affect the folding or extension of the CR3 protein. Upon receptor activation, an antibody (CBRM1/5) epitope is revealed within the I-domain of the CD11b polypeptide, allowing the relative levels of activation to be estimated by flow cytometry (Diamond and Springer 1993).

As detailed in the section 1.4.4, the optimal expression, under both steady state and inflammation, and conformational changes of CR3 on neutrophils and monocytes enables a fine-balance of inflammatory responses. Indeed there is evidence to suggest that CR3 expression and activation determines the capabilities of neutrophils to phagocytose certain microbes, such as *B. pertussis* (Mobberley-schuman and Weiss 2005). Through use of two anti-CD11b monoclonal antibodies - one without conformation specificity (clone ICRF44) and another specific with specificity for the active conformation (clone CBRM1/5) - I measured the effects of the R77H polymorphism on both the cell surface expression and activation of CR3, respectively, under resting and activated conditions, by flow cytometry.

3.2 Results

3.2.1 Identification of neutrophils and monocytes by flow cytometry

I used fresh, leukocyte-enriched, heparinized whole blood from healthy donors (n=20) of Northern European ancestry from the Twins UK NIHR Bioresource (Methods 2.1.1). Individuals were chosen for their homozygosity at rs1143679, and were processed as pairs of opposing genotypes - homozygous WT (R77) and homozygous 77H.

Neutrophils are large, granular cells, which enables easy identification by flow cytometry, without the use cell surface markers specific antibodies. By plotting light forward-scatter (FSC) and side-scatter (SSC), which separate cells by size and granularity, respectively, the large neutrophil population forms a separate cluster respective to other leukocytes (Figure 3.1A).

The unique cell-surface expression of CD14 allows monocytes to be distinguished from other leukocytes of the same size during a whole blood FACS by staining the sample with a fluorescently labelled (in this instance PerCP-Cy5.5) anti-CD14 antibody, (Figure 3.1B). I did not distinguish the monocytes according to their CD14/CD16 subsets, but instead analysed them as a whole population. It has been shown that CD11b is expressed on all monocyte subsets (Geissmann, Jung, and Littman 2003).

Figure 3.1 Identification of neutrophil and monocyte populations by flow cytometry

A) Forward- (x-axis) and side-scatter (y-axis) was used to separate the neutrophil population within a leukocyte-enriched whole blood sample, prior to CR3 expression analysis, as indicated by the polygon gate. B) A PerCP-Cy5.5 conjugated anti-CD14 antibody was used to stain a leukocyte-enriched whole blood sample. By plotting side-scatter (y-axis) against PerCP-Cy5.5 (x-axis) the $CD14^{+}$ monocyte population can be distinguished from other leukocytes of the same size prior to CR3 expression analysis, as indicated by the circular gate.

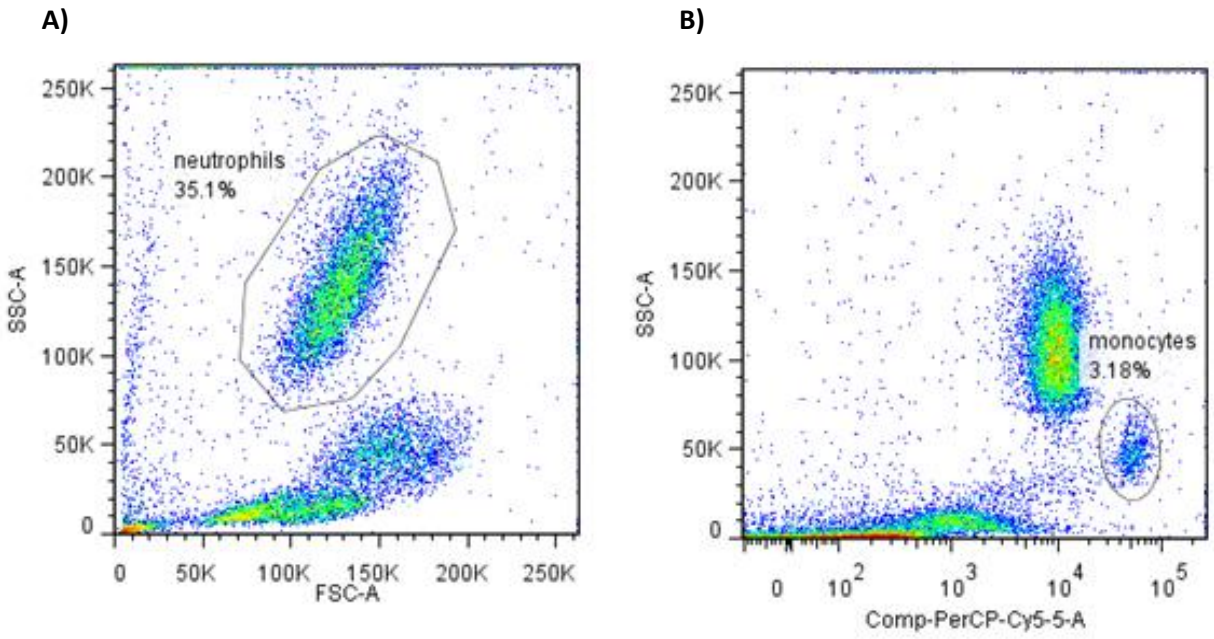

3.2.2 Cell surface expression of CD11b on resting ex vivo monocytes and neutrophils

I measured absolute cell surface expression (Figure 3.2) and percentage of CD11b in its active conformation (Figure 3.3) on resting monocytes and neutrophils. Using a paired t-test, there was no significant difference in the expression of CD11b on resting monocytes (P=0.25) and neutrophils (P=0.33; Figure 3.2), nor was there a significant difference in the percentage of CD11b in its active conformation on resting monocytes (P=0.16) and resting neutrophils (P=0.86; Figure 3.3), between the homozygous genotype groups. I observed low levels of CBRM1/5 positive cells under resting conditions, indicating that the experimental protocol was conducted under sterile conditions that did not significantly activate the leukocytes.

3.2.3 Cell surface expression of CD11b on PMA-stimulated ex vivo monocytes and neutrophils

Phorbol myristate acetate (PMA) is known to upregulate CR3 expression and is commonly used to study its activation (Wright and Meyer 1986; Ma, Plow, and Geng 2004). I measured absolute cell surface expression (Figure 3.2) and percentage of CD11b in its active conformation (Figure 3.3) following PMA-stimulation for 10 minutes at 37°C (Methods 2.2). I observed a ~10-fold increase in CD11b cell surface expression on both monocytes and neutrophils, compared with resting cells, irrespective of genotype (Figure 3.2). Once more, using a paired t-test, no significant differences between genotype groups were observed for CD11b expression on stimulated monocytes (P=0.97) and neutrophils (P=0.42; Figure 3.2), nor were there significant differences in the percentage of activated CD11b on stimulated monocytes (P=0.70) and neutrophils (P=0.47; Figure 3.3).

3.2.4 Increased CD11b expression in one individual under resting conditions

There is one individual - from the 77H genotype group - who repeatedly showed higher expression of CD11b on both resting neutrophils and monocytes, as seen in Figure 3.2. I attempted to identify a variation in the promoter region of the *ITGAM* gene by sequencing ~500bp upstream of the start codon (Methods 2.3). The reverse primer was located in exon 1 of *ITGAM* to ensure good sequencing coverage upstream of the coding region of the gene. I additionally amplified and sequenced the genomic DNA from another healthy control who had not shown elevated expression levels of CD11b on monocytes or neutrophils. However, I did not observe any notable variation in this regulatory region.

Figure 3.2 Cell surface expression of CD11b on neutrophils and monocytes under resting and activated conditions

Leukocyte-enriched whole blood from healthy volunteers (n=20) of either R77 (WT) or 77H homozygous genotypes was incubated with PE-conjugated anti-CD11b (clone ICRF44) and Per-CyP-conjugated anti-CD14 antibodies and analysed by flow cytometry. No significant difference in cell surface expression of CD11b was seen between genotypic groups for either neutrophils (left panel) or monocytes (right panel), under resting (upper panel) or PMA-stimulated (lower panel) conditions, as measured by MFI and compared using a paired two-tailed t-test.

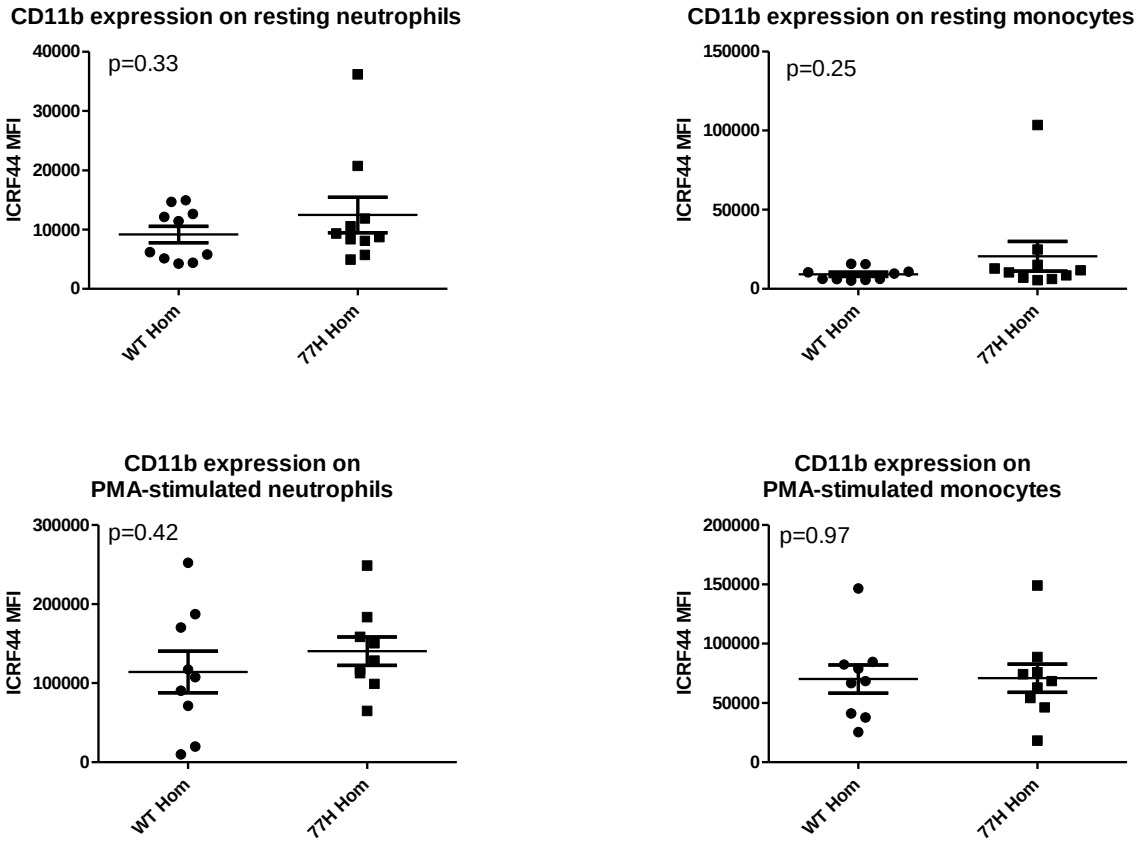

Figure 3.3 Percentage of CD11b present in active conformation on neutrophils and monocytes under resting and activated conditions

Leukocyte-enriched whole blood from healthy volunteers (n=20) of either R77 (WT) or 77H homozygous genotypes was incubated with APC-conjugated activation specific anti-CD11b (clone ICBRM1/5) and Per-CyP-conjugated anti-CD14 antibodies and analysed by flow cytometry. No significant difference in percentage of activated CD11b was seen between genotypic groups for neutrophils (left panel) or monocytes (right panel), under resting (upper panel) or PMA-stimulated (lower panel) conditions, as measured by MFI and compared using a paired two-tailed t-test.

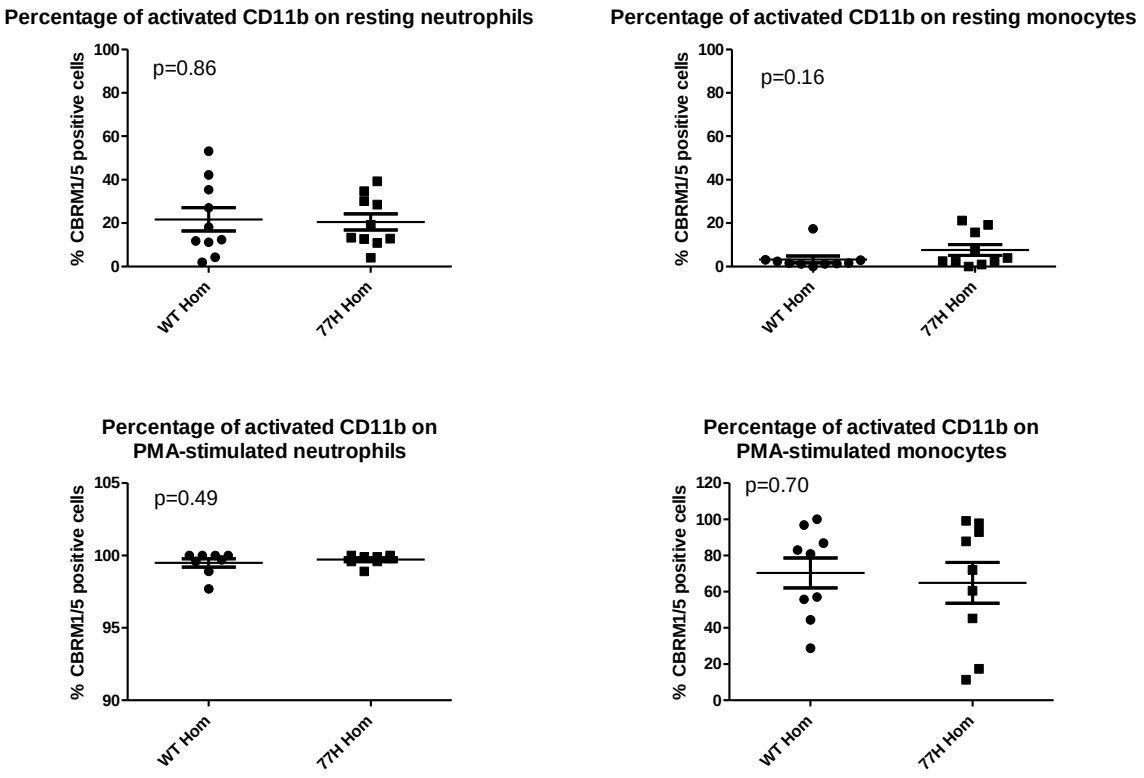

3.3 Discussion

As discussed in section 1.4.2, leukocytes yet to undergo activating stimuli have low densities of cell surface receptors that are involved in inflammatory processes, such as CR3 (Ley 2002). Large intracellular pools of such receptors are stored in secretory vesicles and are available for immediate up-regulation of cell surface expression following appropriate activating signals. Sufficient regulation of this function is of paramount importance to the host organism to avoid leukocyte hypersensitivity and subsequent tissue damage.

My data provide strong evidence that the R77H missense variant does not affect CR3 expression on the cell surface of resting *ex vivo* monocytes and neutrophils (Figure 3.2, Figure 3.3), suggesting that the SLE-associated polymorphism neither affects the absolute levels of translated CD11b polypeptide, nor the heterodimer formation between CD11b and CD18. Furthermore, R77H did not affect the up-regulated cell surface expression of CR3 on either cell type following PMA stimulation (Figure 3.2).In this study, an antibody specific for an I-domain epitope, which is revealed only when CR3 adopts its active conformation state (clone CBRM1/5) (Diamond and Springer 1993), was utilised to measure the effects of the R77H polymorphism on the allosteric activation of CR3 (Hynes 2002). The R77H variant is located in the β-propeller domain of CD11b, which is not thought to be a direct binding site for any of the CR3 ligands. However, as this transmembrane protein carries cell signals and, in doing so, alters its conformation, the R77H variation could affect the protein's cell signalling leading to impaired function. I observed no significant difference between the two homozygous genotype groups, suggesting that the R77H polymorphism does not affect the ability of the CR3 receptor to extend into the fully active conformation on monocytes and neutrophils (Figure 3.3); a necessary change needed for high-affinity ligand-binding.

My work alone does not shed-light on whether or not *ITGAM* gene regulation is altered by the haplotype on which 77H is found in individuals of Northern European ancestry. However, a colleague, Dr Barbara Fürnrohr, used a quantitative PCR (qPCR) method to compare the relative mRNA levels in *ex vivo* PBMCs and monocytes from WT homozygous (n=14) and R77H heterozygous (n=9) healthy controls. No significant difference was observed between genotype groups (Rhodes et al. 2012). Together these data provide strong evidence that there is no expression difference, on an RNA or protein level, associated with the R77H polymorphism.

Since this work was carried out, two additional studies have reported no genotypic difference in the cell surface expression, or activation, of CR3 on *ex vivo* monocytes, macrophages, neutrophils, and dendritic cells of healthy volunteers (Y. Zhou et al. 2013; Fossati-Jimack et al. 2013). Additionally, *in vitro* studies report no difference in expression levels between WT and 77H transfected cells, indicating that the CD11b/CD18 pairing is not affected by this non-synonymous variation (MacPherson et al. 2011).

The use of healthy subjects, as opposed to individuals with disease, is beneficial in studying the effects of genetic variants on *ex vivo* cells as potential confounding factors are reduced (such as drug treatment). Most recently however, a study reported a R77H-dependent reduction of CR3 cell surface expression on, and CD11b mRNA levels in, *ex vivo* monocytes of SLE patients (Maiti et al. 2014). There are, I believe, potential issues with the methodologies applied in this study. The majority of the samples were SLE patients (n=53), and a negative correlation is seen with CR3 cell surface expression and rs1143679 minor allele count (cell surface expression is highest for homozygous WT (GG) and lowest for homozygous risk (AA)). Three samples from heterozygous healthy individuals were also included in the analysis, and the authors conclude that this is sufficient to discount the possibility of confounding factors such as drug use (Maiti et al. 2014). Additionally, CD14 positive selection was applied to isolate monocyte before allelic imbalance assays were performed. CD14 is a co-receptor for TLR ligation, therefore the monocytes could be activated during isolation (Noubir, Hmama, and Reiner 2004). As discussed in section 1.4.4, there is evidence that CR3 interact with the CD14 on the cell surface of monocytes, which adds further complexity to the interpretation of their results (Hawley et al. 2011). In addition, some of the electropherograms used to calculate relative allelic expression appear to show a peak for the ancestral G nucleotide only, and the authors claim this to be extreme allelic imbalance. However, an alternative explanation, of course, is preferential allelic amplification or genotyping error and this is not clearly disproved in the manuscript (Maiti et al. 2014). My work demonstrates no genotypic difference in CR3 expression following PMA activation. It is, however, possible that genotypic differences are present following activation through alternative stimuli (Maiti et al. 2014). More work is needed to establish whether or not the differential expression of CR3 on *ex vivo* cells from SLE patients is indeed genotype specific.

A recent descriptive study reports lower *ITGAM* mRNA levels in PBMCs from SLE patients compared with healthy controls (M. Zhou et al. 2013). Additionally, they found significant decreases in cell surface expression of CD11b on T cells, monocytes, and neutrophils, and correlations with disease activity were observed (M. Zhou et al. 2013). The genotypes of these individuals have not been considered; indeed they also measured *FCGR3A* (CD16a) expression without considering the copy number variation at this locus. It has previously been reported that neutrophils from SLE patients showed significantly elevated levels of cell-surface CR3, as measured by an anti-CD11b antibody, compared with healthy controls, and furthermore, that CR3 expression correlated with disease activity (Buyon et al. 1988). Even though these two studies are contradictory, it is likely that disease status and, in particular, disease activity alter the expression levels of immune complex receptors. However, the results of my work, and that of others (Y. Zhou et al. 2013; Fossati-Jimack et al. 2013), demonstrate that the R77H polymorphism does not affect CD11b expression in healthy controls, suggesting that altered CD11b expression is not a mechanism through which the *ITGAM* association is explained. Here we see an example of how genetic analyses can help delineate between cause and effect of disease status; observations of altered CD11b expression are likely be products of, and not a mechanism contributing to, immune dysregulation.

CR3 activation following PMA stimulation, as measured here, is a model of integrin 'inside-out' activation (section 1.4.2). My results therefore suggest that the R77H variant does not impact on the ability of CR3 to respond to the 'inside-out' transmission of cellular activation signals. TNF, INF-γ, and IL-8 are all reported to increase CR3 expression and activation (Mobberley-schuman and Weiss 2005; Ley 2002). Given the results reported here, I would not predict R77H to impact on the up-regulation and activation of CR3 following stimulation by these pro-inflammatory cytokines. However, the R77H-dependent impairment of CR3 function suggests that the missense variant does indeed affect 'outside-in' signalling (MacPherson et al. 2011). These results cannot be explained by ligand-binding impairment as no difference in ligand association is observed, but are instead attributed to defective downstream signalling transmission (Rhodes et al. 2012).

One individual showed high CD11b expression on both resting neutrophils and monocytes, and this was repeatedly replicated (data not shown). It is possible that this is due to a variation in a regulatory region of *ITGAM*. However, through capillary sequencing, I did not detect a notable variation in the 500bp upstream region of the *ITGAM* start codon. It is probable that a variation is

present beyond the region I surveyed, or indeed that a variation is present in the regulatory region of *ITGB2* (encoding CD18). If the variation is indeed located in the *ITGB2* gene, then it is possible that a higher expression of other CD18 integrins would be observed also; something I did not measure. Given the complexities of gene expression regulation, it was hard to foresee the extent to which I would need to extend the search through sequencing. Additionally, given the individual's CR3 expression on PMA-stimulated cells was not as dramatically different to other individuals within the study, nor were there differences in percentage of CR3 proteins present in the active conformation (Figure 3.3), it is unclear how much of a biological impact this observed higher expression of low-affinity CR3 on resting cells would have on neutrophil and monocyte function. For these two reasons, I decided pursuing the search for putative – possibly even novel - genetic variations was not worthwhile in this project.

Chapter 4: The contribution of rare variants within *ITGAM* to SLE pathogenesis

4.1 Introduction

For most complex diseases, as with SLE, the amount of unexplained genetic variance following very large GWA studies is higher than initially anticipated under the common disease-common variant (CDCV) hypothesis (Reich and Lander 2001; Manolio et al. 2009; So et al. 2011). As discussed in section 1.2.2, rare variants with larger effect sizes than the average disease-associated polymorphism (OR≥2), but present at frequencies that fall below the detectable threshold of most GWA studies (MAF<5%), is one of multiple hypotheses which address this problem of 'missing heritability' (Pritchard 2001; Pritchard and Cox 2002; Eichler et al. 2010). Although these variants are individually rare, they are collectively common, therefore may make a significant contribution to disease risk on the population level and many studies have now successfully identified additional rare variants in GWAS-associated loci (Torgerson et al. 2012; Rivas et al. 2011). Given the robust associated of the non-synonymous polymorphism R77H with SLE, *ITGAM* was a great candidate gene for resequencing in a patient cohort.

Through resequencing 24Kb of the *ITGAM* gene in 73 SLE patients, Ellen Thomas (Imperial College London) successfully identified two non-synonymous rare variants, F941V and G1145S. In this chapter I present the continuation of this work. Firstly, I conducted follow-up genotyping of both rare variants in SLE cohorts to estimate their frequency. Secondly, I assessed the functional effects of these variants on CR3 function by utilising a robust *in vitro* model of phagocytosis. This assay had previously been used to demonstrate the under-functioning effects of the R77H polymorphism (MacPherson et al. 2011; Benjamin Rhodes et al. 2012).

In addition, I used the same *in vitro* model to ascertain whether the CD11b-A858V polymorphism (rs1143683) had any deleterious impact on the phagocytic capabilities of CR3, as there has been speculation of a secondary independent SLE association with this non-synonymous polymorphism (W. Yang et al. 2009), as discussed in section 1.3.1. Since there is precedence for the presence of multiple effects in risk loci of complex diseases, this required further evaluation (Ke 2012).

4.2 Results

4.2.1 Two novel non-synonymous variants discovered through ITGAM resequencing

24kb of the *ITGAM* locus, including all exons and intron-exon boundaries, was resequenced at high-coverage (x105) on the 454 Next Generation Sequencing (NGS) platform in 73 SLE patients of European ancestry (Methods 2.5.1). The 73 cases used in this resequencing study met the ARC classification criteria for SLE, but were not chosen for any further sub-phenotypic reason.

Seventeen candidate rare variants within *ITGAM* were identified from this resequencing (Methods Table 2.1). However, through capillary sequencing I was only able to confirm two of these putative variants, which highlights the need to address potential false positives in NGS data. F941V (chr16:31340577) and G1145S (chr16:31343001) were each confirmed in one patient sample each - 88:2.1 and 50:2.2, respectively (Figure 4.1).

I utilised a large-scale publicly-available sequencing project datasets to screen *ITGAM* on the chromosomes of healthy controls of European ancestry. Neither variant, F941V nor G1145S, is described in the 8600 European-American chromosomes of The National Heart Lung and Blood Institute's (NHLBI) Exome Variant Server (EVS; http://evs.gs.washington.edu/EVS/). This database reports high sequence coverage across the *ITGAM* regions containing the rare variants (Table 4.1) and for this reason is a comparable control dataset for our sequencing data. Therefore, both variants are novel. It is worth noting that neither variant is found in the African-American cohort also included in the database. This was an expected observation as rare variants are population specific.

Figure 4.1 Validation of *ITGAM* rare variants by capillary sequencing

A) Forward sequence of *ITGAM* exon 24 from patient 88:2.1 as visualised by BioEdit software following capillary sequencing. The solid arrow highlights the T/G heterozygous peak encoding the F941V rare variant (codon change = TTC → GTC). B) Reverse sequence of *ITGAM* exon 30 from patient 50:2.2 as visualised by BioEdit software following capillary sequencing. The solid arrow highlights the C/T heterozygous peak encoding the G1145S rare variant (codon change = GGT → AGT), and the dotted line highlights G/A heterozygous peak encoding the P1146S polymorphism (codon change = CCC → TCC) also present in patient 50:2.2.

A

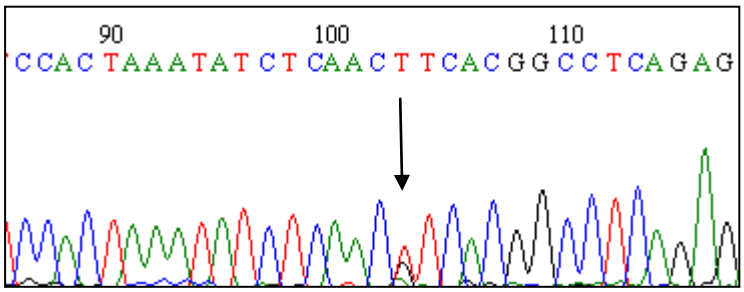

B

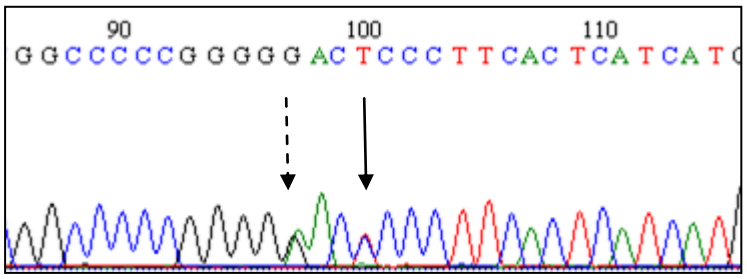

4.2.2 In silico analyses of F941V and G1145S

CD11b codons 941 and 1145 are located in the membrane-proximal extracellular domain and the short cytoplasmic tail of the protein, respectively (Figure 4.2). I used MultAlin (Corpet et al. 1988; http://multalin.toulouse.inra.fr/multalin/) to compare the protein sequences of the four human CD11 molecules that pair with CD18 as part of the β2 integrin family (Figure 4.3). The four proteins CD11a, CD11b, CD11c and CD11d are encoded by *ITGAX, ITGAM, ITGAL,* and *ITGAD,* respectively. The phenylalanine (F) residue at CD11b codon 941, which is located in the membrane-proximal

extracellular domain, is conserved across all four polypeptide sequences. The Glycine (G) residue at CD11b codon 1145 is not shared with any of the other three CD11 proteins. In fact there is no homology at this relative position amongst any the CD11 amino acid sequences. The short cytoplasmic tails of the CD11 molecules vary in length and sequence, and the differences observed are likely to be crucial for their varying functions, and/or intracellular signalling properties (Hynes 2002).

I estimated the pathogenicity of F941V and G1145S using PolyPhen-2 (Adzhubei et al. 2010) and SIFT (Kumar, Henikoff, and Ng 2009). PolyPhen-2 categorises mutations as 'benign', 'possibly damaging' or 'probably damaging' based on pairs of false positive rate (FPR) thresholds. SIFT predicts variants to be deleterious given an output value <0.05 (Methods 2.7.2). F941V was predicted to be deleterious, and G1145S was predicted to be benign, by both algorithms (Table 4.1).

Table 4.1 Genomic details and pathogenicity predictions of *ITGAM* rare variants.

Genomic location, PolyPhen-2 and SIFT predictions of pathogenicity of F941V and G1145S, and sequence coverage in the NHLBI EVS for both F941V and G1145S.

Variant	*ITGAM* region	G37/hg19 Position	Coverage in NHLBI EVS	PolyPhen-2	SIFT
F941V	Exon 24	16:31340577	58.2 ±12.1	Probably damaging (1.00)	Damaging (0)
G1145S	Exon 30	16:31343001	19.3±4.7	Benign (0.319)	Tolerated (0.5)

Figure 4.2 *ITGAM* transcript, CD11b primary protein domains and CR3 protein.

A) *ITGAM* genomic organisation showing relative positions of common polymorphisms (R77H, M441T, A858V), and novel rare variants (F941V, G1145S). B) Primary protein domains of CD11b and the relative location of the missense variants. The β-propellor domain is shown in dark blue; the ligand-binding I-domain is shown in green; light blue represents the other extracellular domains; the transmembrane domain is shown in yellow and the short cytoplasmic tail is represented in orange. C) A cartoon diagram of the CR3 protein (Protein domain ratios = extracellular: transmembrane: cytoplasmic = 1:6:6). The same colours as b) are used to represent the various domains; CD18 is shown in light purple. Asterisks are used to indicate the position of missense variants used in the functional studies - M441T, A858V, F941V and G1145S.

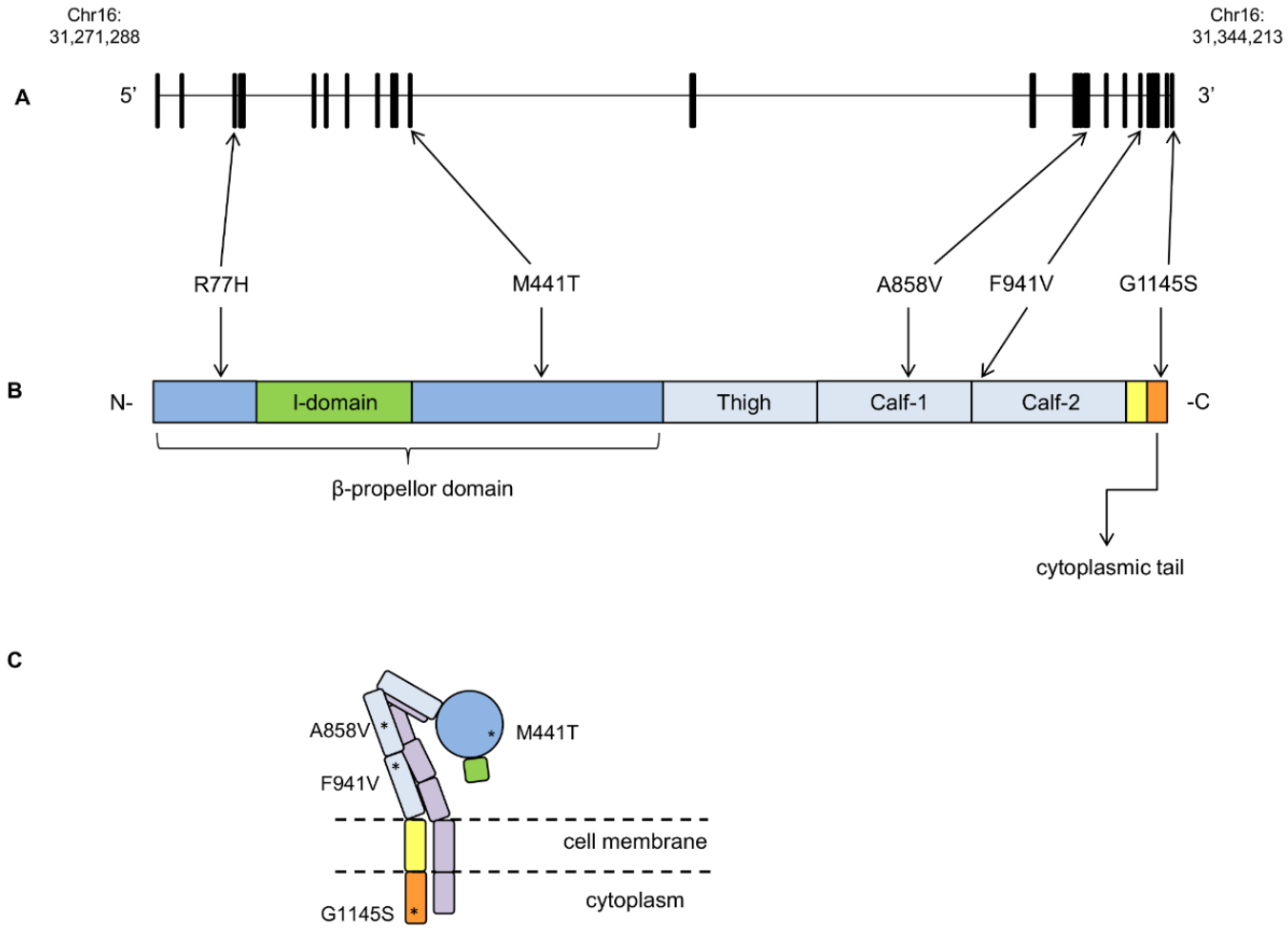

Figure 4.3 Mutalin alignment of human CD11 amino acid sequences

CD18 pairs with CD11b, CD11a, CD11c and CD11d, and together these make up the β2 integrin family. The four CD11 protein sequences (encoded by *ITGAM, ITGAX, ITGAD* and *ITGAL*) were aligned using MutAlin software. The numbers indicate the CD11b codons and all other sequences are aligned relative to this. F941 and G1145 of CD11b are indicated by arrows.

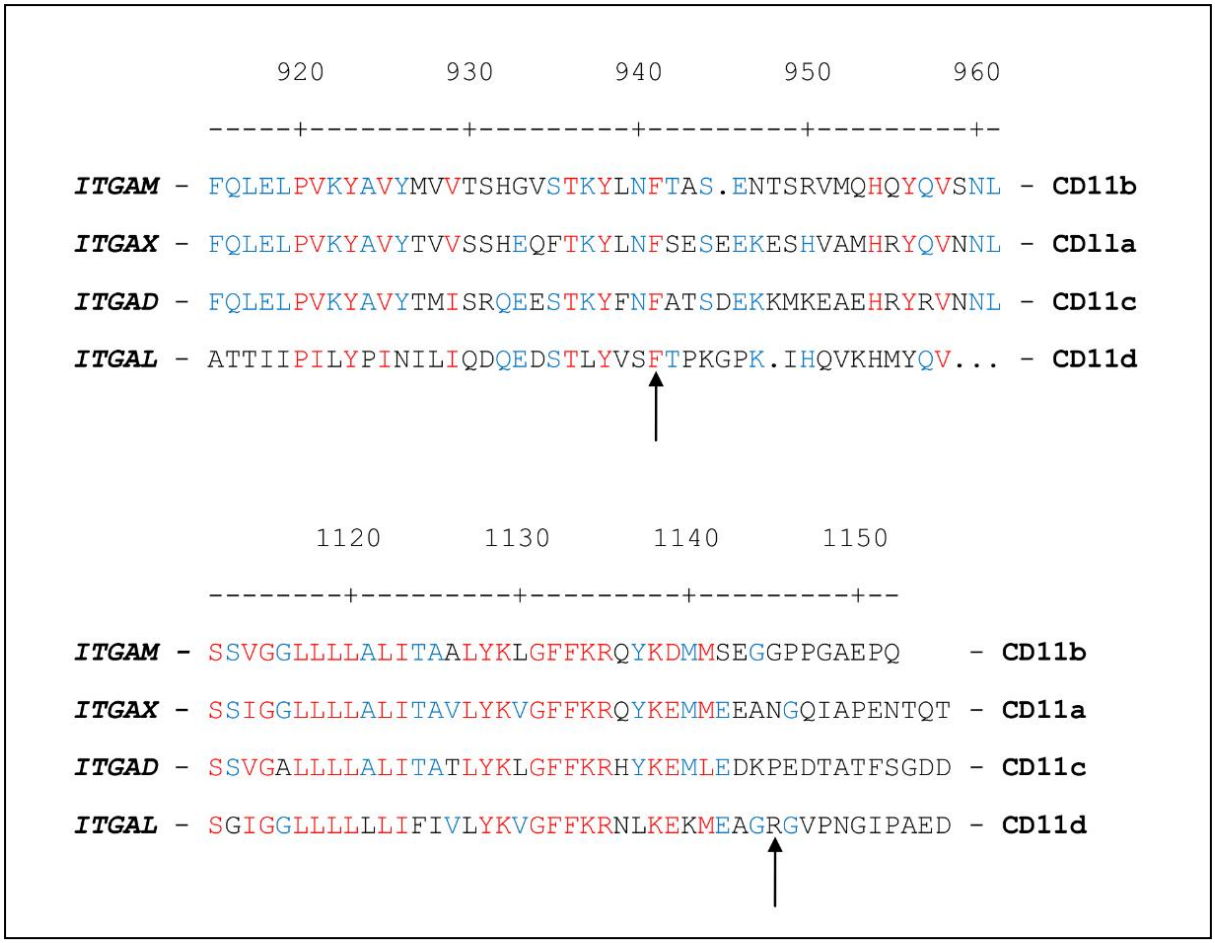

4.2.3 Follow-up genotyping in larger SLE cohorts

4.2.3.1 F941V

F941V was further genotyped in 2107 SLE cases of European ancestry; 1762 were genotyped on an Illumina Custom 384 Chip in the University of Uppsala, Sweden, as part of Prof. Tim Vyse's GWAS replication study (Methods 2.6.2), and an additional 345 samples I genotyped using SSP-PCR (Figure 4.4; Methods 2.6.1). The F941V variant was not observed again in the SLE cohort. I was, however, able to identify the patient's mother (80:1.2) and sibling (88:2.2) as heterozygous for F941V. Neither of which, to the best of my knowledge, have been diagnosed with SLE.

4.2.3.2 G1145S

G1145S did not pass QC analysis following the Illumina Chip genotyping, possibly due to its close proximity (3bp) to the common polymorphism P1146S (as seen in Figure 4.1b). I therefore used capillary sequencing to genotype this variant in 949 SLE cases of European ancestry (Methods 2.6.3). This variant was not observed again in these additional cases. None of the family members of patient 50:2.2, for which DNA was available, carried the G1145S variant. However the father's DNA was not available for genotyping.

Figure 4.4 SSP-PCR genotyping of the F941V variant by agarose gel electrophoresis

The presence of the 3rd amplicon (151bp) indicates 88:2.1 (SLE patient; Lane 6) and 88:2.2 (sibling; Lane 8) are heterozygous for F941V. All other samples are WT homozygous as determined by the absence of the lower size band. Hyper Ladder IV (Lane 1) and water negative control (Lane 4) are also shown.

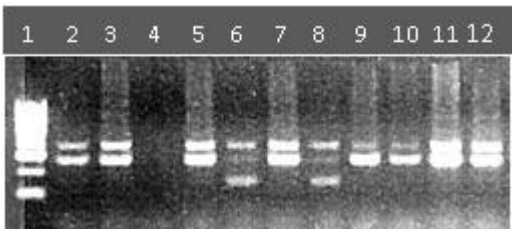

4.2.4 In vitro analyses of rare and common variants

I included two common polymorphisms M441T (rs11861251) and A858V (rs1143683), which are in low (r^2=0.017) and relatively high (r^2=0.551) LD, respectively, with R77H in European populations, in the *in vitro* analyses. The LD scores were calculated with 1000 Genomes Pilot 1 CEU data set using SNAP Pairwise LD (http://www.broadinstitute.org/mpg/snap/ldsearchpw.php). A858V has previously been suggested to be a secondary independent association within *ITGAM* in a Thai population (W. Yang et al. 2009) and therefore I wished to ascertain whether there was functional evidence to support this. I envisaged M441T as a negative control as there is no genetic evidence to suggest this is associated with SLE.

I successfully introduced each of the four variants – F941V, G1145S, M441T, and A858V – individually into a CD11b-pcDNA3.1(-) plasmid vector by site-directed mutagenesis (Methods 2.8.1). Figure 4.5 shows the mutated *ITGAM* sequences from each plasmid, as visualised using BioEdit software following capillary sequencing, compared with the WT sequence as taken from UCSC. I used these plasmids, along with a CD18-pcDNA3.1(-) plasmid, to transiently co-transfect COS-7 cells in order to model the effects of each CD11b variant on CR3 function.

Figure 4.5 *ITGAM* sequences following site-directed mutagenesis.

UCSC sequences surrounding F941, G1145, M441, and A858 of *ITGAM* and corresponding electropherograms showing mutated nucleotides (indicated by arrows) following site-directed mutagenesis.

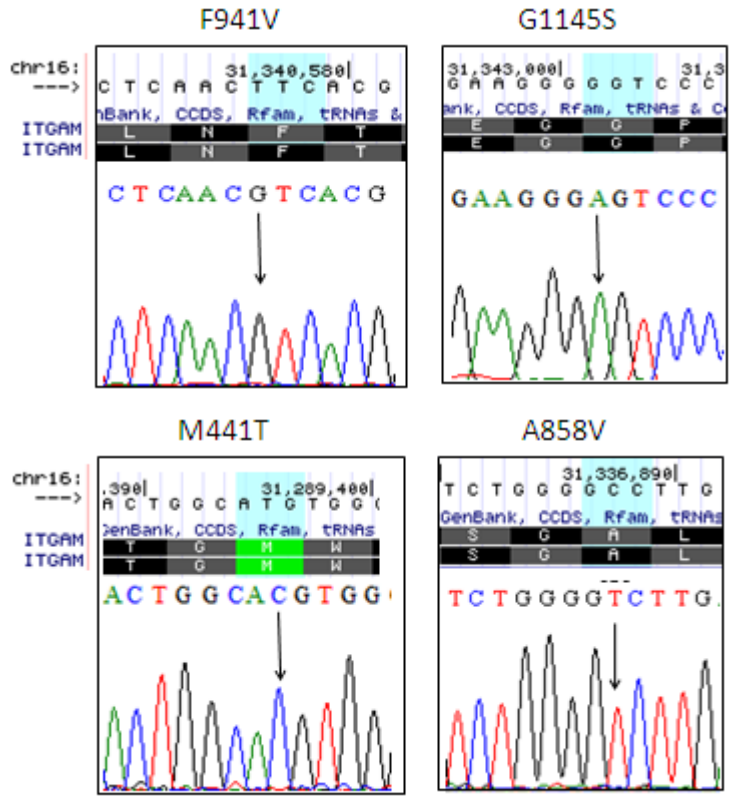

4.2.4.1 Effects of rare and common ITGAM variants on CR3 expression

24 hours following transfection of the COS-7 cells, I measured CR3 expression using a PE-conjugated anti-CD11b (clone ICRF44) monoclonal antibody and compared the mean fluorescence intensity (MFI) of the CD11b positive cells (Methods 2.8.6). No significant difference in cell surface expression of CD11b was observed between WT (n=5, mean ± s.d.; 14445±6982) and M441T (15017±7993), A858V (12377±5130), F941V (14327±4358), or G1145S (12767±5028) CD11b transfected cells (Figure 4.6), suggesting that none of the M441T, A858V, F941V, and G1145S variants affect the transfection efficiency, nor do they affect the non-covalent binding of CD11b to CD18. The same is true for the R77H variant, as shown in Chapter 3 (Rhodes et al. 2012).

Figure 4.6 Expression of CR3 in transfected COS-7 cells.

The MFI of ICRF44-positive COS-7 cells are shown for WT and each of the four CD11b variants No significant difference in cell surface expression of CD11b was observed between WT (mean ± s.d.; 14445±6982) and M441T (15017±7993), A858V (12377±5130), F941V (14327±4358), or G1145S (12767±5028) CD11b transfected cells.

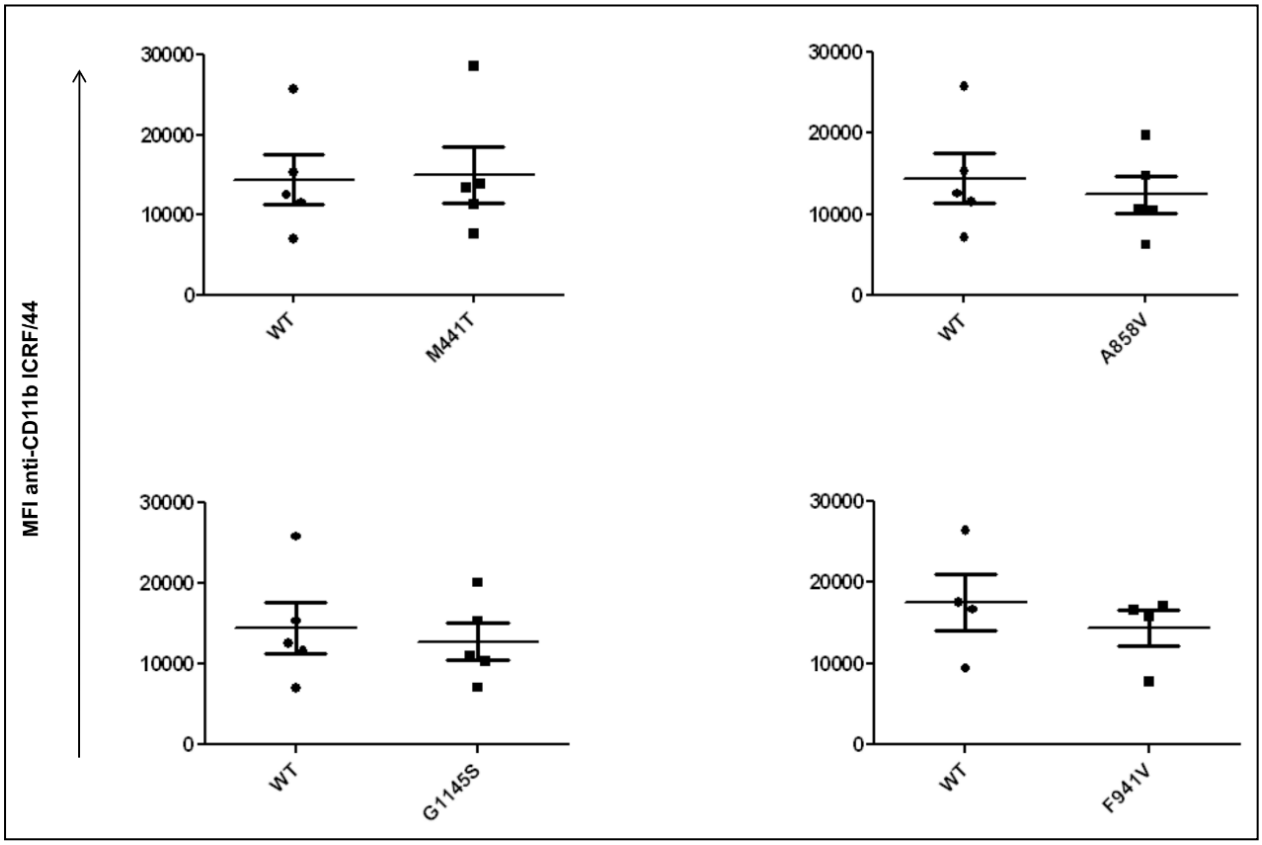

4.2.4.2 Effects of rare and common ITGAM variants on iC3b binding

To test whether the non-synonymous variants affected iC3b binding, I measured the ability of transiently transfected COS-7 cells to associate with iC3b-opsinized sheep red blood cells ($sRBC_{iC3b}$) using an Association Index (Methods 2.8.8). No significant difference was observed when variant CD11b were compared with WT (paired t-test: M441T p=0.79; A858V p=0.69; F941V p=0.61; G1145S p=0.85), indicating that none of the four variants affect the iC3b binding ability of CR3 (Figure 4.7). Given that the four variants are located outside the iC3b-binding site of the protein (Diamond et al. 1993), this was an expected result.

Figure 4.7 Association of CR3-expressing COS-7cells with $sRBC_{iC3b}$.

Association Index = mean number of associated (internal and external) $sRBC_{iC3b}$/100 COS-7 cells. No significant difference was observed between WT and any of four variants. Mean and SEM are shown.

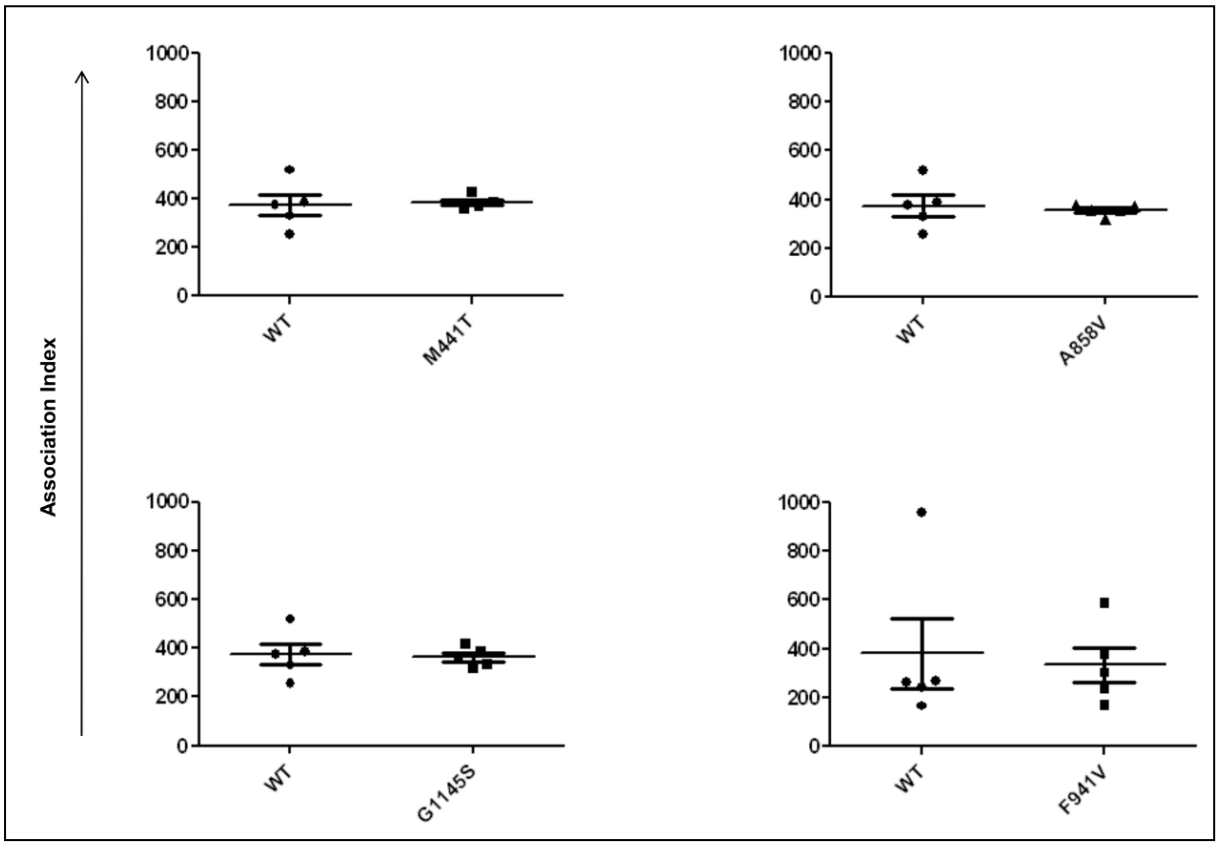

4.2.4.3 Effects of rare and common ITGAM *variants on phagocytosis*

I compared the effects of CD11b variants on CR3-mediated phagocytosis of $sRBC_{iC3b}$ by comparing the Phagocytic Index (Figure 4.8) and Percentage Phagocytosis (Figure 4.9) of CD11b-variant expressing COS-7 cells to WT-CD11b COS-7 cells (Methods 2.8.8). F941V significantly impaired the Phagocytic Index (p=0.002; Figure 4.8) and the percentage phagocytosis (p=0.006; Figure 4.9), and the G1145S variant significantly impaired percentage phagocytosis (p=0.0232; Figure 4.8), when compared with the WT. The reduction in Phagocytic Index between G1145S and WT did not reach statistical significance at the 95% level (p=0.37). Neither of the two common polymorphisms, M441T and A858V, had an effect on the phagocytosis of $sRBC_{iC3b}$ as measured by the Phagocytic Index (Figure 4.8; M441T p=0.74; A858V p=0.92), and percentage phagocytosis (Figure 4.9; M441T p=0.70; A858V p=0.47).

Figure 4.8 Phagocytosis of $sRBC_{iC3b}$ by CR3-expressing COS-7cells as measured by Phagocytic Index.
Phagocytic Index = mean number of internal $sRBC_{iC3b}$/100 COS-7 cells. F941V significantly impairs phagocytosis (p=0.002). No significant difference observed between WT and either common polymorphism M441T (p=0.74) and A858V (p=0.92), or the rare variant G1145S (p=0.37).

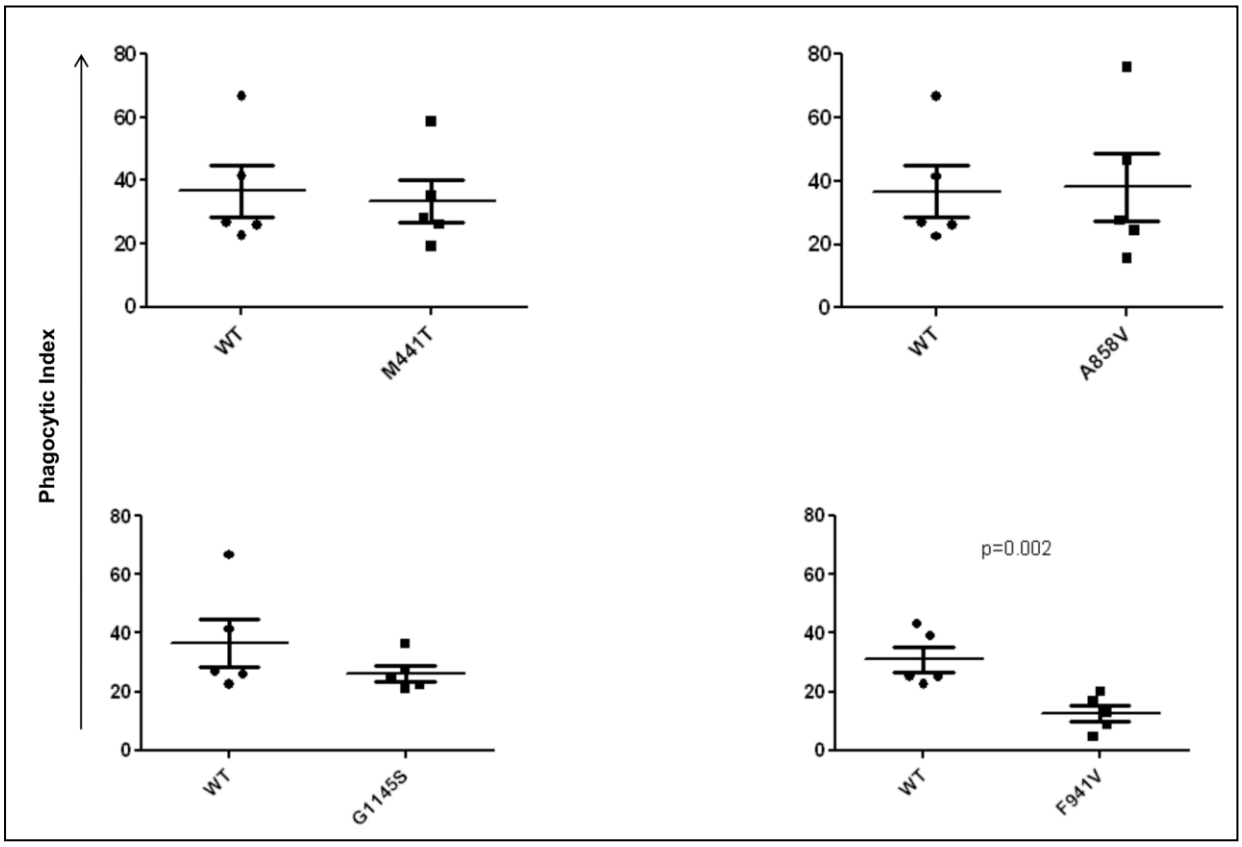

Figure 4.9 Phagocytosis of sRBC$_{iC3b}$ by CR3-expressing COS-7cells as measured by Percentage Phagocytosis.

Percentage Phagocytosis = mean percentage phagocytosis/COS-7 cell. Both rare variants F941V and G1145S significantly impair phagocytosis (p=0.006 and 0.0232, respectively). No significant difference observed between WT and either common polymorphism M441T (p=0.70) and A858V (p=0.47).

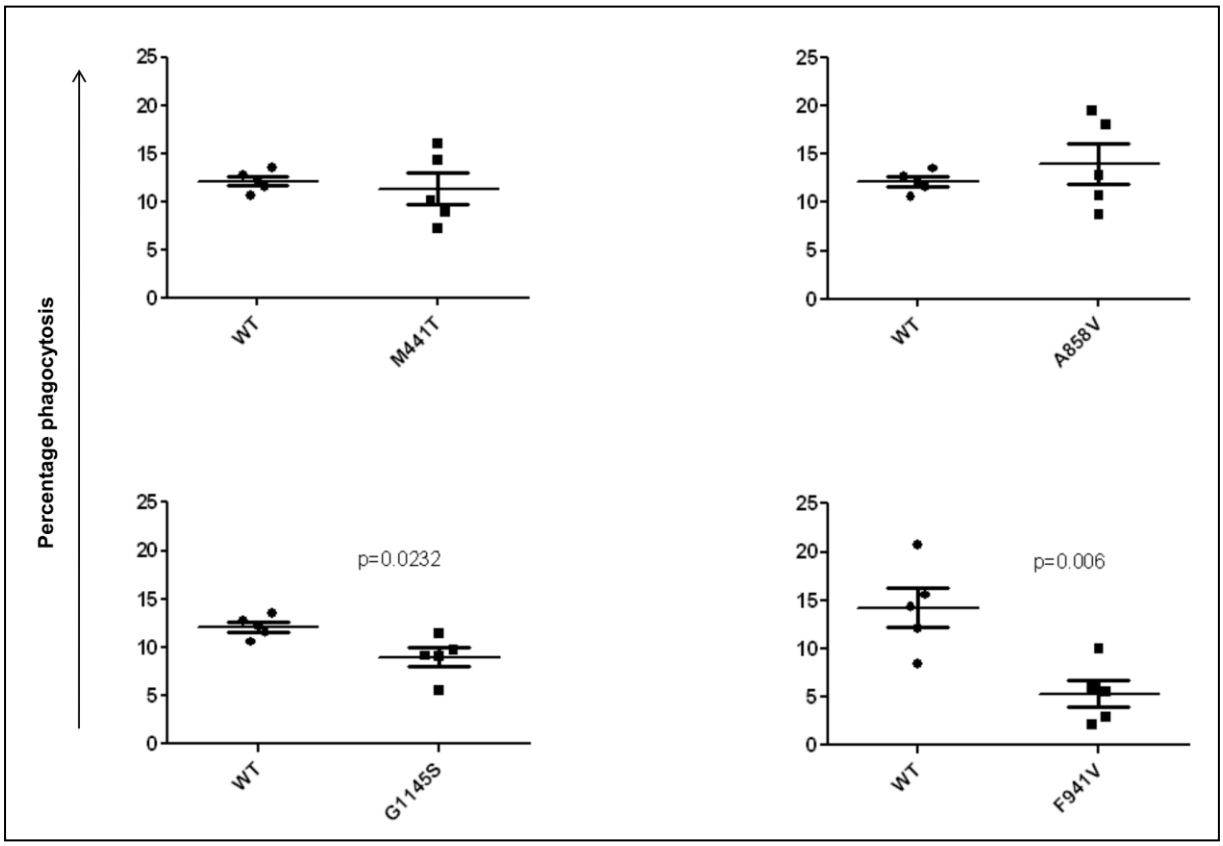

4.2.4.4 Comparison of under-functioning rare variants with R77H

The COS-7 model was used by our group to demonstrate the deleterious effects of the SLE-associated missense polymorphism, R77H, on iC3b-dependent phagocytosis (work carried out by, Dr Ben Rhodes; Rhodes et al. 2012). By using the percentage reduction in phagocytosis compared with WT (set to 100%) for each independent assay, I was able to compare my results to that of the previous R77H study (Figure 4.10). As seen here, G1145S (26%) has a comparable magnitude of effect to that of R77H (31%), whereas F941V (61%) has an even greater effect on phagocytosis.

Figure 4.10 Percentage reduction in phagocytosis of CD11b variants compared with WT

Comparison of the functional impact of the two rare variants to that of the SLE-associated R77H (Rhodes et al. 2012) in transiently transfected COS-7 cells. Mean and SEM are shown.

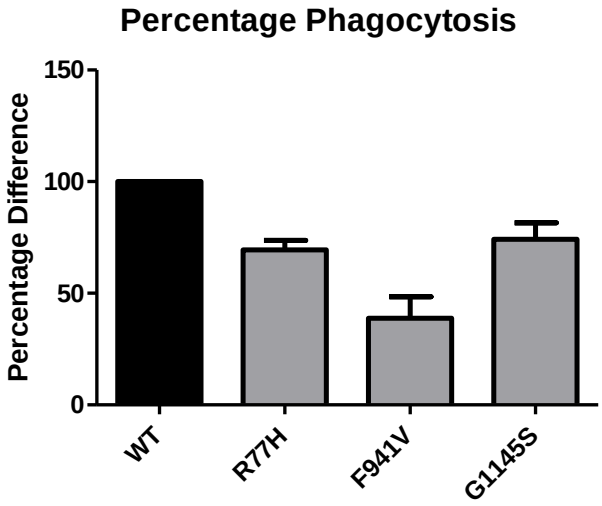

4.3 Discussion

Through use of multiple cell models transfected to express CR3, and *ex vivo* monocytes/monocyte-derived macrophages from healthy volunteers, the SLE-associated R77H variant has been shown to impair phagocytosis of iC3b-coated targets (Rhodes et al. 2012; MacPherson et al. 2011). In addition, the CR3-mediated adhesion to iC3b, ICAM-1, and fibrinogen is significantly reduced by this variant (Rhodes et al. 2012; MacPherson et al. 2011). Adhesion, unlike ligand-binding, requires multiple downstream receptor functions, very much like phagocytosis (Cougoule et al. 2004). Ligand binding, however, by monocytes or neutrophils, is not affected by the R77H polymorphism (Rhodes et al. 2012; MacPherson et al. 2011). It was concluded therefore that R77H affects the "outside-in" signalling of CR3 (MacPherson et al. 2011).

In this chapter I have demonstrated the functional impact of two case-specific rare variants in *ITGAM*. These variants, F941V and G1145S, were identified through the resequencing of *ITGAM* in 73 SLE patients of European ancestry. The *in vitro* model shows both these variants, G1145S and, more strongly, F941V impair CR3-mediated phagocytosis of iC3b-coated targets. The observed detrimental impact on protein function is of a similar (G1145S), or greater (F941V), magnitude to that of the common SLE-associated polymorphism R77H, which is associated with a 31% reduction in phagocytosis (Rhodes et al. 2012). Firstly, these data add further evidence for the coexistence of common and rare variants in genetic loci predisposing to the same disease biology, and secondly, they emphasise the role of under-functioning *ITGAM* variants in SLE pathogenesis.

The targeted resequencing of loci harbouring disease-associated common polymorphisms has successfully identified novel rare variants in a number of other complex genetic diseases such as inflammatory bowel disease, psoriasis and asthma (Torgerson et al. 2012; Rivas et al. 2011; Jordan et al. 2012). Studies in schizophrenia (Need et al. 2012) and epilepsy (Heinzen et al. 2012) identified rare variants through whole-exome sequencing but failed to identify a single variant which reached study-wide significance despite large-scale genotyping in follow-up cohorts. In fact, the schizophrenia study reported that 23% of case-specific variants from the initial sequencing cohort were not observed again in the follow-up cohort (Need et al. 2012). As demonstrated by these two studies, individual rare variants may never reach statistical significance for disease association. In the

follow-up genotyping presented in this chapter, 2107 and 949 additional SLE cases were found to be wild-type for F941V and G1145S, respectively.

Despite the lack of statistical evidence for a contribution of these rare variants to SLE, the functional assessment of these *ITGAM* variants demonstrates their contribution to disease biology. I was able to do this by utilising a robust functional assay that had previously proven successful in delineating the function of the common *ITGAM* R77H variant (Rhodes et al. 2012). Such *in vitro* studies are beneficial to study polymorphisms of interest in isolation from other confounding factors on *ex vivo* cells, particularly the presence of other receptors with similar ligand-specificity. COS-7 cells possess the ability to phagocytose, however they do not express endogenous phagocytic receptors. The introduction of phagocytic receptors through transfection therefore provides a robust model for phagocytosis without confounding factors (Caron 1998).

It has been suggested that impaired phagocytosis is the main mechanism by which R77H confers risk to SLE (Fossati-Jimack et al. 2013). The G1145S variant had a comparable under-functioning effect (26%), whereas F941V had an even greater impact on phagocytosis (61%). It is likely, then, that these rare variants are contributing towards dysfunctional phagocytosis in the two patients in question. As discussed in section 1.1.2, the 'waste disposal' hypothesis is a central paradigm of SLE disease biology and refers to insufficient clearance of apoptotic cells by under-functioning of phagocytes (Gaipl et al. 2007; Pittoni and Valesini 2002; Herrmann et al. 1998). Apoptotic cells are opsonised with soluble ligands of phagocytic receptors, such as complement factors, enabling their effective recognition (Pittoni and Valesini 2002). Defective clearance of apoptotic cells leads to their accumulation and subsequent release of nuclear components. Through presentation by antigen-presenting cells (APCs), such as dendritic cells (DCs), and exposure to cells of the adaptive immune system, this leads to the production of the characteristic autoantibodies to nuclear components (Kelley et al. 2010).

This work does not contribute to the estimate of overall genetic variance explained for SLE, but it does add evidence to the functional importance of the *ITGAM* locus to SLE susceptibility. Furthermore, this work is another example of rare variants located in genetically-associated loci whose contribution to disease risk cannot be estimated by statistical models alone due to their extremely low frequencies. However, given the demonstrated functional impact of these variants,

their contribution to disease pathogenesis cannot be dismissed. In fact, a case report of a CR3 defect in an SLE patient has previously been assumed to be a result of a rare genetic variant (Witte et al. 1993).

Many studies of rare variants in complex diseases are concluding that such variation has negligible contribution to the genetic variance of complex diseases (Hunt et al. 2013). However, until additional methods of analysis are available, the contribution of rare variants to complex diseases should not be dismissed on the basis of non-significant statistical associations alone.

It is interesting to note that both PolyPhen-2 and SIFT predicted the G1145S variant to be benign/tolerated. Some methods of analysis rely on weighted values being applied to rare variants based on these computational predictions (Price et al. 2010). The results of my *in vitro* studies demonstrate how the predictive functions of such algorithms should be taken as a guide only, and where possible, should not be relied upon instead of laboratory tests. Relying heavily on computational predictions in analyses may result in the effects of rare variants being underestimated.

In addition to mechanistic similarities between the novel rare variants and R77H, we also see a similar magnitude of functional effect between R77H and one rare variant, G1145S. This raises an important point about the rare variant paradigm, which is often represented as a negative correlation between allele frequencies and disease risk (Bodmer and Bonilla 2008). Our *in vitro* models suggests a comparable functional effect, despite the large difference in the minor allele frequencies of these two missense variants in SLE cohorts; R77H (MAF =0.2) and G1145S (MAF ≤0.0005). Furthermore, F941V has a comparable MAF (≤0.0002) to that of G1145S, yet has a significantly greater impact on phagocytosis. Despite defective phagocytosis being a robust paradigm in SLE biology, it is, of course, not the only mechanism by which impaired CR3 function predisposes to SLE risk. It is possible, then, that F941V and/or G1145S have variable effect sizes on other CR3 functions, such as the inhibition of Toll 7/8-induced pro-inflammatory cytokines; however, in the absence of *ex vivo* cells from multiple healthy individuals carrying these mutations, or additional suitable *in vitro* assays, we lack a sufficient model for this (C. Han et al. 2010; Rhodes et al. 2012). In this instance, I recognise that it is difficult to estimate the contribution of these rare

variants to SLE risk. However, given their impact on phagocytosis – being equal to, or greater than, that of R77H – I feel it is sufficient to conclude their contribution cannot be dismissed.

My work also expands on the specific understanding of the role of common *ITGAM* variants in SLE pathogenesis, particularly by resolving the uncertainty in the genetic literature concerning the possible additional functional effect of *ITGAM* SNP rs1143683 (A858V). SNP rs1143683 (A858V) and rs1143679 (R77H) are in relatively high LD (r^2=0.55) in European populations and rs1143683 has been suggested as a secondary independent association signal within *ITGAM* in a Thai population (W. Yang et al. 2009). I wished to clarify this issue by including the A858V polymorphism in the *in vitro* model, along with another polymorphism rs11861251 (M441T), which is not a part of the same disease-associated haplotype (r^2=0.017), which I envisaged as a negative control. Neither the A858V nor the M441T polymorphisms affected the CR3-mediated phagocytosis of iC3b-coated targets.

Since my work was carried out, a publication has demonstrated the functional impact of the *ITGAM* polymorphisms rs1143683 and rs1143678, encoding A858V and P1146S present in the calf region and cytoplasmic tail of CD11b, respectively, on *ex vivo* neutrophils, independent of R77H (Y. Zhou et al. 2013). There is perfect LD between rs1143683 (A858V) and rs1143678 (P1146S) and for this reason the functional impact of these variants could not be analysed separately. Even though they report a significant reduction in the phagocytic capabilities of neutrophils from individuals with the 858V/1146S variants, they hypothesise that the affect is attributable to the less conservative P1146S amino acid change (Y. Zhou et al. 2013). My results support this hypothesis of the functional neutrality of A858V. Of particular interest, patient 50:2.2, who harbours the G1145S rare variant, is also heterozygous for the P1146S polymorphism (Figure 4.1b). Through using the Integrative Genomics Viewer (IGV) programme to view aligned 454 sequencing reads (work carried out by Dr Ellen Thomas) we can see that the G1145S rare variant and P1146S polymorphism are in phase on the chromosome. G1145S had the least severe impact on phagocytic function (26% reduction); however, a functional alteration to two sequential amino acids could indeed have an impact greater than the additive effect of the G1145S and P1146S variants considered independently. This patient is also heterozygous for the associated R77H polymorphism (of note, the patient with F941V is homozygous WT for this variant). Heterozygosity of the SLE-associated R77H variant has been shown to be sufficient to significantly impair phagocytosis of iC3b-targets, including opsonised mouse apoptotic thymocytes, by *ex vivo* neutrophils, monocytes, and macrophages (Fossati-Jimack et al.

2013). This study argued that, as the heterozygous genotype is far more common in SLE populations (~20%) than 77H homozygosity (~3%), comparisons between WT with R77H heterozygous samples were more informative (Fossati-Jimack et al. 2013). It is likely, then, that the CR3 functions of patient 50:2.2 are severely affected *in vivo* by the combination of these *ITGAM* variants (discussed further in 7.2.1).

The functional results of the COS-7 model used in this work emphasises that impaired phagocytosis of iC3b opsonised particles, a consequence of defective 'outside-in' signalling is one, but clearly not necessarily the only, functional mechanism underlying the association between specific *ITGAM* risk variants and SLE. It is notable that all three functional variants, R77H, F941V and G1145S, are located in different domains of the CD11b polypeptide (Figure 4.2) but have similar effects on signalling. None appear to directly influence known ligand binding sites (Diamond et al. 1993), but clearly specific amino acids throughout CD11b, from the N-terminal β-propeller (R77) domain through to the C-terminal cytoplasmic tail (G1145) are important in mediating CR3 'outside-in' signals to the cytoplasm.

The 'hypothesis-free' GWAS methodology has proven successful in highlighting novel disease-associated polymorphisms for further functional analysis, but lacks statistical power to prove the association of most rare variants with disease. Recent approaches have identified rare variants in disease-associated loci very successfully, but estimating their contribution to disease risk has proven difficult. Conclusions are leading towards the notion that rare variants contribute little towards genetic variance (Hunt et al. 2013). My work demonstrates that once the functional consequence of a common variant has been clearly elucidated, this knowledge can be reapplied to provide proof of a role for additional candidate rare variants at the same locus. In a relatively small resequencing project, two functional deleterious rare variants at the *ITGAM* locus have been identified. This suggests that further screening of *ITGAM* for rare variants in a larger cohort of SLE cases promises to be worthwhile. If an association-based approach alone had been applied in this study, together with computational predictions, there would be no evidence of any potential contribution of these rare variants to SLE pathogenesis. However, it is not possible to disregard these variants given their genetic location, conservation, and deleterious effects on receptor function. If each of the 52 known SLE susceptibility loci contains a similar high number of modest effect-size rare variants then their contribution to the overall genetic component of disease susceptibility will be not inconsiderable.

However, perhaps we currently lack the correct tools for estimating the contribution of rare variation to complex disease susceptibility.

Chapter 5: Inhibition of NK cell pro-inflammatory responses by CR3 small-molecule agonist

5.1 Introduction

In addition to aiding our understanding of complex pathologies of disease, genetic studies may also provide avenues of directed therapies. Such an example may be true of the *ITGAM* association; a high-throughput screening cell-adhesion assay identified a novel agonist of CR3 which has anti-inflammatory properties (Maiguel et al. 2011; Faridi et al. 2009).

K562 cells stably transfected with CD11b/CD18, which show very little binding to the CR3 natural ligand fibrinogen prior to transfection, were used to identify small molecules that increased CR3-mediated adhesion. Leukadherin-1 (LA1) is a small-molecule agonist that binds specifically to the αA-domain of CD11b, causing allosteric activation of CR3 (Faridi et al. 2009). LA1 has been shown to increase the receptor's affinity for multiple natural ligands in transfected cells and *ex vivo* human neutrophils, demonstrating that its effects are neither ligand- nor cell-specific (Maiguel et al. 2011). Furthermore, by increasing the CR3-mediated adhesion of neutrophils, LA1 decreases cell migration of both *ex vivo* and *in vivo* murine cells, suggesting a potential pharmacological use in inflammatory and autoimmune diseases (Maiguel et al. 2011). In contrast to anti-CD11b activating antibodies, which induce receptor clustering and global CR3 conformational changes, LA1 does not mimic natural ligands. This is thought to provide its therapeutic advantage over activating antibodies (Faridi et al. 2013). Given the demonstrated involvement of CR3 under-functioning in SLE susceptibility (Rhodes et al. 2012; MacPherson et al. 2011; Fossati-Jimack et al. 2013; Maiti et al. 2014), LA1 is a promising avenue for molecular-targeted SLE treatment. Particularly as LA1 stimulated phagocytosis of iC3b-coated sheep red blood cells by CD11b/CD18 transfected K562 cells (Maiguel et al. 2011). Furthermore, sub-phenotype analyses suggest the R77H variant is most strongly associated with renal manifestations of SLE (W. Yang et al. 2009; Kim-Howard et al. 2010), and, of particular interest, LA1 was shown to preserve kidney functions in a murine model of nephritis (Maiguel et al. 2011).

The conclusions of one study, however, suggested a limitation for the potential therapeutic use of LA1 for SLE. Reed and co-workers demonstrated that LA1 pre-treatment of THP-1 cells and *ex vivo* macrophages from healthy human donors significantly reduced the TLR7/8-mediated secretion of

TNF by degrading the adaptor protein MyD88 (Reed et al. 2013). However, despite very modest numbers (n=3), this study concluded that R77H-heterozygosity was sufficient to diminish the LA1 effect in *ex vivo* macrophages (Reed et al. 2013). The MAF of rs1143679 is estimated to be ≈0.15-0.2 in SLE cases across multiple ethnicities (S. Han et al. 2009), and a genotypic restriction on the efficiency of LA1 would indeed be a caveat for its use as an SLE therapeutic.

As discussed in section 1.4.4, there is growing evidence that CR3 acts as a regulator of immune cell signalling (C. Han et al. 2010; Bai et al. 2012). NK cells, in particular the $CD56^{bright}$ subset, are prominent producers of cytokines, yet the role of CR3 on NK cells has yet to be fully explored. It is possible, then, that LA1 could have similar CR3-dependent inhibitory effects on NK cells. Work carried out by Ben Rhodes (King's College London) using *ex vivo* human NK cells from healthy volunteers either homozygous WT (R77) or homozygous risk (77H) demonstrated that pre-treatment with LA1 prior to 24 hour incubation with paired monocyte-derived cytokines (monokines) - IL-12 and IL-15, or IL-12 and IL-18 - significantly reduced the secretion of pro-inflammatory cytokines IFN-γ and TNF, and the chemokine MIP-1β, compared with the vector control (DMSO), as measured by Cytometric Bead Arrays. No difference was observed in IL-8 secretion under either stimulation conditions, indicating an element of specificity to these inhibitory effects (Figure 5.1; manuscript under review). Even though the SLE-associated R77H polymorphism has been shown to affect CR3 function following natural ligand engagement (MacPherson et al. 2011), including its regulatory functions (Rhodes et al. 2012), the R77H variant had no effect on the LA1-mediated inhibition of NK cell cytokine production following monokine stimulation. This result contradicts that of Reed and colleagues discussed above (Reed et al. 2013). However, the study by Ben Rhodes is better able to detect a genotypic effect, firstly due to a much greater sample size (n>20), and secondly due to the use of opposing genotypic groups (R77 v 77H).

In order to understand the mechanism through which CR3 engagement with LA1 down-regulated cytokine secretion in NK cells, as demonstrated by Ben Rhodes (Figure 5.1), I employed an intracellular FACS assay with phospho-specific antibodies (Methods 2.9). I measured the effects of LA1 pre-treatment on the tyrosine phosphorylation of signal transducers and activators of transcription (STAT) and p38 MAPK in NK cells following stimulation with the paired monokines; IL-12 and IL-15, or IL-12 and IL-18.

Figure 5.1 LA1 significantly reduces the production of pro-inflammatory cytokines by NK cells

NK cell pre-treatment with LA1 before IL-12 and IL-15 (n=20; top panel), or IL-12 and IL-18 (n=28; bottom panel) stimulation significantly reduced production of cytokines IFN-γ, TNF, and MIP-1β, but not IL-8. Healthy volunteers were either homozygous WT or homozygous risk for the SLE-associated R77H polymorphism. No genotypic effect was observed.

This work was carried out and these data were provided by Ben Rhodes. The remainder of the data presented in this chapter is my own.

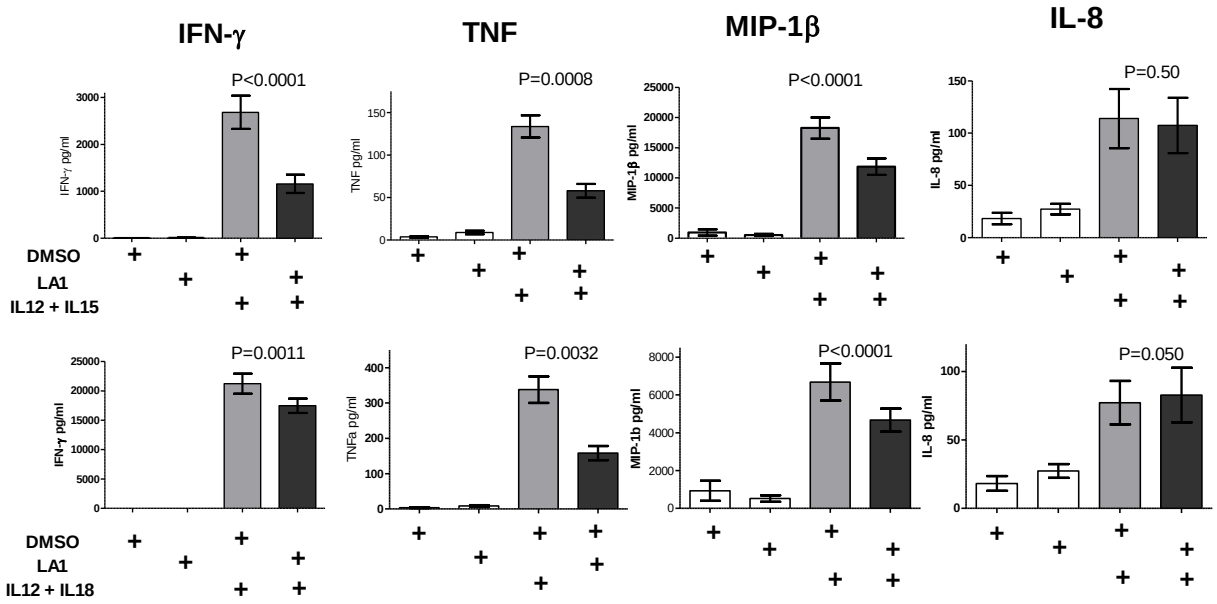

5.2 Results

5.2.1 LA1 does not reduce cell viability in NK cell populations of high purity

I used a negative selection kit to isolate NK cells from whole blood of healthy donors and tested the purity of the cell population using the following cell surface marker antibody panel: anti-CD56 (APC), anti-CD16 (FITC), anti-CD14 (PerCP-Cy5.5), anti-CD3 (Pacific Blue), and anti-CD19 (PE) (Methods 2.9). I consistently observed a high degree of purity, as represented in Figure 5.2. Donors were not selected by R77H genotype because there did not appear to be a genotypic difference in the cytokine secretion assays.

Using a CellTiter-Glo® Luminescent Cell Viability Assay (Methods 2.9.3), I did not observe a significant difference in cell viability of 50,000 NK cells ($0.5x10^6$/ml) following 24 hour incubation with DMSO (vector control) or LA1, either alone or in combination with paired monokines IL-12 and IL-15, or IL-12 and IL-18 (Figure 5.3). Although all conditions resulted in a slight decrease in cell viability when compared with NK cells incubated without any stimulation, it is the comparison of LA1 against its vector control that is of importance for the experiments described here. Therefore, the LA1-mediated reduction in NK cell cytokine production, as observed by Dr Ben Rhodes (Figure 5.1) cannot be attributed to reduced cell viability. This is in concordance with a previous study on the *in vivo* effects of LA1 in mice (Maiguel et al. 2011).

In further Phosflow experiments, NK cells were in fact used at a higher concentration of $1x10^6$/ml, yet LA1 was used at the same concentration (1:2000). Therefore, the cell viability results presented here demonstrate that LA1 is not toxic to NK cells even when the receptor: ligand ratio is double that used in the Phosflow assays.

Figure 5.2 Isolation of NK cells from PBMCs by negative selection yields cell population with high purity Following negative selection from PBMCs, $2x10^5$ cells were stained with anti-CD56 (APC), anti-CD16 (FITC), anti-CD14 (PerCP-Cy5.5), anti-CD3 (Pacific Blue), and anti-CD19 (PE). A) Scatter-plot of APC and FITC staining separates the $CD56^{dim}CD16^{+}$ (Q2) and $CD56^{bright}$ $CD16^{-}$ cells (Q1). An insignificant amount of B) $CD3^{+}$ T cells (Q5), $CD19^{+}$ B cells (Q7), and C) $CD14^{+}$ monocytes (Q10) were observed. Representative data are shown.

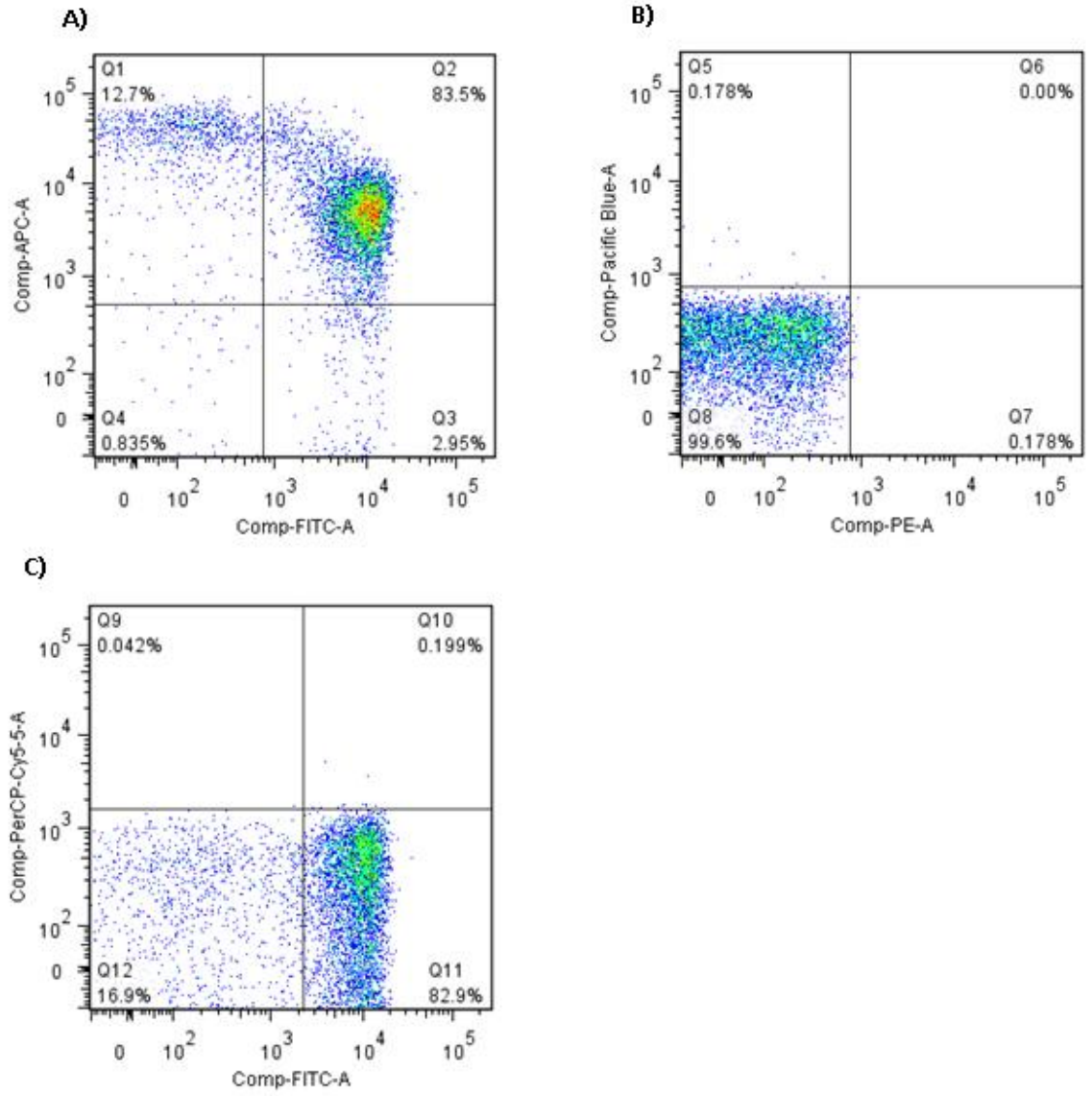

Figure 5.3 LA1 does not reduce NK cell viability The addition of DMSO or LA1, alone or in combination with paired cytokines (IL-12 and IL-15, or IL-12 and IL-18) slightly decreased NK cell viability compared with no stimulation. However, no significant difference in NK cell viability was observed between DMSO plus cytokines, and LA1 plus cytokines (50,000 cells, 24-hour incubation).

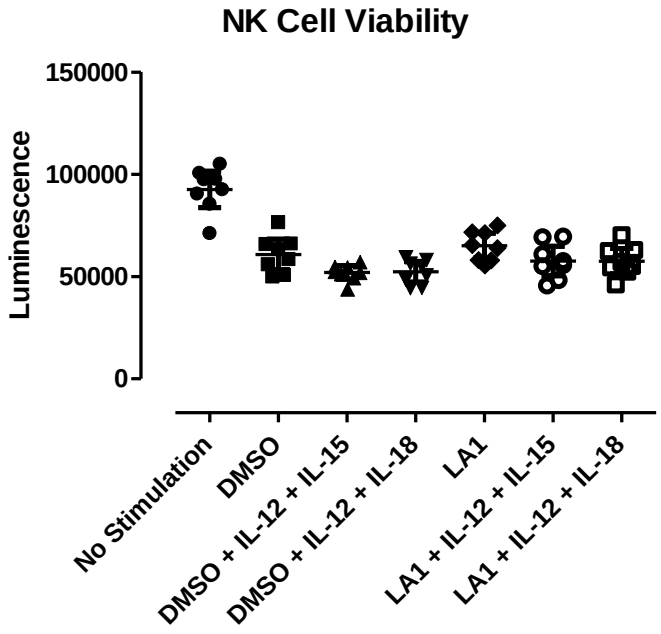

5.2.2 Measuring STAT phosphorylation in NK cells

I surveyed the effects of LA1 on NK cells stimulated with IL-12 and IL-15, or IL-12 and IL-18, by measuring the phosphorylation of three STAT proteins - STAT3, STAT4, and STAT5 - known to be of particular importance in IL-12, IL-15 and IL-18 signalling and NK cell production of IFN-γ, TNF, and MIP-1β, as demonstrated in Figure 5.4 (Nakahira et al. 2001; Carroll, Paunovic, and Gadina 2008; Paunovic et al. 2008; Strengell et al. 2003; Johnston et al. 1995).

Figure 5.4 Cartoon representation of the specificity of STAT and MAPK signalling in, and cytokine and chemokines production by, NK cells following activation with IL-12, IL-15, and IL-18.

IL-15R and IL-12R engagement activates JAKs, which in turn phosphorylate the cytokine receptors, allowing the phosphorylation of specific STATs. Phosphorylated STATs can dimerise, enabling their translocation to the nucleus and subsequent activation of transcription. IL-15 signalling activates STAT3 and STAT5, which are able to form hetero/homodimers. IL-12R signalling is STAT4-dependent. Furthermore, this signalling cascade can induce IL-18Rβ expression. The IL-18Rα chain phosphorylates p38 MAPK; the IL-18Rβ chain, when expressed, ultimately signals through NFκB. The signalling molecules presented in bold were measured with phosphor-specific antibodies. The cytokine and chemokines milieu shown here are those measured in Figure 5.1, and those presented in bold are suppressed by CR3 pre-engagement with Leukadherin-1.

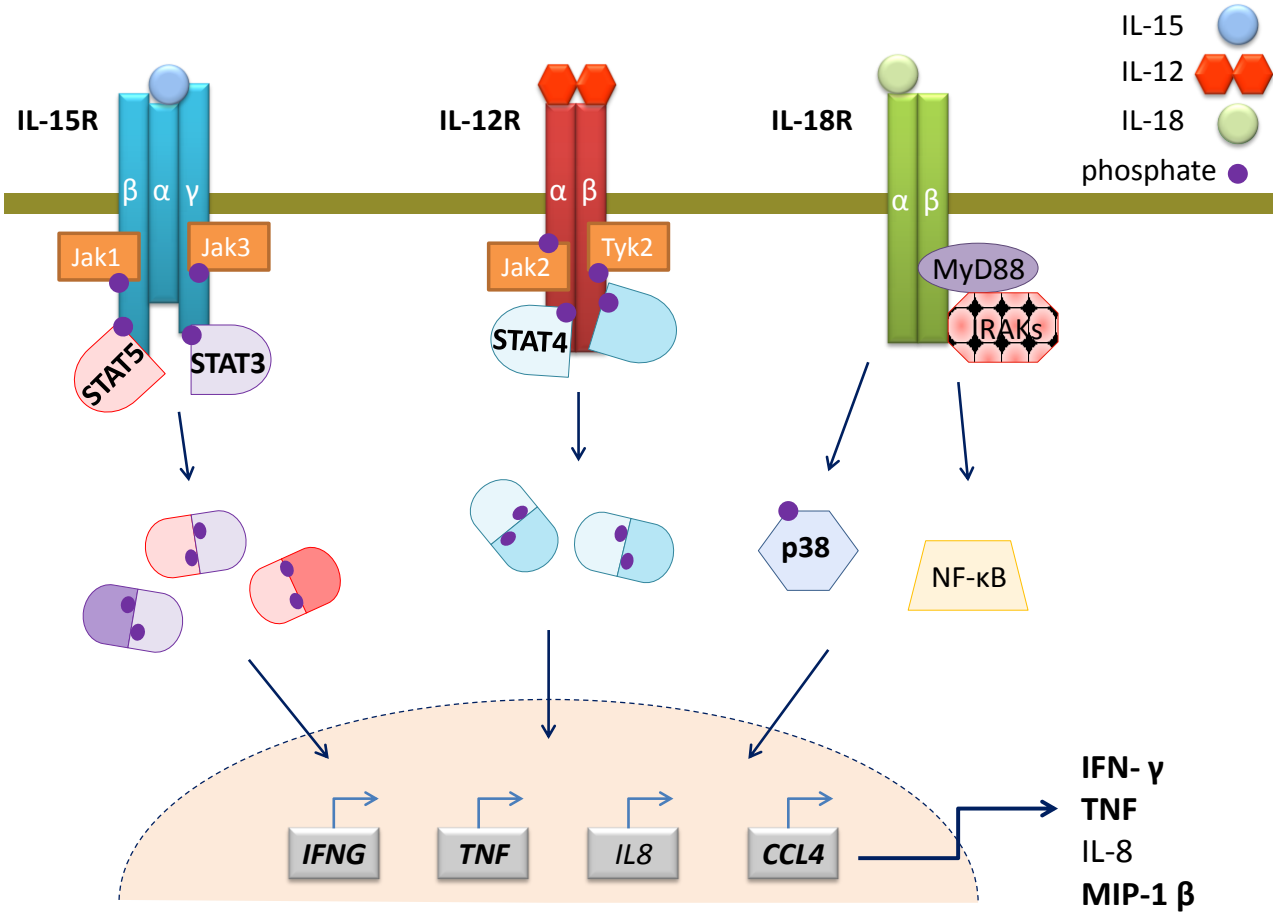

As the cytokine data was measured after 24 hour incubation (Figure 5.1) and the mechanism of LA1-mediated cytokine/chemokine regulation is incompletely understood, I measured the phosphorylation of STAT3, STAT4, and STAT5 at a short time point (10 minutes) and an extended time-point (2 hours). Negative regulation of the JAK-STAT pathway occurs through multiple mechanisms, such as dephosphorylation (e.g. through tyrosine phosphatases deactivation of JAKs) or degradation of activated JAKs/STATs (e.g. as seen with suppressors of cytokine signalling (SOCS)). By taking early and late time-point measurements, I hoped to be able to test whether LA1 decreased the rate of phosphorylation or increased the rate of dephosphorylation.

For each individual volunteer, NK cells with DMSO and LA1 pre-treatment, but no cytokine stimulation (T=0), were used to calculate the fold-change of median fluorescence intensity at the indicated time points (Figure 5.5). I also used a Pacific Blue-conjugated anti-CD56 antibody to enable the delineation of the $CD56^{bright}$ NK cell population during FlowJo analysis (Methods 2.9.7).

Figure 5.5 Fold-change of STAT5 phosphorylation as observed using phospho-specific antibodies

Median fluorescent intensity (MFI) values were measured prior to monokine stimulation (red histogram) and at specific time-points following monokine stimulation (blue histogram). Fold-changes in STAT phosphorylation were calculated by dividing MFI following stimulation by the basal MFI (Methods 2.9.8). Representative data from one experiment shows fluorescence of APC-conjugated anti-pSTAT5 before (red) and after (blue) IL-12 and IL-15 stimulation.

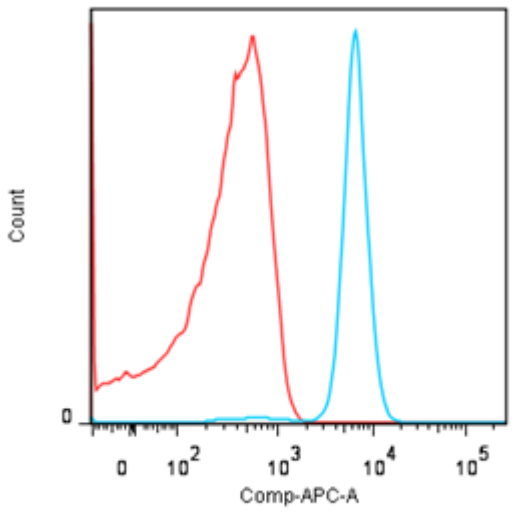

5.2.3 The effects of LA1 on STAT phosphorylation following IL-12 and IL-15 stimulation

I observed a large fold-change increase in STAT5 phosphorylation, in both total and $CD56^{bright}$ NK cell populations, after 10 minutes stimulation with IL-12 and IL-15. STAT5 is known to be a key mediator of IL-15 signalling in NK cells (Johnston et al. 1995; Strengell et al. 2003). Furthermore, pre-treatment with LA1 significantly reduced this fold-change in both total ($p=0.02$) and $CD56^{bright}$ ($p=0.004$) NK cell populations (Willcoxon's matched paired test; Figure 5.6a). STAT5 phosphorylation was still elevated at similar levels after 2 hours, but the LA1 effect was no longer significant (Figure 5.6a).

An increase in STAT4 phosphorylation was also seen following IL-12 and IL-15 stimulation, although the rate of this increase was much slower; the fold-change observed after 2 hours incubation with the paired monokines was much greater than that observed after 10 minutes (Figure 5.6b). LA1 did not appear to affect the phosphorylation of STAT4 (Figure 5.6b). A very modest fold-change in STAT3 phosphorylation was seen at both time points and, once again, LA1 did not appear to affect this (Figure 5.6c).

5.2.4 LA1 delays the IL-15-mediated phosphorylation of STAT5

STAT phosphorylation is very proximal in cell signalling cascades, and, given the LA1-mediated reduction in pSTAT5 after 10 minutes incubation with IL-12 and IL-15, this suggested that LA1 is reducing the rate of phosphorylation, as opposed to triggering a negative feedback loop.

I used scatter plots with anti-pSTAT5 (APC) on the x-axis and anti-CD56 (Pacific Blue) on the y-axis, as shown in Figure 5.7a, to compare the shift in pSTAT5 positivity. The y-axis gate is set to distinguish $CD56^{dim}$ and $CD56^{bright}$ populations; pSTAT5 positivity was set at $>10^3$ log-APC. Using this gating strategy, I compared the shift in percentage pSTAT5 positivity across nine independent experiments. Pre-treatment with LA1 significantly lowered the percentage of pSTAT5 positive cells (Q8; Figure 5.7a) at 10 minutes, in both $CD56^{dim}$ ($p=0.03$) and $CD56^{bright}$ ($p=0.004$) cells (Willcoxon's matched paired test; Figure 5.7b).

Figure 5.6 The effect of LA1 on STAT phosphorylation in IL-12 and IL-15 activated NK cells

LA1 pre-treatment significantly decreases the fold-change in pSTAT5 (A), but not pSTAT4 (B) or pSTAT3 (C), at 10 minutes (left panel). No significant difference was seen at 2 hours (right panel).

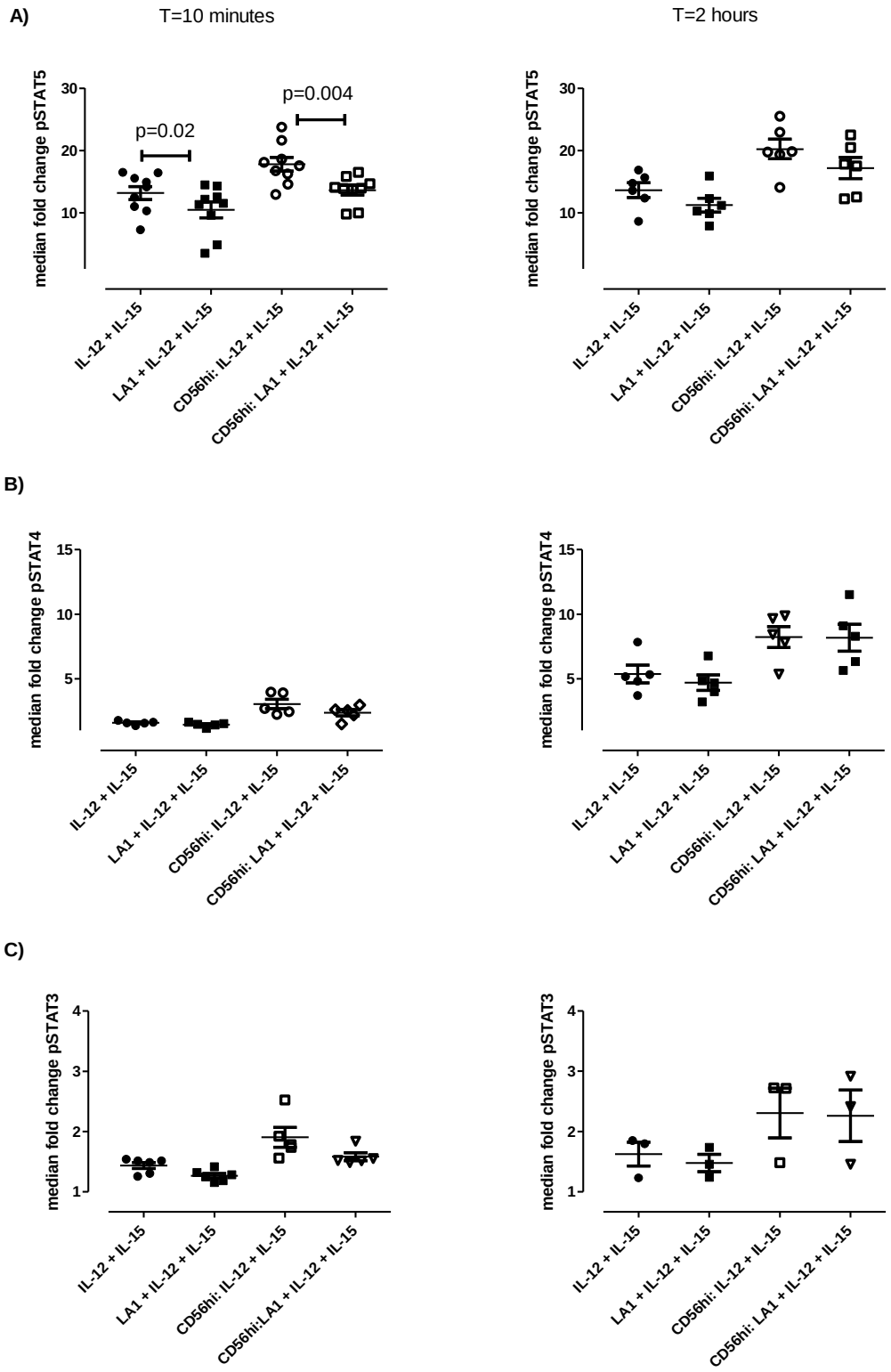

Figure 5.7 Reduced pSTAT5 positive cell population following LA1 pre-treatment

A) Scatter-plots show pSTAT5 (x-axis) and CD56 (y-axis) staining, before (left panel) and after (right panel) 10 minutes incubation with IL-12 and IL-15. Representative data from one experiment shows the effects of DMSO (top panel) and LA1 (bottom panel) pre-treatment. B) Comparison of percentages of cells positive for pSTAT5 at 10 minutes across nine independent experiments.

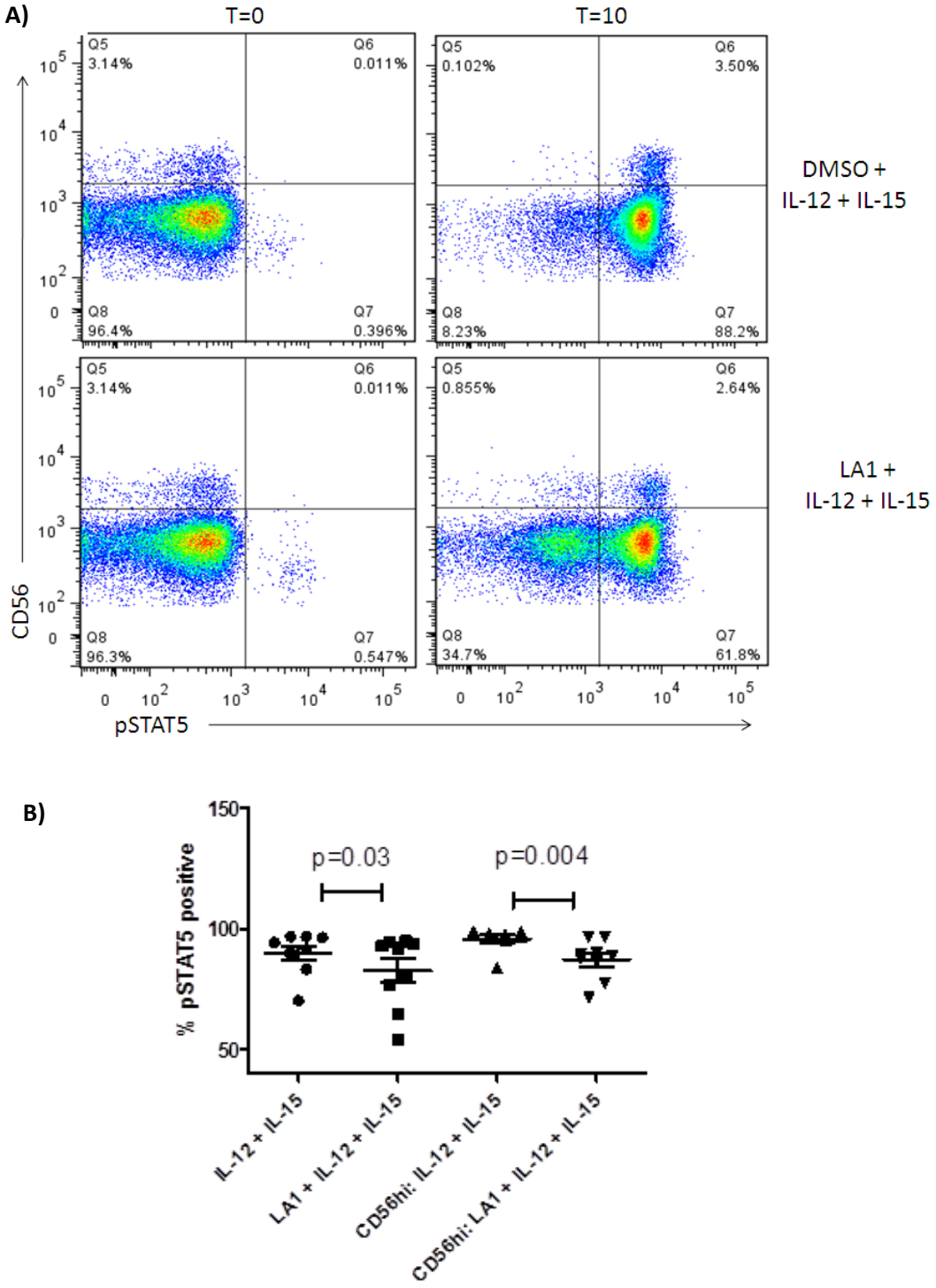

5.2.5 The effects of LA1 on STAT phosphorylation following IL-12 and IL-18 stimulation

IL-12-mediated STAT4 tyrosine phosphorylation is critical to induce IL-18Rβ expression (Kunikata et al. 1998; Nakahira et al. 2001; Sareneva, Julkunen, and Matikainen 2000). This is paramount for IL-18 signal transduction, as the IL-18Rα chain alone binds IL-18 but does not induce a pro-inflammatory signalling cascade (Nold-Petry et al. 2009; Hyun Kim et al. 2001; Wu et al. 2003). Measuring STAT4 tyrosine phosphorylation in this instance was therefore fulfilling two functions: directly measuring the effects of LA1 on IL-12R signalling, and indirectly measuring the potential affect of LA1 on IL-18Rβ expression (Nakahira et al. 2001).

An increase in pSTAT4 was observed following incubation with IL-12 and IL-18, and the fold-change was much greater after 2 hours incubation compared with that after 10 minutes (Figure 5.8b). The fold-change in pSTAT4 observed under both IL-12 and IL-15, and IL-12 and IL-18 activation are similar, suggesting that phosphorylation of STAT4 is mainly a result of IL-12 signalling, as previously reported (Matikainen et al. 2001). However, LA1 pre-treatment did not affect STAT4 phosphorylation (Figure 5.8b).

As expected, no increase in pSTAT5 was seen at either time point after IL-12 and IL-18 stimulation (Figure 5.8a). Similarly, no increase in pSTAT3 was observed at either time point (Figure 5.8c).

Figure 5.8 Fold-changes of pSTATs in NK cells activated with IL-12 and IL-18

LA1 pre-treatment does not affect the fold-change in pSTAT5 (A), pSTAT4 (B) or pSTAT3 (C), at either time points, 10 minutes (left panel) and 2 hours (right panel).

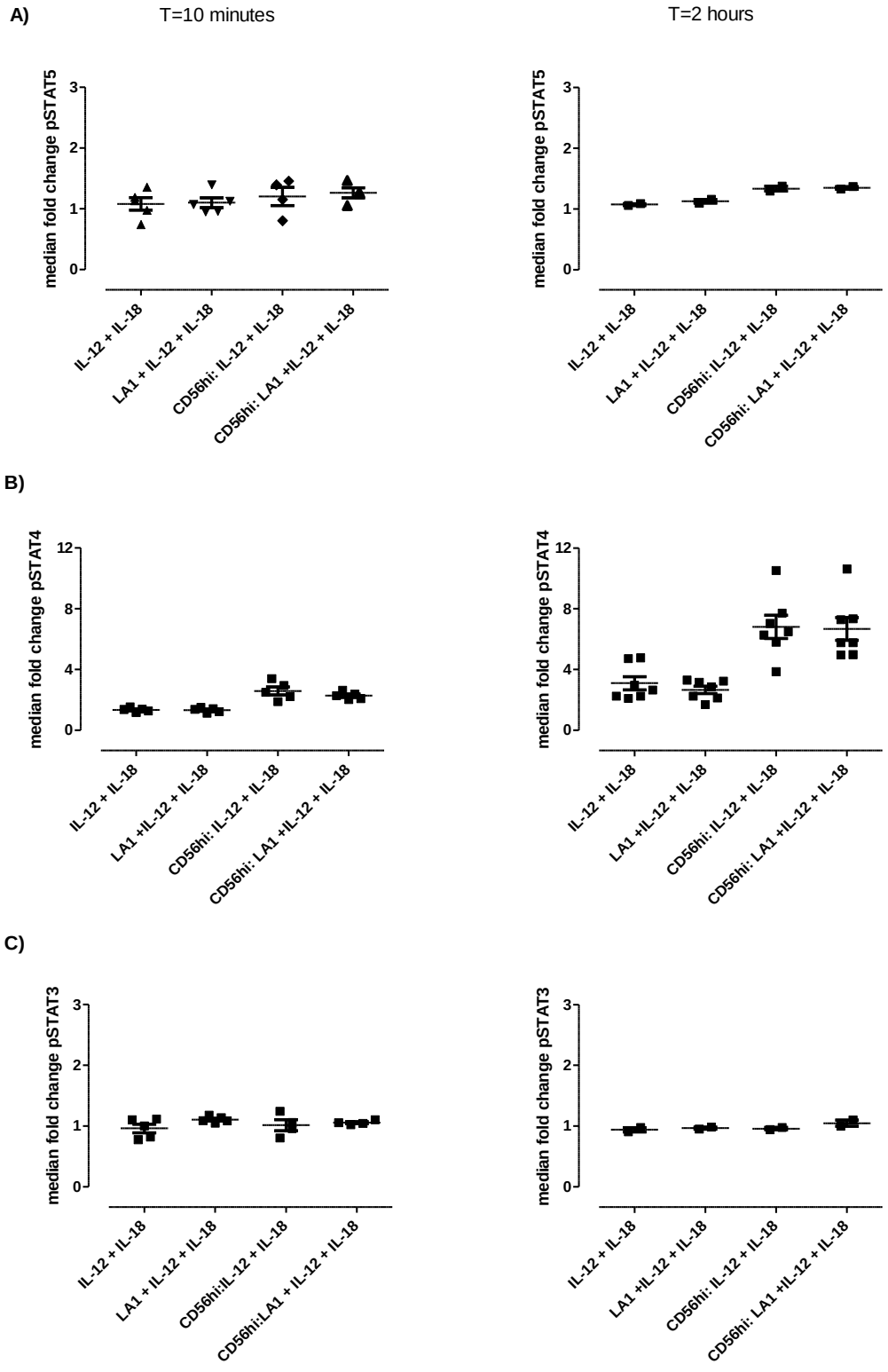

5.2.6 The effect of LA1 pre-treatment on the time-course of STAT phosphorylation

The contrast between the kinetics of STAT4 and STAT5 phosphorylation observed across two time-points – the former exhibiting a slower rate of phosphorylation, and the latter showing rapid yet sustained phosphorylation (Figures 5.5 and 5.7) – suggested that the time-courses of phosphorylation for the three STAT molecules may be of interest. I therefore wished to expand the range of time points to construct time-courses of phosphorylation.

Under the same experimental conditions, and in addition to 10 minutes and 2 hours, I measured the fold-change in median fluorescence intensity at 5, 30, and 60 minutes. In some instances, measurements were also taken after three and four hours of monokine activation (Figure 5.9 and Figure 5.10). These experiments were limited by the number of NK cells obtained from each donor sample, therefore I was unable to measure all STATs across every time point.

LA1 pre-treatment reduced the fold-change in pSTAT5 across all time points in both total and $CD56^{bright}$ NK cells following IL-12 and IL-15 activation (Figure 5.9a), adding further evidence that inhibition of IL-15-mediated STAT5 tyrosine phosphorylation is a possible mechanism through which LA1 inhibits NK cell cytokine production (Figure 5.1). Interestingly, despite IL-12 and IL-18 activation appearing not to induce an increase in pSTAT5 in the initial study with T=10 minutes and T=2 hours, a two-fold increase in the $CD56^{bright}$ subset was observed after 60 minutes incubation with the paired monokines (Figure 5.10a). However, unlike the down-regulation observed under the IL-15 activation, pre-treatment with LA1 did not affect the fold-change of pSTAT5 in this instance.

Overall, the combination of IL-12 and IL-15 increased the fold-change in pSTAT4 (Figure 5.9b) more so than that of IL-12 and IL-18 (Figure 5.10b). Even though STAT4 is known to be a key signalling molecule for IL-12-mediated signalling, IL-15 has also been shown to signal through STAT4 tyrosine phosphorylation (Strengell et al. 2003). My data suggest that IL-12 and IL-15 synergistically induce a greater degree of STAT4 tyrosine phosphorylation.

A modest increase in pSTAT3, with the greatest level of phosphorylation seen at 30 and 60 minutes, was observed following IL-12 and IL-15 stimulation (Figure 5.9c). Once more, due to the number of

NK cells obtained from whole blood being the limiting factor in these experiments, there is a great deal of variability in pSTAT3 fold-change under the IL-12 and IL-15 activated cells, and I feel further experiments are needed to confirm there is indeed no LA1 effect on STAT3 tyrosine phosphorylation. Very little change in pSTAT3 was observed following IL-12 and IL-18 stimulation. Although the fold-change was slightly higher in LA1 treated cells, the fold-change was very modest and therefore unlikely to be indicative of a functional difference (Figure 5.10c).

Under both activating conditions, the $CD56^{bright}$ NK cells consistently showed a greater degree of STAT tyrosine phosphorylation. This observation is in concordance with the paradigm that $CD56^{bright}$ cells produce greater levels of cytokines (Fehniger et al. 1999; Cooper, Fehniger, and Caligiuri 2001).

Figure 5.9 Time course of STAT tyrosine phosphorylation following IL-12 and IL-15 activation

The effects of DMSO (black) and LA1 (red) pre-treatment on (A) pSTAT5, (B) pSTAT4, and (C) pSTAT3 fold-change in total (left panel) and CD56^{bright} (right) NK cell activated with IL-12 and IL-15.

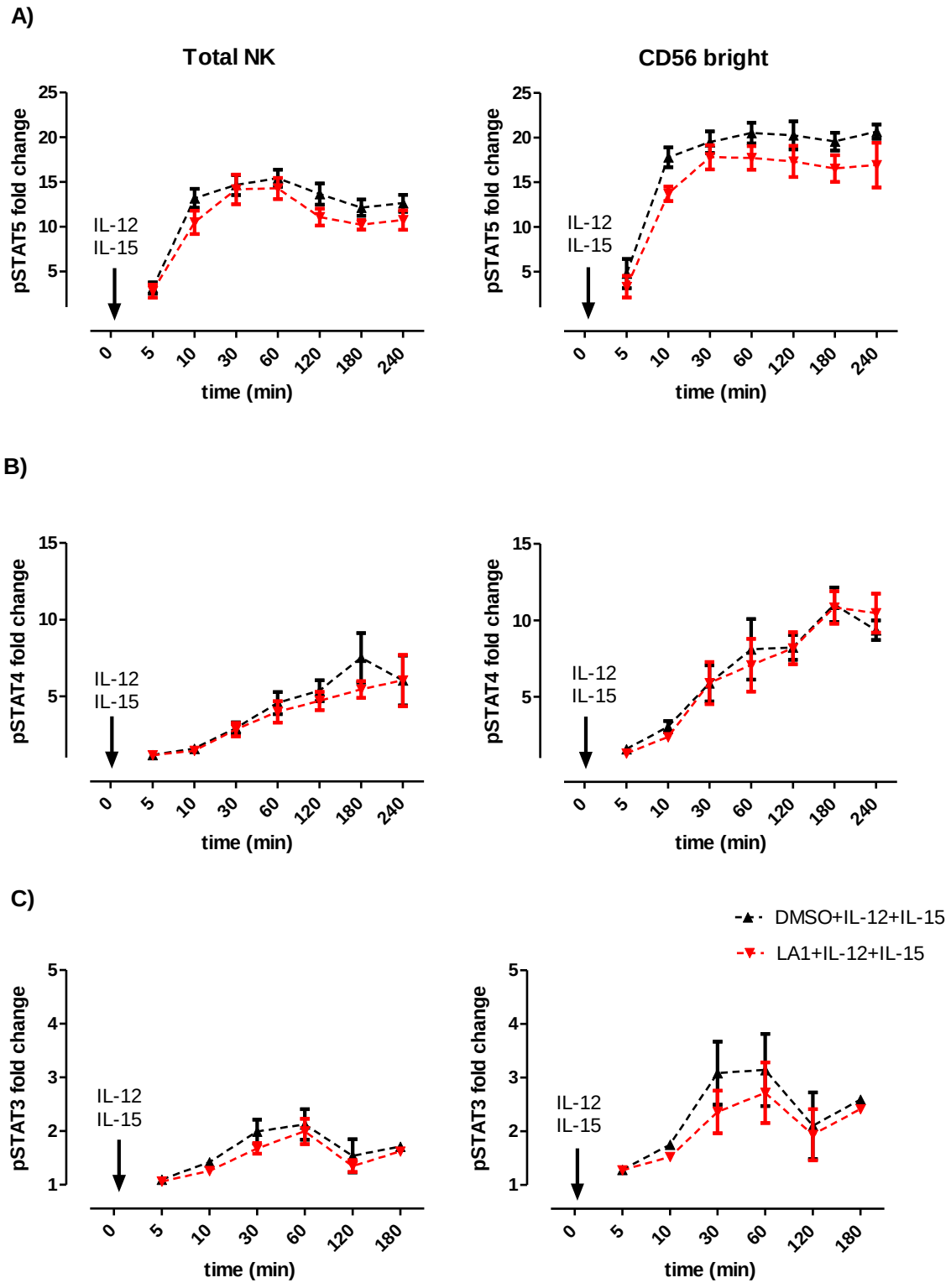

Figure 5.10 Time course of STAT tyrosine phosphorylation following IL-12 and IL-18 activation

The effects of DMSO (black) and LA1 (red) pre-treatment on (A) pSTAT5, (B) pSTAT4, and (C) pSTAT3 fold-change in total (left panel) and CD56^{bright} (right) NK cells activated with IL-12 and IL-18.

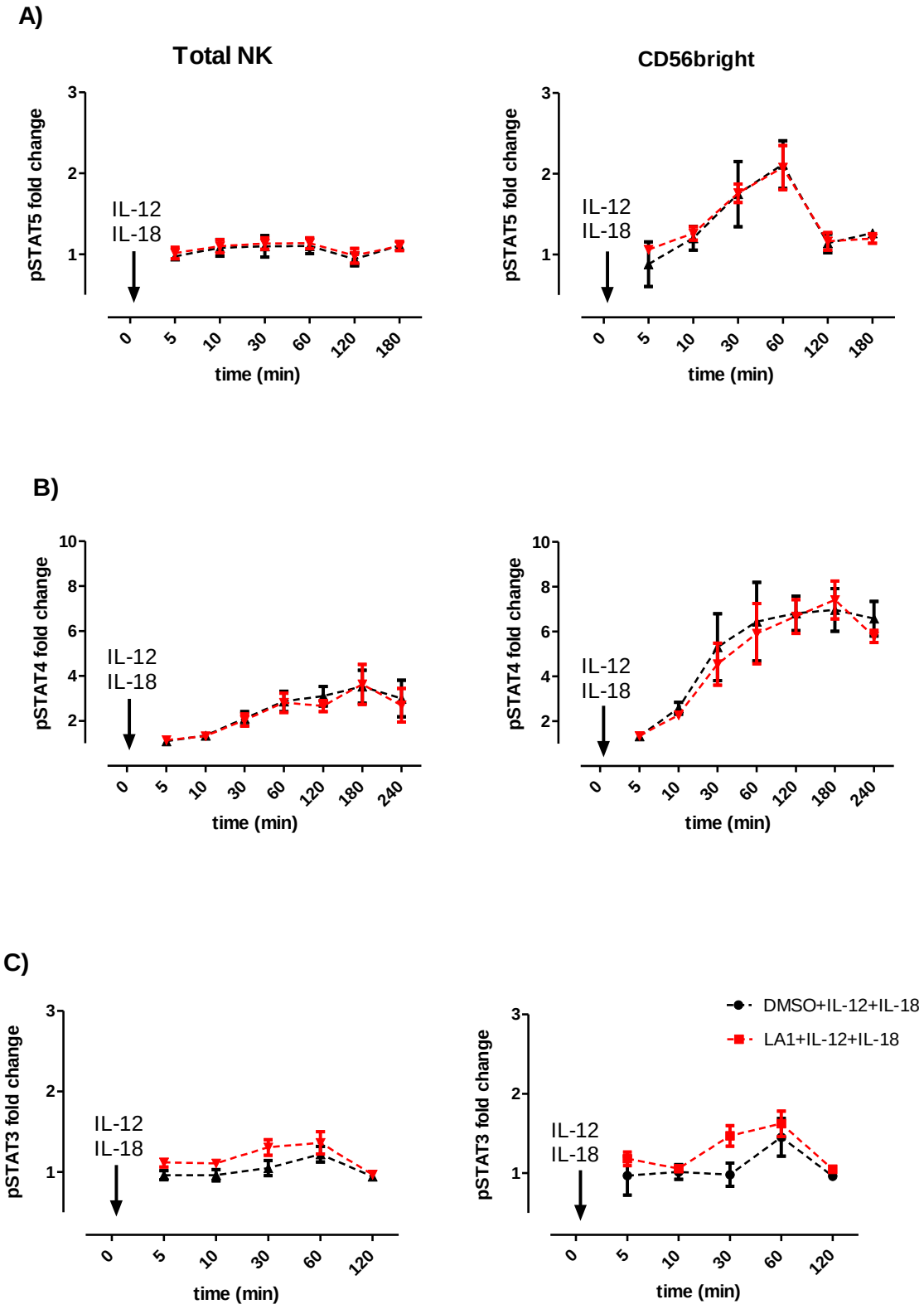

5.2.7 LA1 does not affect p38 MAPK phosphorylation in IL-12 and IL-18 activated NK cells

The two receptor chains that form the IL-18 receptor complex – IL-18α and IL-18Rβ – have different functions and utilise different signalling pathways. The former, which binds IL-18, utilises the MAP kinases and, through inhibition of its expression, has been shown to harbour inhibitory functions (Nold-Petry et al. 2009; Carroll, Paunovic, and Gadina 2008); the latter recruits MyD88 and is essential for IL-18R pro-inflammatory signalling (Adachi et al. 1998; Suzuki et al. 2003). I saw very modest changes in phospho-p38 following IL-12 and IL-18 activation, and LA1 did not appear to affect this (Figure 5.11). As described above, my STAT4 data did not suggest dysregulation of IL-18Rβ expression was a potential mechanism for LA1-mediated effects on IL-18 signalling. Therefore, it is very possible that LA1 affects IL-18Rβ signalling; a potential area for future work.

Figure 5.11 Time course of p38 MAPK phosphorylation following IL-12 and IL-18 activation

The effects of DMSO (black) and LA1 (red) pre-treatment on the fold-change of phosphor-p38 MAPK in total (left panel) and CD56^{bright} (right) NK cell activated with IL-12 and IL-18.

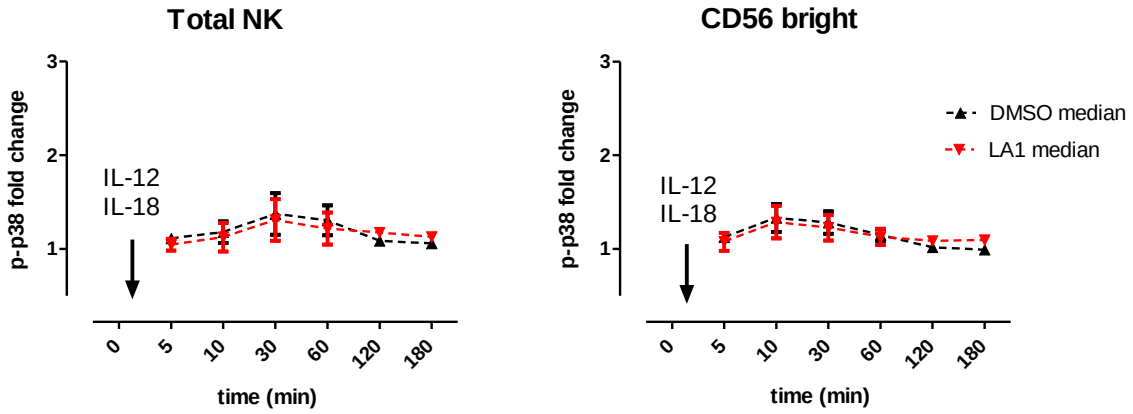

5.3 Discussion

In this chapter I have demonstrated that LA1 significantly reduces the IL-15-mediated fold-change in STAT5 tyrosine phosphorylation, in both total NK cells and the $CD56^{bright}$ subset, through a mechanism of decreasing the rate of phosphorylation. Synergistic activation of NK cells with paired monocyte-derived cytokines has been shown to produce a milieu of pro-inflammatory cytokines and chemokines (Fehniger et al. 1999). Even though stimulation with individual cytokines has been shown to result in relatively modest quantities of secreted products, IL-15 alone stimulates NK cells to produce large quantities of MIP-1β and TNF (Fehniger et al. 1999). Also, IL-15 alone has been shown to activate *IFNG* gene expression and IFN-γ protein production (Strengell et al. 2003). Therefore, it is possible that the reduced fold-change in STAT5 tyrosine phosphorylation presented in this chapter at least partly explain the reduced production of IFN-γ, TNF, and MIP-1β by IL-12 and IL-15 activated NK cells (Figure 5.11).

Furthermore, the data presented here suggest that LA1-mediated CR3 signalling interferes with the events that take place upstream of or during STAT5 phosphorylation: the activation of JAK kinases on the IL-15 receptor chains, the subsequent recruitment or binding of STAT5 to the phosphorylated receptor chains, or the phosphorylation of STAT5. Specifically, activation of JAK1 and JAK3 associated with the IL-2Rβ and γ_c-chains, respectively, have been shown to be crucial for STAT5 tyrosine phosphorylation in response to IL-15 (Johnston et al. 1995; Carroll, Paunovic, and Gadina 2008). It is possible, then, that LA1 has JAK kinase specificity, in which case other JAK1- and JAK3-dependent cytokine signalling pathways may also be affected (Jian-Xin Lin, Judy Mietz 1996).

A CR3-mediated effect on JAK kinases has recently been shown in human monocytes/macrophages. IL-13-mediated up-regulation of CD36 expression on activated human monocytes/macrophages is inhibited by pre-ligation of CR3 with either anti-CD18 or anti-CD11b antibodies (Yakubenko et al. 2013). CR3 activation blocks the phosphorylation of IL-13 receptor-associated Jak-2 and Tyk-2 kinases, which further inhibits the downstream tyrosine and serine phosphorylation of STAT1, STAT3, and STAT6 (Yakubenko et al. 2013). These effects were dependent on CR3 ligation occurring before cellular activation. Interestingly, this demonstrated agonist chronology is also paramount for the LA1-mediated effects on TLR signalling; TLR activation before CR3 ligation with LA1 overrides its regulatory effects (Reed et al. 2013).

On the other hand, interleukins can activate common JAKs yet their downstream signalling can diverge at the STAT level; it is the tyrosine-based motifs in the receptor components that dictate their STAT specificity (Stahl et al. 1995; Johnston et al. 1995). For instance, IL-12 and IL-13 both utilise Jak-2 and Tyk-2, yet IL-13, unlike IL-12, does not phosphorylate STAT4 (Yakubenko et al. 2013). In this chapter I have shown the effects of LA1 on IL-15R signalling; therefore LA1-mediated effects could be specific for IL-2Rβ or the common γ_c-chain. For example, if the observed effects were a product of common γ_c-chain-specificity, LA1 could plausibly regulate the signalling of all other IL-2-family cytokine receptors which contain the γ_c-chain: IL-2, IL-4, IL-9, and IL-21 (Lin and Leonard 2000). Particularly as all common γ_c-chain-containing receptors have been shown to signal through STAT5 (Lischke 1998). The IL-2Rβ, on the other hand, is only shared by IL-2 and IL-15 receptor complexes (Lin and Leonard 2000). Therefore, measuring the effects of LA1 on the NK cell activating effects of other cytokines may help delineate the molecular mechanisms of LA1-mediated NK cell regulation and determine the level at which its specificity lies: cytokine receptor, JAK, or STAT.

An unexpected observation was that of a short-lived, two-fold increase in STAT5 phosphorylation in $CD56^{bright}$ cells after 60 minutes incubation with IL-12 and IL-18 (Figure 5.10a). The demonstration that LA1 pre-treatment did not affect this suggests that its effects are not STAT5-specific. However, the involvement of STAT5 in IL-12 or IL-18 signalling has not been previously described; therefore any further interpretation of this observation is very difficult.

The epitope of the anti-pSTAT5 antibody used in this study identifies the phosphorylated tyrosine at amino acid 694 (Y694) of STAT5A. However, the orthologous phosphorylation site in STAT5B is Y699, and by comparing the flanking amino acid sequences of these tyrosine residues, we can see that the antibody is not predicted to differentiate between the STAT5A and STAT5B isoforms (Table 5.1). If I had the ability to measure both STAT5 isoforms independently, it is possible that I would see a fold-change difference in only one isoform. Therefore, the reduction presented in this chapter could indeed be a modest estimation of the true effects of LA1 on STAT5 signalling. That is, if only one of STAT5A or STAT5B tyrosine phosphorylation is inhibited by LA1, the results obtained by the anti-pSTAT5 antibody may be diluted. It may be possible to estimate STAT5 isoform specificity by using a qPCR with STAT5A and STAT5B specific targets to delineate which, if not both, STAT5 isoform is regulated by CR3 (Basham et al. 2008).

Table 5.1 Comparison of STAT5A and STAT5B peptide sequences surrounding the anti-pSTAT5 antibody epitope pY694

The amino acid sequence surrounding the Y694 (bold) of STAT5A is identical to the orthologous amino acid sequence in STAT5B (Y699). Therefore the anti-pSTAT5 antibody will recognise both isoforms when they are phosphorylated.

STAT5 Isoform	Peptide Sequence
STAT5A	VDG**Y**VKPQIK
STAT5B	VDG**Y**VKPQIK

In addition to forming homodimers, under certain conditions, which are incompletely understood, STATs can form heterodimers, and STAT5 has been shown to heterodimerise with STAT3. Indeed, the ability to induce homo- or heterodimers may be indicative of yet another level on which signalling specificity is controlled by cytokine receptors (Delgoffe and Vignali 2013). Furthermore, STAT3 and STAT5 have been shown to reciprocally regulate IL-17 production (X. Yang et al. 2011). The LA1-mediated effects on pSTAT5 presented here may therefore indirectly affect STAT3; either by skewing the cellular ratio of pSTAT5:pSTAT3, or by reducing the possibility of pSTAT3-pSTAT5 heterodimer formation.

IL-18 binds the IL-18Rα chain, but, in the absence of IL-18Rβ expression, no pro-inflammatory signal is induced (Suzuki et al. 2003; Adachi et al. 1998; Hyun Kim et al. 2001; Wu et al. 2003). Absence or inhibition of IL-18Rα leads to the somewhat paradoxical increase in MAP kinase signalling and cytokine production, due to the anti-inflammatory properties of IL-18Rα (Nold-Petry et al. 2009; Lewis and Dinarello 2006). I saw a short-lived, modest increase in phosphorylated p38 MAPK, but no evidence that LA1 affected this.

IL-15 and IL-12 have been shown to induce IL-18Rβ expression (Hyun Kim et al. 2001; Kunikata et al. 1998; Nakahira et al. 2001). For this reason, without IL-12 or IL-15 co-stimulation, IL-18 does not induce IFN-γ (Kunikata et al. 1998). STAT4 signalling is paramount to the IL-12-mediated induction of IL-18Rβ expression (Sareneva, Julkunen, and Matikainen 2000; Nakahira et al. 2001). Therefore, the

observation that LA1 pre-treatment did not affect STAT4 tyrosine phosphorylation suggests dysregulation of IL-12-mediated IL-18Rβ expression is not a likely mechanism of LA1 function. However, it would be of interest to confirm this by measuring the cell surface expression of IL-18Rβ following IL-12 activation, with and without LA1 pre-treatment.

It was not possible to include members of the IL-18Rβ signalling cascade in my flow cytometry experiment, due to the lack of phospho-specific antibodies. IL-18Rβ recruits MyD88, which in turn phosphorylates IRAK1 and IRAK4, ultimately leading to NFκB translocation (Strengell et al. 2003; Carroll, Paunovic, and Gadina 2008; Kanakaraj et al. 1999). It is likely, then, that LA1 may interfere with the IL-18Rβ signalling cascade, and it is of particular interest that the LA1-mediated inhibition of TLR-signalling in monocytes/macrophages is thought to be MyD88-dependent (C. Han et al. 2010; Reed et al. 2013).

CR3 engagement has been shown to have regulatory effects in cell types including monocytes, macrophages, and dendritic cells (Rhodes et al. 2012; C. Han et al. 2010; Bai et al. 2012). Furthermore, the SLE-associated R77H variant has been shown to negatively affect these regulatory functions. Using the U937 monocyte cell line, Macpherson and colleagues demonstrated elevated levels of IL-6 production in CD11b-77H-expressing cells compared with CD11b-WT (MacPherson et al. 2011). Additionally, pre-treatment of *ex vivo* monocytes with iC3b-coated RBCs prior to TLR7/8 engagement with the R848 agonist results in reduced secretion of pro-inflammatory cytokines IL-1β, IL-6 and TNFα. However, this regulatory effect is significantly less pronounced in 77H-homozygous cells (Rhodes et al. 2012).

It is possible that CR3 plays a similar regulatory role on NK cells. However, the role of CR3 on NK cells is incompletely understood and is often overlooked in reviews of the topic (Fagerholm et al. 2013). The combined work presented in this chapter is the first study of the effects of LA1 on NK cell function. The lack of a genotypic effect in the regulation of NK cell cytokine production demonstrates how LA1-mediated allosteric activation of CR3 is very different to that of natural ligands. Even though the effects of R77H on the functions of NK cells have not been addressed, this SLE-associated variant is likely to have functional consequences given the multitude of effects already demonstrated using various *in vitro* models and *ex vivo* cells (MacPherson et al. 2011; Rhodes et al. 2012; Fossati-Jimack et al. 2013). In addition, LA1 does not mimic natural ligands (Faridi

et al. 2013). Therefore, the results of this study are not a model for the role of CR3 on NK cells following natural ligand ligation and should not be extrapolated as such.

There are reports in the literature of pro-inflammatory roles of CR3 (Fan and Edgington 1993). One study using human monocytes reported that ligation of CD11b with antibodies or soluble CD23 induced the production of MIP-1α and MIP-1β (R. Rezzonico 2001). These data are very much in contrast with LA1-mediated effects presented here, which highlight the contrasting effects of CR3 ligands. However, ligand avidity has been shown to dramatically influence CR3 signalling, which may explain these paradoxical results (Wang et al. 2010).

Given the cellular distribution of CR3 expression, in an *in vivo* setting LA1 is likely to have very significant systemic regulatory effects. CR3 ligation with anti-CD11b antibodies or iC3b suppresses IL-12 production by bacteria-infected or IFN-γ-stimulated monocytes (Marth and Kelsall 1997; Yoshida et al. 1998), and a recent study shows that *Leishmania major*-mediated inhibition of IL-12 secretion by macrophages is CR3-dependent (Ricardo-Carter et al. 2013). Once more, the effects of specific CR3 ligands should not be used to predict the effects of other agonists, as stated above. However, if LA1 were also to suppress IL-12 production by monocytes, coupled with its demonstrated regulatory effects on monokine-stimulated NK cells, LA1 could lead to a significant systemic decrease in pro-inflammatory cytokines.

In summary, the work presented in this chapter demonstrates that LA1:

- Inhibits the IL-15-mediated STAT5 tyrosine phosphorylation
- Does not affect IL-12-mediated STAT4 tyrosine phosphorylation, and for this reason is unlikely to affect the IL-12-mediated induction of IL-18Rβ expression
- Does not affect the p38 MAPK phosphorylation following IL-18 signalling.

As described in this discussion, further experiments are of both great importance and interest to further our understanding of the regulatory effects of LA1. These experiments are summarised in Chapter 7.

Chapter 6: Genetic interaction within the *FCGR* locus

6.1 Introduction

Reduced copy number of *FCGR3B* on chromosome 1q23.3 is robustly associated with SLE (P_{meta}=9.1x10^{-7}, OR=1.59; McKinney & Merriman, 2012), and has been shown to be strongly correlated with the CD16b protein expression and function (Morris et al. 2010; Willcocks et al. 2008). Within the same complex *FCGR* genomic locus, homozygosity of the minor allele of the rs1050501 polymorphism (Chr1:161643798) located in exon 5 of *FCGR2B* and encoding a non-synonymous coding variant I232T within the transmembrane domain of inhibitory receptor CD32b, has also been shown to be associated with SLE (P_{meta}=8 x10^{-6}, OR=1 .73; Willcocks et al., 2010). This polymorphism has been shown to reduce the inhibitory function of CD32b on B cells and macrophages (Xiaoli Li et al. 2003; Kono et al. 2005; Clatworthy et al. 2007). Studies in Southeast Asian cohorts have shown consistent associations between *FCGR2B*-232T homozygosity and SLE (Chen et al. 2006; Kyogoku et al. 2002; Siriboonrit et al. 2003; Chu et al. 2004), whereas studies in European cohorts have been inconsistent, with some, albeit small, studies failing to find a significant association (Xiaoli Li et al. 2003; V. Magnusson 2004). It is possible that the lower minor allele (C) frequency in European populations (MAF=0.1) compared with that in Southeast Asians (MAF=0.22-0.25), resulting in reduced power to detect an association, explains these discrepancies (Clatworthy et al. 2007; Chen et al. 2006; Siriboonrit et al. 2003; Kyogoku et al. 2002; Chu et al. 2004). Nonetheless, the *FCGR2B*-I232T effect has consistently been shown to be in the same direction and meta-analyses have successfully demonstrated a strong disease association with *FCGR2B*-232T homozygosity (Willcocks et al. 2010; Niederer et al. 2010b).

The *FCGR3B* copy number variable region spans ~85Kb of the *FCGR* locus, and, in addition to the complete absence of the *FCGR3B* gene, a deletion also amalgamates the coding region of *FCGR2B* with the regulatory region of *FCGR2C* resulting in the ectopic expression of the inhibitory receptor CD32b on NK cells (Mueller et al. 2013), as discussed previously in section 1.7.4.

In this study I wished to investigate whether the SLE-association with reduced *FCGR3B* copy number was partly explained by the ectopic expression of *FCGR2B*. I genotyped the *FCGR2B*-I232T polymorphism (rs1050501) and estimated *FCGR3B* copy number variation (CNV) in SLE cases and

healthy controls of European ancestry to test for a genetic interaction between the two SLE-associated variations. If it is possible to identify epistasis between associated variants, we may find that we have explained far more disease heritability than previously thought (Zuk et al. 2012).

6.2 Results

6.2.1 Genotyping FCGR2B-I232T

I used PCR amplification followed by capillary sequencing (Figure 6.1) to genotype the rs1050501 SNP (*FCGR2B*-I232T) in 627 SLE cases and 864 controls (Methods 2.1.2). Due to the high sequence identity between the 5' regions of *FCGR2B* and *FCGR2C* (see Introduction 1.7.1) it is paramount to design PCR primers that will provide *FCGR2B* specificity for accurate genotyping of the rs1050501 polymorphism. I used primers as described previously (P. Zhou et al. 2008; Morris et al. 2010), whereby PCR specificity is achieved from the reverse primer, which anneals to intron 5 of the *FCGR2B* gene (chr1:161645840-161645862), downstream of the *FCGR2B*/*C* homologous region.

I did not observe a deviation from Hardy-Weinberg equilibrium for the rs1050501 genotype frequencies within the control samples (χ^2=0.71; p=0.4). Also, I observed a MAF of 0.10, which is consistent with a previous estimates in European cohorts (Clatworthy et al. 2007). Therefore I am confident in the accuracy of my genotype results (Table 6.1a).

6.2.2 FCGR2B-I232T Case/Control Analysis

I used chi-squared tests (2x2 contingency table; df =1) to compare allele frequencies of the rs1050501 variant between cases and controls, as summarised in Table 6.1c. I did not observe a significant difference at the 95% level using 627 SLE cases and 864 controls (χ^2=0.8; p=0.37). 232T-homozygosity has previously been associated with SLE (Kyogoku et al. 2002; Willcocks et al. 2010). I observed no evidence of an association between 232T-homozygosity (genotype = CC) and disease risk at the 95% level (Table 6.1b; p=0.17; Fisher's exact test). The genotype frequencies for the control group - 0.987 for TT and TC combined, and 0.013 for CC (232T-homozygous) - correlate very strongly with those reported by Willcocks and colleagues, in which the 1958 Birth Cohort was also used (Willcocks et al. 2010). This indicates a high degree of reproducibility in the genotyping of rs1050501. The low MAF (0.1) resulted in very small numbers for the homozygous risk group in both

cases and controls (Table 6.1a). However, the cohort size (n=1491) is comparable to a previous study which detected an association (n=1622; Willcocks et al., 2010), suggesting I had sufficient power.

Figure 6.1 *FCGR2B* rs1050501 genotyping by capillary sequencing

(A) An ethidium bromide-stained agarose gel as observed under UV-transillumination showing the 3Kb amplified fragment of *FCGR2B* following Long-Range PCR amplification. The Hyper Ladder I DNA ladder (Lane 1) and PCR negative control (Lane 3) are shown. (B) Electropherogram representations of all three possible genotypes – TT, TC, and CC - of the rs1050501 SNP following capillary sequencing.

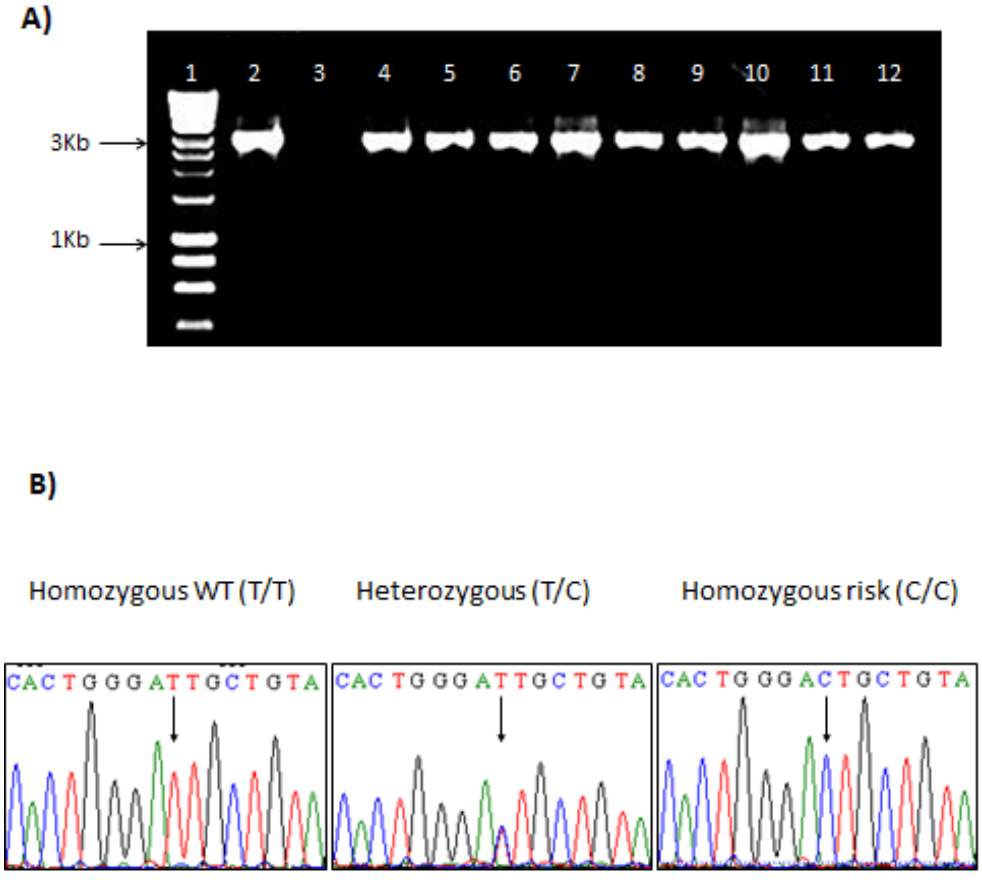

Table 6.1 *FCGR2B* rs1050501 genotyping results for cases and controls.

A) Absolute genotype counts and calculated frequencies are presented for 627 cases and 864 controls. No deviation from Hardy-Weinberg was observed in controls (χ^2=0.71; p=0.4). B) Combined genotype counts and frequencies of homozygous WT (TT) and heterozygous (TC) compared with homozygous risk (CC). No significant difference in 232T-homozygosity was observed (p=0.17; Fisher's exact test). C) Absolute allele counts and calculated frequencies for 1254 SLE chromosomes and 1728 control chromosomes. No significant difference was observed between allele frequencies (χ^2=0.8; p=0.37).

A)

rs1050501	Cases (n=627)		Controls (n=864)	
genotype	n	Frequency	n	Frequency
TT	516	0.823	701	0.811
TC	108	0.172	152	0.176
CC	3	0.005	11	0.013

B)

rs1050501	Cases (n=627)		Controls (n=864)	
genotype	n	Frequency	n	Frequency
TT or TC	624	0.995	853	0.987
CC	3	0.005	11	0.013

C)

rs1050501	Cases (n=1254)		Controls (n=1728)	
allele	n	Frequency	n	Frequency
T	1140	0.909	1554	0.899
C	114	0.091	174	0.101

Figure 6.2 *FCGR2B*-I232T (rs1050501) genotype and allele frequencies

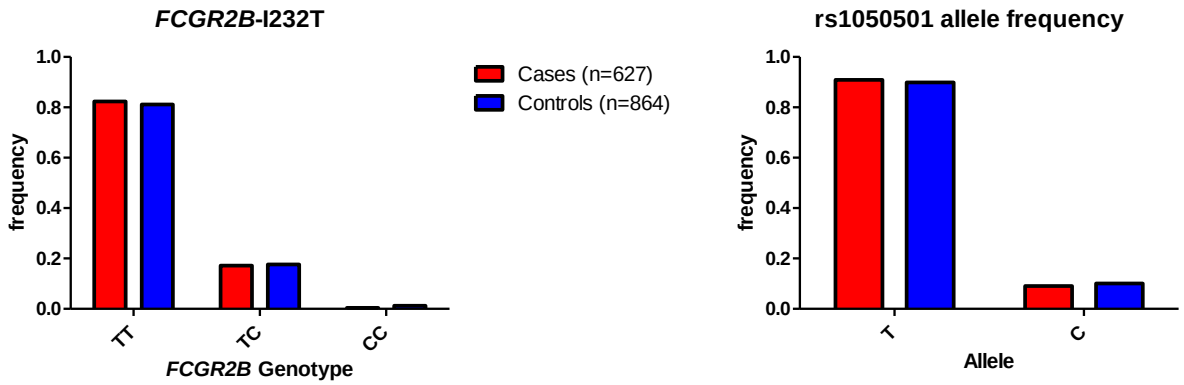

6.2.3 Meta-analysis of FCGR2B association

I conducted a meta-analysis by combining my data with that of five independent cohorts of European ancestry: Swedish (n=491; V. Magnusson 2004), European American (n=285; Li et al. 2003), UK (n=1622; Willcocks et al. 2010), Swedish (n=544; Niederer et al. 2010b), and UK (n=650; Niederer et al. 2010b), as reported fully in the supplementary data of two publications (Niederer et al. 2010b; Willcocks et al. 2010). As stated above, my control cohort was partly made up by samples from the 1958 Birth Cohort, as was the UK cohort from the study by Willcocks and colleagues. Therefore, to avoid the potential of duplicate samples, I removed the data for the 494 samples from the 1958 Birth Cohort included in my genotyping, leaving 370 controls from the TwinsUK Bioresource cohort (Methods 2.1.2). This reduced my final sample size to 997.

I combined the data, as summarised in Table 6.2, and performed a meta-analysis using a total of 1830 cases and 2759 controls (n=4589; Figure 6.3). I found strong evidence for an association with 232T-homozygosity (χ^2= 11.34; p=0.0008; OR=1.90 (1.28-2.81)).

Table 6.2 Summary data of the *FCGR2B*-232T homozygosity and SLE risk meta-analysis.

The combined rs1050501 genotype data from six independent cohorts of European ancestry: UK (n=997; this study), Swedish (n=491; V. Magnusson 2004), European American (n=285; Li et al. 2003), UK (n=1622; Willcocks et al. 2010), Swedish (n=544; Niederer et al. 2010b), and UK (n=650; Niederer et al. 2010b). 232T-homozygosity is strongly associated with SLE risk (p=0.0008; OR=1.90).

Rs1050501	Cases (n=1830)		Controls (n=2759)	
genotype	n	Frequency	n	Frequency
TT or TC	1770	0.97	2711	0.98
CC	60	0.03	48	0.02

Figure 6.3 Forest plot of the *FCGR2B*-232T-homozygosity and SLE meta-analysis.

Meta-analysis of 1830 cases and 2759 controls from six case/control studies shows the strong association of *FCGR2B*-232T homozygosity and SLE.

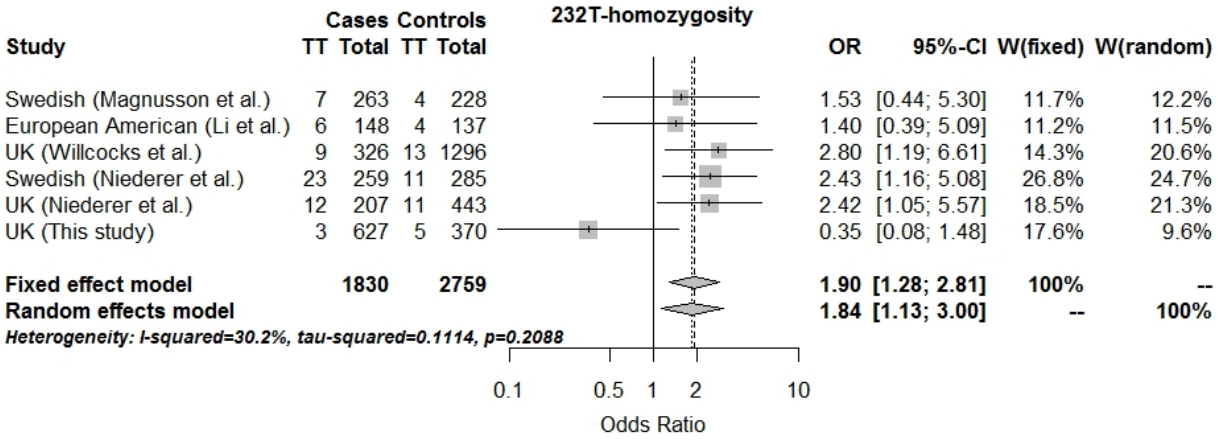

6.2.4 Measuring FCGR3B CNV

The prologue ratio test (PRT) is a robust methodology for estimating gene copy number within a copy number variable region (Armour et al. 2007). The PRT test has been used to measure copy number variation across several loci (Boteva et al. 2012; Fode et al. 2011; X.-J. Zhou et al. 2012), including *FCGR3B* (Morris et al. 2010; Niederer et al. 2010b).

I used this robust assay to measure the *FCGR3B* copy number in the SLE cases and healthy controls (Methods Figure 2.3). 561 SLE cases and 708 healthy controls (Methods 2.1.2) were successfully genotyped for both the *FCGR2B*-I232T variant and *FCGR3B* CNV. The results are summarised by genotype in Table 6.3 and by allele in Table 6.4, and displayed in Figure 6.3.

There was no difference in rs1050501 allelic frequency between the *FCGR2B*-I232T only data (n=1491; Table 6.1c) and the samples with both *FCGR2B*-I232T and *FCGR3B* CNV (n=1269; Table 6.4a) for cases (χ^2=0.043) or controls (χ^2=0.046), indicating there was no rs1050501 genotype-specific bias in the samples that failed the *FCGR3B* CNV assay.

Table 6.3 *FCGR2B* rs1050501 genotyping results conditioned on *FCGR3B* copy number

Genotype counts and frequencies for rs1050501 genotype groups, and combined TT and TC genotype groups are displayed for A) Total samples (not conditioned on *FCGR3B* copy number), B) Conditioned on two or more copies (no deletion) of *FCGR3B*. (C) Results conditioned on fewer than two copies of *FCGR3B* (at least one gene deletion). No significant difference in 232T-homozygosity was observed between case and control when genotype counts for combined groups (TT or TC) and homozygous risk (CC) were compared using Fisher's exact test for (A) p=0.25 and (B) p=0.25.

A)

rs1050501	Cases (n=561)		Controls (n=708)	
genotype	Absolute	Frequency	Absolute	Frequency
TT	460	0.820	572	0.808
TC	98	0.175	127	0.179
TT or TC	558	0.995	699	0.987
CC	3	0.005	9	0.013

B)

rs1050501	Cases (n=498)		Controls (n=654)	
genotype	Absolute	Frequency	Absolute	Frequency
TT	407	0.817	523	0.800
TC	88	0.177	122	0.187
TT or TC	495	0.994	645	0.986
CC	3	0.006	9	0.014

C)

rs1050501	Cases (n=63)		Controls (n=54)	
genotype	Absolute	Frequency	Absolute	Frequency
TT	53	0.841	49	0.907
TC	10	0.159	5	0.093
TT or TC	63	1.00	54	1.00
CC	0	0.00	0	0.00

Table 6.4 *FCGR2B* rs1050501 allelic results conditioned on *FCGR3B* copy number

Total rs1050501 allele counts and relative calculated frequencies are displayed for A) Total samples (not conditioned on *FCGR3B* copy number). B) Results conditioned on two or more copies (no deletion) of *FCGR3B*. (C) Results conditioned on fewer than two copies of *FCGR3B* (at least one gene deletion). N values refer to number of chromosomes. No significant difference was observed between case and control allele counts in any group: χ^2=0.67 (p=0.41), 0.99 (p=0.32), and 1.06 (p=0.30) for A, B, and C, respectively.

A)

rs1050501	Cases (n=1122)		Controls (n=1416)	
Allele	Absolute	Frequency	Absolute	Frequency
T	1018	0.907	1271	0.898
C	104	0.093	145	0.102

B)

rs1050501	Cases (n=996)		Controls (n=1308)	
Allele	Absolute	Frequency	Absolute	Frequency
T	902	0.906	1168	0.893
C	94	0.094	140	0.107

C)

rs1050501	Cases (n=126)		Controls (n=108)	
Allele	Absolute	Frequency	Absolute	Frequency
T	116	0.921	103	0.954
C	10	0.079	5	0.046

6.2.5 FCGR2B-I232T and FCGR3B CN Interaction

I combined the rs1050501 genotype groups TT (homozygous WT) and TC (heterozygous) for cases (n=498) and controls (n=654) without a *FCGR3B* deletion (CN≥2; Table 6.3b) to test for an association with minor allele (CC) homozygosity (232T-homozygosity). No significant difference between cases and controls was observed (p=0.25; Fisher's exact test). Furthermore, I used a chi-squared test (2x2 contingency table; df =1) to compare the allele counts of the rs1050501 variant between cases (n=498) and controls (n=654) without a *FCGR3B* deletion (CN≥2), as summarised in Table 6.4b. No difference was observed at the 95% significance level (χ^2=0.99; p=0.32).

I did not observe homozygosity of the rs1050501 minor allele (C) together with a reduced CN (<2) of *FCGR3B* in any individual from either the case or control cohort, therefore I could not test for a 232T-homozygosity effect. This could be expected given the MAF of ~0.10 (therefore q^2=0.01) and the small sample size within the *FCGR3B* <2 cohorts. The estimated 'C' allele frequency in cases with *FCGR3B* deletion is 0.079 (Table 6.4c). Therefore I should expect to observe 232T-homozygosity by increasing the sample size to n=160. However, the equivalent MAF in controls is 0.046 (Table 6.4c), and 232T-homozygosity would not be expected to be observed in fewer than 466 samples.

I compared the allele counts of the rs1050501 variant between cases (n=63) and controls (n=54) with at least one *FCGR3B* deletion (CN<2), as summarised in Table 6.3c. Despite observing a higher frequency of the minor allele (C) in cases with reduced *FCGR3B* CN compared with controls (Figure 6.4c), this did not reach significance at the 95% level (Fisher's exact test p=0.42). An interaction between *FCGR2B*-I232T and *FCGR3B*-CNV was tested for by fitting an additive logistic regression model (SLE status as the outcome) using the statistical computing language R. The interaction term was not significant (p=0.09).

Figure 6.4 *FCGR2B*-I232T genotype and allele frequencies conditioned on *FCGR3B* copy number

Frequencies in A) total samples irrespective of *FCGR3B* copy number, B) samples conditioned on ≥2 copies *FCGR3B* and C) samples conditioned on <2 copies *FCGR3B*. No significant difference between cases and controls was observed in 232T-homozygosity (p=0.25 Fisher's exact test) or allele frequencies (p=0.32; chi-squared) in B, or allele frequencies (p=0.42; Fisher's exact test) in C.

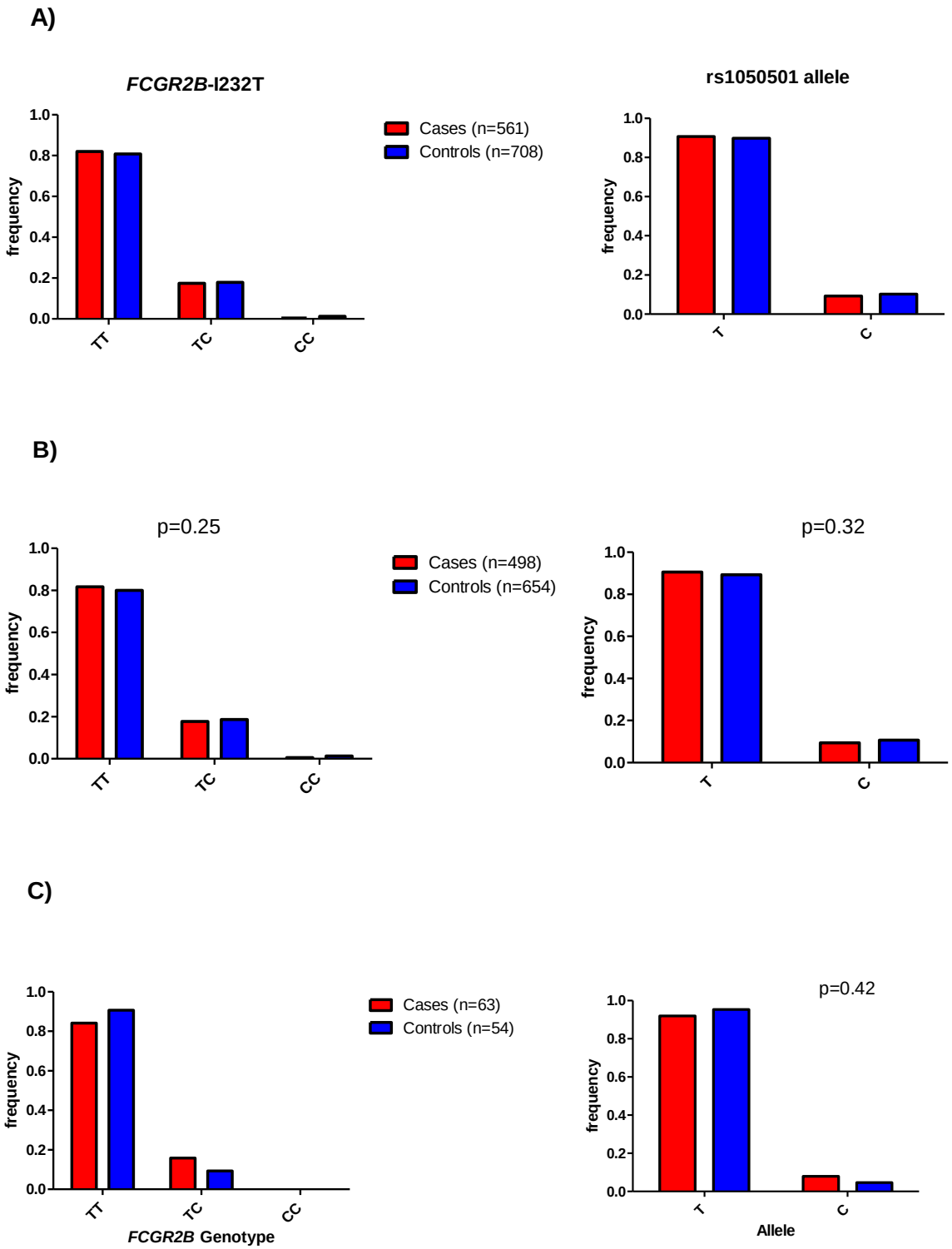

6.3 Discussion

The paradigm of 'missing heritability' in recent years has focused on as-of-yet unidentified genetic variants that, once identified, are expected to increase the amount of heritability of complex diseases explained by additive genetic variation. However, this paradigm assumes an additive model of contribution for each genetic variant, both known and unknown (Zuk et al. 2012). Without fully exploring the possibility of epistasis between associated genetic variants, whereby the combined effect of two risk factors is greater than the sum of the effects of the individual variants, we may be underestimating the amount of heritability explained (Eichler et al. 2010). In which case, at least part of what is currently considered as 'missing heritability' could in fact be 'phantom heritability' due to the assumption that the heritability of complex diseases is largely additive (Zuk et al. 2012). Indeed, gene-gene interactions between associated SNPs in SLE have been successfully identified in recent years in European and Chinese populations, as discussed in section 1.2.4 (X. Zhou et al. 2012; Hughes et al. 2012; Leng et al. 2012; Zuo et al. 2014).

The *FCGR* locus is of particular interest in this instance following the recent identification of ectopically expressed CD32b on NK cells as a result of the *FCGR3B* gene deletion (Mueller et al. 2013). This molecular peculiarity presents a fascinating *a priori* hypothesis of potential genetic interaction. Additionally, perhaps the true effect size of the *FCGR2B*-232T association with SLE is underestimated without the consideration of *FCGR3B* CNV. That is, the under-functioning CD32b-232T variant may also contribute to SLE risk when ectopically expressed on NK cells, as has been demonstrated with B cells and macrophages (Floto et al. 2005; Kono et al. 2005). The ectopic expression of CD32b does not abolish its B cell expression (Mueller et al. 2013). Such an under-functioning effect on an additional cell type may lead to an increased effect size when considered together with reduced *FCGR3B* CN. In the absence of this *FCGR3B* CNV consideration, studies could potentially be underestimating the contribution of *FCGR2B*-232T to SLE susceptibility.

Reduced CN at *FCGR3B*, which is among the strongest genetic risk factors for SLE (OR=1.59), has been shown to be correlated with reduced CD16b expression on and immune complex uptake by neutrophils – the only cell type on which this receptor is expressed (Willcocks et al. 2008; Morris et al. 2010). However, the ectopic expression of *FCGR2B*, a direct product of a *FCGR3B* gene deletion, may also contribute to the functional explanation behind this robust disease association.

Evidence exists that when expressed on NK cells, *FCGR2B* maintains its inhibitory function (van der Heijden et al. 2012). Although, the functional effect of the I232T variant on NK cells has yet to be explored. I hoped this study would provide further evidence of function: an observed genetic interaction would suggest a further contribution from the *FCGR2B*-I232T variant to SLE risk via ectopic expression on NK cells. I observed a trend towards reduced MAF in controls (0.046) compared with cases (0.079), which suggest CD32b-232T could also be deleterious when ectopically expressed on NK cells.

The hypothesis at the heart of this study is one of *cis* interaction. Therefore not knowing which rs1050501 allele is in phase with the *FCGR3B* deletion in I232T heterozygotes is problematic. By extracting mRNA from NK cells and genotyping rs1050501 using cDNA, it would be possible to be confident in the phase. Genotyping would essentially be 'haploid' with respect to *FCGR2B* as its expression in NK cells will be expressed from one chromosome only, allowing confident haplotype phasing (Mueller et al. 2013).

I did not observe an association between *FCGR2B*-232T homozygosity and SLE, as previously reported in European cohorts (Niederer et al. 2010b; Willcocks et al. 2010). However, combining my data with previously published genotypes yielded a significant association of 232T-homozygosity and SLE (Figure 6.3). I am confident in my genotyping of the rs1050501 SNPs as I did not see a deviation from HWE (χ^2=0.71) and neither forward nor reverse primers used in this assay contain any known SNPs as observed using UCSC genome browser. The SLE cases used in this study were not selected for any subphenotypes or for disease severity. It is perhaps possible that such differences in the SLE cohorts between studies contribute to the power to detect associations.

Studies in East Asian cohorts have yielded consistent results of *FCGR2B*-232T association. This is likely to be due to increased power due to the elevated MAF in these populations (MAF=0.22-0.25), which is possibly driven by positive selective pressure due to its observed protective effect against the progression of severe malaria following infection (OR=0.5), which is strongly associated with childhood mortality (Clatworthy et al. 2007). The same protective effect, as well as SLE susceptibility, from the *FCGR2B*-232T variant has also been shown in a Kenyan cohort (Willcocks et al. 2010). Once again, possibly due to positive selection pressures, there is an observed elevated MAF in the Kenyan population (0.25) compared with Europeans (Willcocks et al. 2010). The frequency of the *FCGR3B*

deletion is also higher in these populations (Niederer et al. 2010b). Interestingly, the elevated frequencies of *FCGR3B* deletion is thought to be another example of positive selection pressures as a result of infectious agents (Machado et al. 2012). Together, the higher frequencies of both SLE susceptibility variants of the *FCGR* locus in these populations are likely to provide more adequate power to detect an interaction.

The trend toward increases in minor allele frequency in cases (0.079) compared with controls (0.046) within individuals with an *FCGR3B* deletion suggests it may be possible to detect a genetic interaction with an increased sample size in an European cohort, or by conducting this study with cohorts known to have higher MAFs. An earlier study also observed a trend toward an interaction in an European cohort (Niederer et al. 2010b). A meta-analysis could prove fruitful in this instance, as with the 232T association, in Europeans.

Given the known ectopic expression of CD32b on NK cells due to the *FCGR3B* deletion, this issue is worth pursuing (Mueller et al. 2013). With individual ORs approaching 2, both *FCGR* variants considered here are among the strongest risk factors for SLE. However, exploring this putative interaction may reveal that their effect sizes are underestimated when considered independently.

Chapter 7: Conclusions

7.1 Summary of findings

The results of the work presented in this thesis, which I believe to be novel contributions to the field, can be summarised as follows:

- The SLE-associated R77H variant in CD11b, encoded by rs1143679 in *ITGAM*, does not affect expression of CR3, under resting nor activated states, on the cell surface of monocytes and neutrophils from healthy volunteers of European ancestry.
- Two case-specific non-synonymous rare variants in *ITGAM*, F941V and G1145S, impair CR3-mediated phagocytosis of iC3b coated targets *in vitro.*
- Two non-synonymous polymorphism within *ITGAM*, M441T (rs11861251) and A858V (rs1143683), do not affect phagocytosis in the same *in vitro* model, reducing the evidence of a secondary SLE association with the latter.
- The small-molecule CR3 agonist, LA1, reduces cytokine and chemokines production by monokine-activated NK cells, and inhibits IL-15-mediated STAT5 phosphorylation.
- An increased frequency of *FCGR2B*-I232 (WT) alleles is seen in a control cohort conditioned on *FCGR3B* gene deletion, compared with SLE cases. This suggests the possibility of a genetic interaction between the two SLE-associated variants, which may contribute further to disease risk.

There are, of course, some limitations to these results, and conclusions could be aided by further experimental work. I have addressed each of these below.

7.2 Limitations and future work

7.2.1 Rare Variants in ITGAM

In Chapter 4 I demonstrated that two newly identified case-specific non-synonymous *ITGAM* rare variants, F941V and G1145S, impair CR3-mediated phagocytosis of iC3b coated targets *in vitro.* I believe the identification of case-specific, functionally deleterious rare variants within *ITGAM* adds further support to the role of CR3 in SLE pathogenesis.

Although it has been suggested that defective phagocytosis is the primary cause of the R77H association (Fossati-Jimack et al. 2013), R77H has been demonstrated to affect many other CR3 functions (MacPherson et al. 2011). Unfortunately, the rarity of the two novel variants, F941V and G1145S, meant that *ex vivo* studies were not feasible. Therefore, my analysis of their functional impact was limited to the availability of *in vitro* models. Although I can conclude that neither affects iC3b-binding, and both affect phagocytosis, it would be of great interest to ascertain their effects on other CR3 functions. Particularly as the F941V variant had an even greater impact (61% reduction) on phagocytosis than R77H (31%), it is possible that other functions are more dramatically affected too.

In addition, the minor allele of G1145S is in phase with the minor allele of P1146S on the chromosome. A recent study, published after the completion of my work, suggests P1146S also effects CR3 function on neutrophils (Y. Zhou et al. 2013). The phenomenon of an additive functional effect of both rare and common variants within the same polypeptide molecule is of particular interest when considering the contribution of rare variants to complex disease susceptibility. It would be possible to model this by introducing additional variants by site-directed mutagenesis to the CD11b plasmids. It would have been very interesting to introduce the P1146S to the pcDNA3.1(-)-*ITGAM*(G1145S) plasmid and measure the impact of these two sequential missense variants on iC3b-dependent phagocytosis. Following the evidence presented by Zhou and colleagues (Y. Zhou et al. 2013), I would suspect that an even greater reduction in phagocytic function would be seen. Additionally, given the location of amino acids 1145 and 1146 in the short cytoplasmic tail of CD11b, it is possible that, in addition to the 'outside-in' signalling effects measured by the phagocytic assay, an effect on 'inside-out' signalling would also been seen. Of course, a suitable *in vitro* model, which is hitherto unavailable, would be needed to measure such functional consequences.

The study by Zhou and colleagues also reports diminished phagocytosis of IgG-coated targets by both 77H/A858/P1146 and R77/858V/1146S neutrophils (Y. Zhou et al. 2013), due to the disrupted cooperation between CR3 and CD16b (Krauss et al. 1994). This is of particular interest to SLE, suggesting variants within *ITGAM* may affect the ability of neutrophils to phagocytose immune complexes as well as iC3b-coated targets (such as apoptotic cells). It would also be of interest to explore whether the rare variants, particularly F941V due to its close proximity to the β-glucan domain on CD11b, also affect this cooperation.

7.2.2 Effects of LA1 on CR3 functions

In addition to aiding our understanding of complex pathologies of disease, genetic studies may also provide avenues of directed therapies. Genetic analyses have highlighted *ITGAM* polymorphisms as important in disease susceptibility, and functional studies have confirmed the R77H-mediated impairments to CR3 function (Nath et al. 2008; MacPherson et al. 2011). A high-throughput screening cell-adhesion assay was used to identify LA1, a novel agonists of CR3, discussed in detail in Chapter 5 (Faridi et al. 2009). The therapeutic potential, then, for LA1 to target this under-functioning in inflammatory disease is a great example of translational research (Maiguel et al. 2011). In Chapter 5 I demonstrate that LA1 acts by inhibiting IL-15-mediated STAT5 phosphorylation, resulting in reduced levels of cytokine and chemokines production. However, there are a number of potential avenues of future work in order to fully conclude my results, as discussed in section 5.3, which can be summarised as follows:

- Increase the sample size in order to reduce variability in pSTAT3 fold-change following IL-12 and IL-15 activation to confirm there is indeed no LA1 effect on STAT3 tyrosine phosphorylation
- Survey the effects of LA1 on the IL-18Rβ signalling cascade: MyD88 recruitment, IRAK phosphorylation, and NF-κB translocation
- Measure IL-18Rβ expression to support the notion that LA1 does not affect the STAT4-mediated induction of its expression
- Survey the effects of LA1 on other cytokine receptor signalling pathways, in particular those containing the common γ_c and IL-2Rβ
- Determine if LA1 effects harbour STAT5A or STAT5B specificity

Furthermore, it is of paramount importance to investigate the effects of LA1 on other CR3-mediated functions. In contradiction to a previous study whereby R77H-heterozygosity was enough to disrupt the inhibitory functions of LA1 pre-treatment on TLR-activated monocytes (Reed et al. 2013), the R77H genotype did not appear to affect the ability of LA1 to reduce NK cell cytokine/chemokines production, as demonstrated by the work of Dr Ben Rhodes (manuscript under review). This is a very important observation in the potential of LA1 as an SLE treatment, as the MAF of rs1143679 (R77H) is ≈0.15-0.2 in SLE cases across multiple ethnicities (S. Han et al. 2009). It would therefore be of pivotal importance to further explore the possibility of the genotype-dependent differential effects of LA1 on CR3 function. As previously discussed, one of the key R77H-mediated impairments is under-functioning of CR3 phagocytosis (Fossati-Jimack et al. 2013), and moreover the 'waste-disposal hypothesis' is a key disease paradigm in SLE (Herrmann et al. 1998). LA1 has been demonstrated to stimulated phagocytosis of iC3b coated sheep red blood cells by CD11b/CD18 transfected K562 cells (Maiguel et al. 2011). It would be of great interest to determine whether LA1 is able to augment the impaired phagocytosis observed with 77H-expressing COS-7 cells (Rhodes et al. 2012), using the same *in vitro* model as applied to the functional study of *ITGAM* rare variants in Chapter 4.

7.2.3 FCGR interaction

In Chapter 6 of this thesis I explored the possibility of a genetic interaction between two SLE-associated variants within the *FCGR* locus. In addition to *FCGR3B* CNV (OR=1.59) and *FCGR2B*-232T homozygosity (OR=1.73) being among the strongest risk factors for SLE, it has been demonstrated that *FCGR3B* gene deletion results in ectopic expression of CD32b on NK cells (Mueller et al. 2013). It is possible, then, that part of the genetic effect of reduced *FCGR3B* copy number is explained by this ectopic expression. Although I observed increased frequency of *FCGR2B*-I232 (WT) alleles in a control cohort conditioned on *FCGR3B* gene deletion, compared with SLE cases, the size of my study was under-powered to detect a significant difference given the relatively low MAFs of both variants in European populations (Willcocks et al. 2010). Additionally, I did not observe 232T-homozygosity together with *FCGR3B* deletion, and the association of rs1050501 association is only seen in 232T-homozygosity (Kyogoku et al. 2002).

However, I believe the trend observed in my data suggests that it is worthwhile to pursue this putative interaction using larger cohorts of European ancestry. Additionally, conducting a genetic

interaction analysis with samples from South East Asian or East African populations, which have elevated rs1050501 MAFs (Clatworthy et al. 2007) and increased frequency of *FCGR3B* CNV (Niederer et al. 2010b) thought to be due to selective pressures, may be fruitful. There are existing data suggesting allele frequency differences affect the ability to replicate interactions between populations (X. Zhou et al. 2012)

Given the vast amount of genetic variants now known to be associated with SLE, hypothesis-free searches for interactions are likely to be hindered by multiple-testing restrictions. However, using functional knowledge to develop *a priori* hypotheses of interactions is likely to be more fruitful and informative (Sun and Kardia 2010). For instance, there has long been *in vitro* evidence that CR3 facilitates CD16b-mediated phagocytosis (Krauss et al. 1994), and that the CR3 lectin-like domain is a binding site for sCD16 (Galon et al. 1996). Recently, functional evidence suggests R77H impairs neutrophil phagocytosis of IgG-coated targets presumably through the impaired interaction between CR3 and CD16b (Y. Zhou et al. 2013). Known protein interactions could therefore aid our search for informative genetic interactions, and increase our understanding of the genetic variance contributing to SLE heritability.

References

Abbas, Lichtmann, Pillai. 2012. *Cellular and Molecular Immunology, 7th Edition*.

Adachi, O, T Kawai, K Takeda, M Matsumoto, H Tsutsui, M Sakagami, K Nakanishi, and S Akira. 1998. "Targeted Disruption of the *MyD88* Gene Results in Loss of IL-1- and IL-18-Mediated Function." *Immunity* 9 (1): 143–50.

Adzhubei, Ivan a, Steffen Schmidt, Leonid Peshkin, Vasily E Ramensky, Anna Gerasimova, Peer Bork, Alexey S Kondrashov, and Shamil R Sunyaev. 2010. "A Method and Server for Predicting Damaging Missense Mutations." *Nature Methods* 7 (4): 248–49.

Aitman, Timothy J, Rong Dong, Timothy J Vyse, Penny J Norsworthy, Michelle D Johnson, Jennifer Smith, Jonathan Mangion, et al. 2006. "Copy Number Polymorphism in *Fcgr3* Predisposes to Glomerulonephritis in Rats and Humans." *Nature* 439 (7078): 851–55.

Alarcón-Segovia, Donato, Marta E Alarcón-Riquelme, Mario H Cardiel, Francisco Caeiro, Loreto Massardo, Antonio R Villa, and Bernardo a Pons-Estel. 2005. "Familial Aggregation of Systemic Lupus Erythematosus, Rheumatoid Arthritis, and Other Autoimmune Diseases in 1,177 Lupus Patients from the GLADEL Cohort." *Arthritis and Rheumatism* 52 (4): 1138–47.

Anaya, Juan-Manuel, Xana Kim-Howard, Sampath Prahalad, Alejandra Cherñavsky, Carlos Cañas, Adriana Rojas-Villarraga, John Bohnsack, et al. 2011. "Evaluation of Genetic Association between an *ITGAM* Non-Synonymous SNP (rs1143679) and Multiple Autoimmune Diseases." *Autoimmunity Reviews* 11 (4): 276–80.

Arbuckle, Melissa R, Micah T McClain, Mark V Rubertone, R Hal Scofield, Gregory J Dennis, Judith a James, and John B Harley. 2003. "Development of Autoantibodies before the Clinical Onset of Systemic Lupus Erythematosus." *The New England Journal of Medicine* 349 (16): 1526–33.

Armour, John a L, Raquel Palla, Patrick L J M Zeeuwen, Martin den Heijer, Joost Schalkwijk, and Edward J Hollox. 2007. "Accurate, High-Throughput Typing of Copy Number Variation Using Paralogue Ratios from Dispersed Repeats." *Nucleic Acids Research* 35 (3): e19.

Baechler, Emily C, Franak M Batliwalla, George Karypis, Patrick M Gaffney, Ward a Ortmann, Karl J Espe, Katherine B Shark, et al. 2003. "Interferon-Inducible Gene Expression Signature in Peripheral Blood Cells of Patients with Severe Lupus." *Proceedings of the National Academy of Sciences of the United States of America* 100 (5): 2610–15.

Baechler, Emily C, Peter K Gregersen, and Timothy W Behrens. 2004. "The Emerging Role of Interferon in Human Systemic Lupus Erythematosus." *Current Opinion in Immunology* 16 (6): 801–7.

Bai, Yi, Cheng Qian, Li Qian, Feng Ma, Jin Hou, Yongjian Chen, Qingqing Wang, and Xuetao Cao. 2012. "Integrin CD11b Negatively Regulates TLR9-Triggered Dendritic Cell Cross-Priming by Upregulating microRNA-146a." *Journal of Immunology* 188 (11): 5293–5302.

Ballestar, Esteban. 2011. "Epigenetic Alterations in Autoimmune Rheumatic Diseases." *Nature Reviews. Rheumatology* 7 (5): 263–71.

Basham, Beth, Manjiri Sathe, Jeffrey Grein, Terrill McClanahan, Annalisa D'Andrea, Emma Lees, and Anne Rascle. 2008. "In Vivo Identification of Novel STAT5 Target Genes." *Nucleic Acids Research* 36 (11): 3802–18.

Becker, Kevin G. 2004. "The Common Variants/multiple Disease Hypothesis of Common Complex Genetic Disorders." *Medical Hypotheses* 62 (2): 309–17.

Bird, Adrian. 2007. "Perceptions of Epigenetics." *Nature* 447 (7143): 396–98.

Bodmer, Walter, and Carolina Bonilla. 2008. "Common and Rare Variants in Multifactorial Susceptibility to Common Diseases." *Nature Genetics* 40 (6): 695–701.

Bogdanos, Dimitrios P, Daniel S Smyk, Eirini I Rigopoulou, Maria G Mytilinaiou, Michael a Heneghan, Carlo Selmi, and M Eric Gershwin. 2012. "Twin Studies in Autoimmune Disease: Genetics, Gender and Environment." *Journal of Autoimmunity* 38 (2-3): 156–69.

Bolin, Karin, Johanna K Sandling, Agneta Zickert, Andreas Jönsen, Christopher Sjöwall, Elisabet Svenungsson, Anders a Bengtsson, et al. 2013. "Association of *STAT4* Polymorphism with Severe Renal Insufficiency in Lupus Nephritis." *PloS One* 8 (12): e84450.

Boteva, Lora, David L Morris, Josefina Cortés-Hernández, Javier Martin, Timothy J Vyse, and Michelle M a Fernando. 2012. "Genetically Determined Partial Complement C4 Deficiency States Are Not Independent Risk Factors for SLE in UK and Spanish Populations." *American Journal of Human Genetics* 90 (3): 445–56.

Breunis, Willemijn B, Edwin van Mirre, Judy Geissler, Nadja Laddach, Gertjan Wolbink, Ellen van der Schoot, Masja de Haas, Martin de Boer, Dirk Roos, and Taco W Kuijpers. 2009. "Copy Number Variation at the *FCGR* Locus Includes *FCGR3A*, *FCGR2C* and *FCGR3B* but Not *FCGR2A* and *FCGR2B*." *Human Mutation* 30 (5): 640–50.

Buyon JP, Shadick N, Berkman R, Hopkins P, Dalton J, Weissmann G, Winchester R, Abramson SB. 1988. "Surface Expression of Gp 165/95, the Complement Receptor CR3, as a Marker of Disease Activity in Systemic Lupus Erythematosus." *Clinical Immunology and Immunopathology* 46 (1): 141–49.

Carmona, F David, Carmen P Simeon, Lorenzo Beretta, Patricia Carreira, Madelon C Vonk, Raquel Ríos-Fernández, Gerard Espinosa, et al. 2011. "Association of a Non-Synonymous Functional Variant of the *ITGAM* Gene with Systemic Sclerosis." *Annals of the Rheumatic Diseases* 70 (11): 2050–52.

Caron, E. 1998. "Identification of Two Distinct Mechanisms of Phagocytosis Controlled by Different Rho GTPases." *Science* 282 (5394): 1717–21.

Carroll, H P, V Paunovic, and M Gadina. 2008. "Signalling, Inflammation and Arthritis: Crossed Signals: The Role of Interleukin-15 and -18 in Autoimmunity." *Rheumatology* 47 (9): 1269–77.

Castillejo-López, Casimiro, Angélica M Delgado-Vega, Jerome Wojcik, Sergey V Kozyrev, Elangovan Thavathiru, Ying-Yu Wu, Elena Sánchez, et al. 2012. "Genetic and Physical Interaction of the B-Cell Systemic Lupus Erythematosus-Associated Genes *BANK1* and *BLK*." *Annals of the Rheumatic Diseases* 71 (1): 136–42.

Chen, Ji-Yih, Chin Man Wang, Chung-Chun Ma, Shue-Fen Luo, Jeffrey C Edberg, Robert P Kimberly, and Jianming Wu. 2006. “Association of a Transmembrane Polymorphism of Fcgamma Receptor IIb (*FCGR2B*) with Systemic Lupus Erythematosus in Taiwanese Patients.” *Arthritis and Rheumatism* 54 (12): 3908–17.

Cheng, Kuang-Fu, and Jin-Hua Chen. 2013. “Detecting Rare Variants in Case-Parents Association Studies.” *PloS One* 8 (9): e74310.

Chu, Z T, N Tsuchiya, C Kyogoku, J Ohashi, Y P Qian, S B Xu, C Z Mao, J Y Chu, and K Tokunaga. 2004. “Association of Fcgamma Receptor IIb Polymorphism with Susceptibility to Systemic Lupus Erythematosus in Chinese: A Common Susceptibility Gene in the Asian Populations.” *Tissue Antigens* 63 (1): 21–27.

Chung, Sharon a, Kimberly E Taylor, Robert R Graham, Joanne Nititham, Annette T Lee, Ward a Ortmann, Chaim O Jacob, et al. 2011. “Differential Genetic Associations for Systemic Lupus Erythematosus Based on Anti-dsDNA Autoantibody Production.” *PLoS Genetics* 7 (3): e1001323.

Clatworthy, Menna R, Lisa Willcocks, Britta Urban, Jean Langhorne, Tom N Williams, Norbert Peshu, Nicholas A Watkins, R Andres Floto, and Kenneth G C Smith. 2007. “Systemic Lupus Erythematosus-Associated Defects in the Inhibitory Receptor Fc RIIb Reduce Susceptibility to Malaria.” *Proceedings of the National Academy of Sciences* 104 (21): 7169–74.

Conrad, Donald F, Dalila Pinto, Richard Redon, Lars Feuk, Omer Gokcumen, Yujun Zhang, Jan Aerts, et al. 2010. “Origins and Functional Impact of Copy Number Variation in the Human Genome.” *Nature* 464 (7289): 704–12.

Cooper, Gregory M, and Jay Shendure. 2011. “Needles in Stacks of Needles: Finding Disease-Causal Variants in a Wealth of Genomic Data.” *Nature Reviews. Genetics* 12 (9): 628–40.

Cooper, M , T Fehniger, and M Caligiuri. 2001. “The Biology of Human Natural Killer-Cell Subsets.” *Trends in Immunology* 22 (11): 633–40.

Cooper, M. 2001. “Human Natural Killer Cells: A Unique Innate Immunoregulatory Role for the CD56bright Subset.” *Blood* 97 (10): 3146–51.

Corpet, Florence, Laboratoire De Genetique Cellulaire, Inra Toulouse, and Castanet Tolosan. 1988. “Multiple Sequence Alignment with Hierarchical Clustering.” *Nucleic Acids Research* 16 (22): 10881–90.

Cougoule, Céline, Agnès Wiedemann, Jenson Lim, and Emmanuelle Caron. 2004. “Phagocytosis, an Alternative Model System for the Study of Cell Adhesion.” *Seminars in Cell & Developmental Biology* 15 (6): 679–89.

Deapen D, Escalante A, Weinrib L, Horwitz D, Bachman B, Roy-Burman P, Walker A, Mack TM. 1992. “A Revised Estimate of Twin Concordance in Systemic Lupus Erythematosus.” *Arthritis and Rheumatism* (3): 311–18.

Delgoffe, Greg M, and Dario a a Vignali. 2013. “STAT Heterodimers in Immunity: A Mixed Message or a Unique Signal?” *Jak-Stat* 2 (1): e23060–5.

Diamond, M S, J Garcia-Aguilar, J K Bickford, a L Corbi, and T a Springer. 1993. “The I Domain Is a Major Recognition Site on the Leukocyte Integrin Mac-1 (CD11b/CD18) for Four Distinct Adhesion Ligands.” *The Journal of Cell Biology* 120 (4): 1031–43.

Diamond, M S, and T Springer. 1993. “A Subpopulation of Mac-1 (CD11b/CD18) Molecules Mediates Neutrophil Adhesion to ICAM-1 and Fibrinogen.” *The Journal of Cell Biology* 120 (2): 545–56.

Dunne, J. L. 2002. “Control of Leukocyte Rolling Velocity in TNF-Alpha -Induced Inflammation by LFA-1 and Mac-1.” *Blood* 99 (1): 336–41.

Dunne, Jessica L, Robert G Collins, Arthur L Beaudet, Christie M Ballantyne, and Klaus Ley. 2003. “Mac-1, but Not LFA-1, Uses Intercellular Adhesion Molecule-1 to Mediate Slow Leukocyte Rolling in TNF-Alpha-Induced Inflammation.” *Journal of Immunology* 171 (11): 6105–11.

Edwards, Steven W. 1995. “Cell Signalliug by Integrins and Immunoglobulin Receptors in Primed Neutrophils.” *Trends in Biochemical Sciences* (9): 362–67.

Eichler, Evan E, Jonathan Flint, Greg Gibson, Augustine Kong, Suzanne M Leal, Jason H Moore, and Joseph H Nadeau. 2010. “Missing Heritability and Strategies for Finding the Underlying Causes of Complex Disease.” *Nature Reviews. Genetics* 11: 446–50.

Fagerholm, S C, M MacPherson, M J James, C Sevier-Guy, and C S Lau. 2013. “The CD11b-Integrin (*ITGAM*) and Systemic Lupus Erythematosus.” *Lupus* 22 (7): 657–63.

Fan, Sao-tah, and Thomas S Edgington. 1993. “Lntegrin Regulation of Leukocyte Inflammatory Functions. CD11b/ CD18 Enhancement of the Tumor Necrosis Factor-Alpha Responses of Monocytes.” *Journal of Immunology* 150 (7): 2972–80.

Fanciulli, Manuela, Penny J Norsworthy, Enrico Petretto, Rong Dong, Lorraine Harper, Lavanya Kamesh, Joanne M Heward, et al. 2007. “*FCGR3B* Copy Number Variation Is Associated with Susceptibility to Systemic, but Not Organ-Specific, Autoimmunity.” *Nature Genetics* 39 (6): 721–23.

Faridi, Mohd Hafeez, Mehmet M Altintas, Camilo Gomez, Juan Camilo Duque, Roberto I Vazquez-Padron, and Vineet Gupta. 2013. “Small Molecule Agonists of Integrin CD11b/CD18 Do Not Induce Global Conformational Changes and Are Significantly Better than Activating Antibodies in Reducing Vascular Injury.” *Biochimica et Biophysica Acta* 1830 (6): 3696–3710.

Faridi, Mohd Hafeez, Dony Maiguel, Constantinos J Barth, Darren Stoub, Ruth Day, Stephan Schürer, and Vineet Gupta. 2009. “Identification of Novel Agonists of the Integrin CD11b/CD18.” *Bioorganic & Medicinal Chemistry Letters* 19 (24): 6902–6.

Fehniger, Todd A, Manisha H Shah, Matthew J Turner, Jeffrey B Vandeusen, Susan P Whitman, Megan A Cooper, Kazuhiro Suzuki, Mark Wechser, Frederico Goodsaid, and Michael A Caligiuri. 1999. “Differential Cytokine and Chemokine Gene Expression by Human NK Cells Following Activation with IL-18 or IL-15 in Combination with IL-12: Implications for the Innate Immune Response.” *Journal of Immunology* 162: 4511–20.

Fernando, Michelle M A, Lora Boteva, David L Morris, Bi Zhou, Yee Ling Wu, Liisa Lokki, Chack Yung Yu, John D Rioux, Edward J Hollox, and Timothy J Vyse. 2010. “Assessment of Complement *C4* Gene Copy Number Using the Paralog Ratio Test.” *Human Molecular Genetics* 31 (7): 866–74.

Floto, R Andres, Menna R Clatworthy, Karen R Heilbronn, Dalya R Rosner, Paul a MacAry, Angela Rankin, Paul J Lehner, et al. 2005. “Loss of Function of a Lupus-Associated FcgammaRIIb Polymorphism through Exclusion from Lipid Rafts.” *Nature Medicine* 11 (10): 1056–58.

Fode, Peder, Cathrine Jespersgaard, Robert J Hardwick, Helen Bogle, Michael Theisen, Daniel Dodoo, Martin Lenicek, et al. 2011. “Determination of Beta-Defensin Genomic Copy Number in Different Populations: A Comparison of Three Methods.” *PloS One* 6 (2): e16768.

Fossati-Jimack, Liliane, Guang Sheng Ling, Andrea Cortini, Marta Szajna, Talat H Malik, Jacqueline U McDonald, Matthew C Pickering, H Terence Cook, Philip R Taylor, and Marina Botto. 2013. “Phagocytosis Is the Main CR3-Mediated Function Affected by the Lupus-Associated Variant of CD11b in Human Myeloid Cells.” *PloS One* 8 (2): e57082.

Gaipl, Udo S, Luis E Munoz, Gerhard Grossmayer, Kirsten Lauber, Sandra Franz, Kerstin Sarter, Reinhard E Voll, et al. 2007. “Clearance Deficiency and Systemic Lupus Erythematosus (SLE).” *Journal of Autoimmunity* 28 (2-3): 114–21.

Galon, Jcrme, Jean-franqois Gauchat, Noelle Mazipres, Roberto Spagnoli, Walter Storkus, Michael Lotze, Jean-yves Bonnefoy, Wolf-herman Fridman, and Catherine Saut. 1996. “Soluble Fcy Receptor Type 111 (FcyRIII, CDl6) Triggers Cell Activation Through Interaction with Complement Receptors.” *Journal of Immunology* 157: 1184–92.

Geissmann, Frederic, Steffen Jung, and Dan R Littman. 2003. “Blood Monocytes Consist of Two Principal Subsets with Distinct Migratory Properties.” *Immunity* 19 (1): 71–82.

Gourley, Mark, and Frederick W Miller. 2007. “Mechanisms of Disease: Environmental Factors in the Pathogenesis of Rheumatic Disease.” *Nature Clinical Practice. Rheumatology* 3 (3): 172–80.

Groth, M, C Wiegand, K Szafranski, K Huse, M Kramer, P Rosenstiel, S Schreiber, J Norgauer, and M Platzer. 2010. “Both Copy Number and Sequence Variations Affect Expression of Human *DEFB4*.” *Genes and Immunity* 11 (6). Nature Publishing Group: 458–66.

Han, Chaofeng, Jing Jin, Sheng Xu, Haibo Liu, Nan Li, and Xuetao Cao. 2010. “Integrin CD11b Negatively Regulates TLR-Triggered Inflammatory Responses by Activating Syk and Promoting Degradation of MyD88 and TRIF via Cbl-B.” *Nature Immunology* 11 (8): 734–42.

Han, Shizhong, Xana Kim-Howard, Harshal Deshmukh, Yoichiro Kamatani, Parvathi Viswanathan, Joel M Guthridge, Kenaz Thomas, et al. 2009. “Evaluation of Imputation-Based Association in and around the Integrin-Alpha-M (*ITGAM*) Gene and Replication of Robust Association between a Non-Synonymous Functional Variant within *ITGAM* and Systemic Lupus Erythematosus (SLE).” *Human Molecular Genetics* 18 (6): 1171–80.

Hardwick, Robert J, Lee R Machado, Luciana W Zuccherato, Suzanne Antolinos, Yali Xue, Nyambura Shawa, Robert H Gilman, et al. 2011. “A Worldwide Analysis of Beta-Defensin Copy Number Variation Suggests Recent Selection of a High-Expressing *DEFB103* Gene Copy in East Asia.” *Human Mutation* 32 (7): 743–50.

Harley, John B, Marta E Alarcón-Riquelme, Lindsey a Criswell, Chaim O Jacob, Robert P Kimberly, Kathy L Moser, Betty P Tsao, et al. 2008. “Genome-Wide Association Scan in Women with Systemic Lupus Erythematosus Identifies Susceptibility Variants in *ITGAM, PXK, KIAA1542* and Other Loci.” *Nature Genetics* 40 (2): 204–10.

Hawley, Kelly L, Chris M Olson, Juan M Iglesias-pedraz, Nicolás Navasa, and Jorge L Cervantes. 2011. "CD14 Cooperates with Complement Receptor 3 to Mediate MyD88-Independent Phagocytosis of Borrelia Burgdorferi." *Proceedings of the National Academy of Sciences*, 14–18.

Hayakawa, Yoshihiro, and MJ Smyth. 2006. "CD27 Dissects Mature NK Cells into Two Subsets with Distinct Responsiveness and Migratory Capacity." *The Journal of Immunology* (176): 1517–24.

Heinzen, Erin L, Chantal Depondt, Gianpiero L Cavalleri, Elizabeth K Ruzzo, Nicole M Walley, Anna C Need, Dongliang Ge, et al. 2012. "Exome Sequencing Followed by Large-Scale Genotyping Fails to Identify Single Rare Variants of Large Effect in Idiopathic Generalized Epilepsy." *American Journal of Human Genetics* 91 (2): 293–302.

Henderson, R B, L H Lim, P a Tessier, F N Gavins, M Mathies, M Perretti, and N Hogg. 2001. "The Use of Lymphocyte Function-Associated Antigen (LFA)-1-Deficient Mice to Determine the Role of LFA-1, Mac-1, and alpha4 Integrin in the Inflammatory Response of Neutrophils." *The Journal of Experimental Medicine* 194 (2): 219–26.

Henriques, Ana, Luís Teixeira, Luís Inês, Maria Luísa Pais, José António, and Artur Paiva. 2013. "NK Cells Dysfunction in Systemic Lupus Erythematosus: Relation to Disease Activity." *Clinical Rheumatology* (32): 805–13..

Herrmann M, Voll RE, Zoller OM, Hagenhofer M, Ponner BB, Kalden JR. 1998. "Impaired Phagocytosis of Apoptotic Cell Material by Monocyte-Derived Macrophages from Patients with Systemic Lupus Erythematosus." *Arthritis and Rheumatism* July (41): 1241–50.

Hervier, Baptiste, Vivien Beziat, Julien Haroche, Alexis Mathian, Pierre Lebon, Pascale Ghillani-Dalbin, Lucile Musset, Patrice Debré, Zahir Amoura, and Vincent Vieillard. 2011. "Phenotype and Function of Natural Killer Cells in Systemic Lupus Erythematosus: Excess Interferon-Γ Production in Patients with Active Disease." *Arthritis and Rheumatism* 63 (6): 1698–1706.

Hochreiter-Hufford, Amelia, and Kodi S Ravichandran. 2013. "Clearing the Dead: Apoptotic Cell Sensing, Recognition, Engulfment, and Digestion." *Cold Spring Harbor Perspectives in Biology* 5 (1)

Hollox, Edward J, Jan-christoph Detering, and Tushna Dehnugara. 2013. "Group An Integrated Approach for Measuring Copy Number Variation at the *FCGR3* (CD16) Locus." *Human Mutation* 30 (3): 477–84.

Hollox, Edward J, Ulrike Huffmeier, Patrick L J M Zeeuwen, Raquel Palla, Jesús Lascorz, Diana Rodijk-Olthuis, Peter C M van de Kerkhof, et al. 2008. "Psoriasis Is Associated with Increased Beta-Defensin Genomic Copy Number." *Nature Genetics* 40 (1): 23–25.

Hom, Geoffrey, Robert R Graham, Barmak Modrek, Kimberly E Taylor, Ward Ortmann, Sophie Garnier, Annette T Lee, et al. 2008. "Association of Systemic Lupus Erythematosus with *C8orf13-BLK* and *ITGAM-ITGAX*." *The New England Journal of Medicine* 9 (358): 900–909.

Hüffmeier, Ulrike, Judith G M Bergboer, Tim Becker, John a Armour, Heiko Traupe, Xavier Estivill, Eva Riveira-Munoz, et al. 2010. "Replication of *LCE3C-LCE3B* CNV as a Risk Factor for Psoriasis and Analysis of Interaction with Other Genetic Risk Factors." *The Journal of Investigative Dermatology* 130 (4): 979–84.

Hughes, Travis, Adam Adler, Jennifer a Kelly, Kenneth M Kaufman, Adrienne H Williams, Carl D Langefeld, Elizabeth E Brown, et al. 2012. “Evidence for Gene-Gene Epistatic Interactions among Susceptibility Loci for Systemic Lupus Erythematosus.” *Arthritis and Rheumatism* 64 (2): 485–92.

Hulspas, Ruud, Maurice R G O’Gorman, Brent L Wood, Jan W Gratama, and D Robert Sutherland. 2009. “Considerations for the Control of Background Fluorescence in Clinical Flow Cytometry.” *Cytometry. Part B, Clinical Cytometry* 76 (6): 355–64.

Hunt, Karen a, Vanisha Mistry, Nicholas a Bockett, Tariq Ahmad, Maria Ban, Jonathan N Barker, Jeffrey C Barrett, et al. 2013. “Negligible Impact of Rare Autoimmune-Locus Coding-Region Variants on Missing Heritability.” *Nature* 498 (7453): 232–35.

Hynes, Richard O. 2002. “Integrins: Bidirectional , Allosteric Signaling Machines.” *Cell* (110): 673–87.

Hyun Kim, S., L. L. Reznikov, R. J. L. Stuyt, C. H. Selzman, G. Fantuzzi, T. Hoshino, H. a. Young, and C. a. Dinarello. 2001. “Functional Reconstitution and Regulation of IL-18 Activity by the IL-18Rbeta Chain.” *The Journal of Immunology* 166 (1): 148–54.

Javierre, Biola M, Agustin F Fernandez, Julia Richter, Fatima Al-Shahrour, J Ignacio Martin-Subero, Javier Rodriguez-Ubreva, Maria Berdasco, et al. 2010. “Changes in the Pattern of DNA Methylation Associate with Twin Discordance in Systemic Lupus Erythematosus.” *Genome Research* 20 (2): 170–79..

Jego, Gaetan, A Karolina Palucka, Jean-philippe Blanck, Cecile Chalouni, Virginia Pascual, and Jacques Banchereau. 2003. “Plasma Cell Differentiation through Type I Interferon and Interleukin 6.” *Immunity* 19: 225–34.

Jian-Xin Lin, Judy Mietz, et al. 1996. “Cloning of Human Stat5B. Reconstitution of interleukin-2-induced STAT5A adn STAT5B DNA binding activity in COS-7 cells.” *Journal of Biological Chemistry* 271 (18): 10738–44.

Johnston, J a, C M Bacon, D S Finbloom, R C Rees, D Kaplan, K Shibuya, J R Ortaldo, S Gupta, Y Q Chen, and J D Giri. 1995. “Tyrosine Phosphorylation and Activation of STAT5, STAT3, and Janus Kinases by Interleukins 2 and 15.” *Proceedings of the National Academy of Sciences of the United States of America* 92 (19): 8705–9.

Jordan, Catherine T, Li Cao, Elisha D O Roberson, Shenghui Duan, Cynthia a Helms, Rajan P Nair, Kristina Callis Duffin, et al. 2012. “Rare and Common Variants in *CARD14*, Encoding an Epidermal Regulator of NF-kappaB, in Psoriasis.” *American Journal of Human Genetics* 90 (5): 796–808.

Kanakaraj, P, K Ngo, Y Wu, a Angulo, P Ghazal, C a Harris, J J Siekierka, P a Peterson, and W P Fung-Leung. 1999. “Defective Interleukin (IL)-18-Mediated Natural Killer and T Helper Cell Type 1 Responses in IL-1 Receptor-Associated Kinase (IRAK)-Deficient Mice.” *The Journal of Experimental Medicine* 189 (7): 1129–38.

Kawai, Kazushige, Nelson H Tsuno, Mika Matsuhashi, Joji Kitayama, Takuya Osada, Jun Yamada, Takeshi Tsuchiya, et al. 2005. “CD11b-Mediated Migratory Property of Peripheral Blood B Cells.” *The Journal of Allergy and Clinical Immunology* 116 (1): 192–97.

Ke, Xiayi. 2012. “Presence of Multiple Independent Effects in Risk Loci of Common Complex Human Diseases.” *American Journal of Human Genetics* 91 (1): 185–92.

Keinan, Alon, and Andrew G Clark. 2012. “Recent Explosive Human Population Growth Has Resulted in an Excess of Rare Genetic Variants.” *Science* 336 (6082): 740–43.

Kelley, James M, Jeffrey C Edberg, and Robert P Kimberly. 2010. “Pathways: Strategies for Susceptibility Genes in SLE.” *Autoimmunity Reviews* 9 (7): 473–76.

Kim-Howard, Xana, Amit K Maiti, Juan-Manuel Anaya, Gail R Bruner, Elizabeth Brown, Joan T Merrill, Jeffrey C Edberg, et al. 2010. “*ITGAM* Coding Variant (rs1143679) Influences the Risk of Renal Disease, Discoid Rash and Immunological Manifestations in Patients with Systemic Lupus Erythematosus with European Ancestry.” *Annals of the Rheumatic Diseases* 69 (7): 1329–32.

Kinashi, Tatsuo. 2006. “Adhere Upright: A Switchblade-like Extension of beta2 Integrins.” *Immunity* 25 (4): 521–22.

Kono, Hajime, Chieko Kyogoku, Takeshi Suzuki, Naoyuki Tsuchiya, Hiroaki Honda, Kazuhiko Yamamoto, Katsushi Tokunaga, and Zen-Ichiro Honda. 2005. “FcgammaRIIB Ile232Thr Transmembrane Polymorphism Associated with Human Systemic Lupus Erythematosus Decreases Affinity to Lipid Rafts and Attenuates Inhibitory Effects on B Cell Receptor Signaling.” *Human Molecular Genetics* 14 (19): 2881–92.

Krauss, John C, Haryoung Poo, Wei Xue, Laura Mayo-bond, Howard R Pettyzt, and F Todd Ill. 1994. “Reconstitution of Antibody-Dependent Phagocytosis in Fibroblasts Expressing Fcγ Receptor IIIB and the Complement Receptor 3.” *Journal of Immunology* (153): 1769.

Kumar, Prateek, Steven Henikoff, and Pauline C Ng. 2009. “Predicting the Effects of Coding Non-Synonymous Variants on Protein Function Using the SIFT Algorithm.” *Nature Protocols* 4 (7): 1073–81.

Kunikata, T, K Torigoe, S Ushio, T Okura, C Ushio, H Yamauchi, M Ikeda, H Ikegami, and M Kurimoto. 1998. “Constitutive and Induced IL-18 Receptor Expression by Various Peripheral Blood Cell Subsets as Determined by Anti-hIL-18R Monoclonal Antibody.” *Cellular Immunology* 189 (2): 135–43.

Kyogoku, Chieko, Hilde M Dijstelbloem, Naoyuki Tsuchiya, Yoko Hatta, Hitoshi Kato, Akihiro Yamaguchi, Toru Fukazawa, et al. 2002. “Fcgamma Receptor Gene Polymorphisms in Japanese Patients with Systemic Lupus Erythematosus: Contribution of *FCGR2B* to Genetic Susceptibility.” *Arthritis and Rheumatism* 46 (5): 1242–54.

Lee, Young Ho, and Swapan K Nath. 2005. “Systemic Lupus Erythematosus Susceptibility Loci Defined by Genome Scan Meta-Analysis.” *Human Genetics* 118 (3-4): 434–43.

Lefort, Craig T, Young-Min Hyun, Joanne B Schultz, Foon-Yee Law, Richard E Waugh, Philip a Knauf, and Minsoo Kim. 2009. “Outside-in Signal Transmission by Conformational Changes in Integrin Mac-1.” *Journal of Immunology* 183 (10): 6460–68.

Leng, Rui-Xue, Wei Wang, Han Cen, Mo Zhou, Chen-Chen Feng, Yan Zhu, Xiao-Ke Yang, et al. 2012. “Gene-Gene and Gene-Sex Epistatic Interactions of *MiR146a, IRF5, IKZF1, ETS1* and *IL21* in Systemic Lupus Erythematosus.” *PloS One* 7 (12): e51090.

Levy, David E, and Isabelle J Marié. 2012. “STATus Report on Tetramers.” *Immunity* 36 (4): 553–55.

Lewis, Eli C, and Charles a Dinarello. 2006. “Responses of IL-18- and IL-18 Receptor-Deficient Pancreatic Islets with Convergence of Positive and Negative Signals for the IL-18 Receptor.” *Proceedings of the National Academy of Sciences of the United States of America* 103 (45): 16852–57.

Ley, Klaus. 2002. “Integration of Inflammatory Signals by Rolling Neutrophils.” *Immunological Reviews* 186 (7): 8–18.

Li, Bingshan, and SM Leal. 2008. “Methods for Detecting Associations with Rare Variants for Common Diseases: Application to Analysis of Sequence Data.” *The American Journal of Human Genetics* 83: 311–21.

Li, Heng, and Richard Durbin. 2009. “Fast and Accurate Short Read Alignment with Burrows-Wheeler Transform.” *Bioinformatics* 25 (14): 1754–60.

Li, L-H, H Yuan, H-F Pan, W-X Li, X-P Li, and Dong-Qing Ye. 2010. “Role of the Fcgamma Receptor IIIA-V/F158 Polymorphism in Susceptibility to Systemic Lupus Erythematosus and Lupus Nephritis: A Meta-Analysis.” *Scandinavian Journal of Rheumatology* 39 (2): 148–54.

Li, Xiaoli, Jianming Wu, Robert H Carter, Jeffrey C Edberg, Kaihong Su, Glinda S Cooper, and Robert P Kimberly. 2003. “A Novel Polymorphism in the Fcgamma Receptor IIB (CD32B) Transmembrane Region Alters Receptor Signaling.” *Arthritis and Rheumatism* 48 (11): 3242–52.

Li, Xinrui, Jianming Wu, Travis Ptacek, David T Redden, Elizabeth E Brown, Graciela S Alarcón, Rosalind Ramsey-Goldman, et al. 2013. “Allelic-Dependent Expression of an Activating Fc Receptor on B Cells Enhances Humoral Immune Responses.” *Science Translational Medicine* 5 (216): 1-10

Li, Zhang. 1999. “The A B 2 Integrin and Its Role in Neutrophil Function.” *Cell Research* 9: 171–78.

Lin, Dan-Yu, and Zheng-Zheng Tang. 2011. “A General Framework for Detecting Disease Associations with Rare Variants in Sequencing Studies.” *American Journal of Human Genetics* 89 (3): 354–67.

Lin, J X, and W J Leonard. 2000. “The Role of Stat5a and Stat5b in Signaling by IL-2 Family Cytokines.” *Oncogene* 19 (21): 2566–76.

Lin, Jian-Xin, Peng Li, Delong Liu, Hyun Tak Jin, Jianping He, Mohammed Ata Ur Rasheed, Yrina Rochman, et al. 2012. “Critical Role of STAT5 Transcription Factor Tetramerization for Cytokine Responses and Normal Immune Function.” *Immunity* 36 (4): 586–99.

Ling, Guang Sheng, Jason Bennett, Kevin J Woollard, Marta Szajna, Liliane Fossati-Jimack, Philip R Taylor, Diane Scott, Guido Franzoso, H Terence Cook, and Marina Botto. 2014. “Integrin CD11b Positively Regulates TLR4-Induced Signalling Pathways in Dendritic Cells but Not in Macrophages.” *Nature Communications* 5 (1): 1–11.

Lischke, a. 1998. “The Interleukin-4 Receptor Activates STAT5 by a Mechanism That Relies upon Common Gamma -Chain.” *Journal of Biological Chemistry* 273 (47): 31222–29.

Lövgren, Tanja, Maija-Leena Eloranta, Ullvi Båve, Gunnar V Alm, and Lars Rönnblom. 2004. "Induction of Interferon-Alpha Production in Plasmacytoid Dendritic Cells by Immune Complexes Containing Nucleic Acid Released by Necrotic or Late Apoptotic Cells and Lupus IgG." *Arthritis and Rheumatism* 50 (6): 1861–72.

Luo, Bing-Hao, Christopher V Carman, and Timothy a Springer. 2007. "Structural Basis of Integrin Regulation and Signaling." *Annual Review of Immunology* 25 (1): 619–47.

Ma, Yan-Qing, Edward F Plow, and Jian-Guo Geng. 2004. "P-Selectin Binding to P-Selectin Glycoprotein Ligand-1 Induces an Intermediate State of alphaMbeta2 Activation and Acts Cooperatively with Extracellular Stimuli to Support Maximal Adhesion of Human Neutrophils." *Blood* 104 (8): 2549–56.

Machado, Lee R, Jennifer Bowdrey, Eliford Ngaimisi, Abiy Habtewold, Omary Minzi, Eyasu Makonnen, Getnet Yimer, et al. 2013. "Copy Number Variation of Fc Gamma Receptor Genes in HIV-Infected and HIV-Tuberculosis Co-Infected Individuals in Sub-Saharan Africa." *PloS One* 8 (11): e78165.

Machado, Lee R, Robert J Hardwick, Jennifer Bowdrey, Helen Bogle, Timothy J Knowles, Manuela Sironi, and Edward J Hollox. 2012. "Evolutionary History of Copy-Number-Variable Locus for the Low-Affinity Fcγ Receptor: Mutation Rate, Autoimmune Disease, and the Legacy of Helminth Infection." *American Journal of Human Genetics* 90 (6): 973–85.

MacPherson, Matthew, Hwee San Lek, Alan Prescott, and Susanna C Fagerholm. 2011. "A Systemic Lupus Erythematosus-Associated R77H Substitution in the CD11b Chain of the Mac-1 Integrin Compromises Leukocyte Adhesion and Phagocytosis." *The Journal of Biological Chemistry* 286 (19): 17303–10.

Madsen, Bo Eskerod, and Sharon R Browning. 2009. "A Groupwise Association Test for Rare Mutations Using a Weighted Sum Statistic." *PLoS Genetics* 5 (2): e1000384.

Maiguel, Dony, Mohd Hafeez Faridi, Changli Wei, Yoshihiro Kuwano, Keir M Balla, Dayami Hernandez, Constantinos J Barth, et al. 2011. "Small Molecule-Mediated Activation of the Integrin CD11b/CD18 Reduces Inflammatory Disease." *Science Signaling* 4 (189): 1-14.

Maiti, Amit K, Xana Kim-Howard, Prasenjeet Motghare, Vandana Pradhan, Kek Heng Chua, Celi Sun, María Teresa Arango-Guerrero, et al. 2014. "Combined Protein- and Nucleic Acid-Level Effects of rs1143679 (R77H), a Lupus-Predisposing Variant within *ITGAM*." *Human Molecular Genetics*(3): 1–16.

Manolio, Teri A, Francis S Collins, Nancy J Cox, David B Goldstein, Lucia A Hindorff, David J Hunter, Mark I McCarthy, et al. 2009. "Finding the Missing Heritability of Complex Diseases." *Nature* (461): 747–53.

Marth, T, and B L Kelsall. 1997. "Regulation of Interleukin-12 by Complement Receptor 3 Signaling." *The Journal of Experimental Medicine* 185 (11): 1987–95.

Matikainen, S, a Paananen, M Miettinen, M Kurimoto, T Timonen, I Julkunen, and T Sareneva. 2001. "IFN-Alpha and IL-18 Synergistically Enhance IFN-Gamma Production in Human NK Cells: Differential Regulation of Stat4 Activation and IFN-Gamma Gene Expression by IFN-Alpha and IL-12." *European Journal of Immunology* 31 (7): 2236–45.

McKenna, Aaron, Matthew Hanna, Eric Banks, Andrey Sivachenko, Kristian Cibulskis, Andrew Kernytsky, Kiran Garimella, et al. 2010. “The Genome Analysis Toolkit: A MapReduce Framework for Analyzing next-Generation DNA Sequencing Data.” *Genome Research* 20 (9): 1297–1303.

McKinney, Cushla, and Tony R Merriman. 2012. “Meta-Analysis Confirms a Role for Deletion in *FCGR3B* in Autoimmune Phenotypes.” *Human Molecular Genetics* 21 (10): 2370–76.

Metes, D, L K Ernst, W H Chambers, a Sulica, R B Herberman, and P a Morel. 1998. “Expression of Functional CD32 Molecules on Human NK Cells Is Determined by an Allelic Polymorphism of the FcgammaRIIC Gene.” *Blood* 91 (7): 2369–80.

Meyer, Matthias, Udo Stenzel, and Michael Hofreiter. 2008. “Parallel Tagged Sequencing on the 454 Platform.” *Nature Protocols* 3 (2): 267–78.

Mobberley-schuman, Paula S, and Alison A Weiss. 2005. “Influence of CR3 (CD11b / CD18) Expression on Phagocytosis of Bordetella Pertussis by Human Neutrophils.” *Infection and Immunity* 73 (11): 7317–23.

Molokhia, Mariam, Manuela Fanciulli, Enrico Petretto, Alan Leslie Patrick, Paul McKeigue, Amy L Roberts, Tim J Vyse, and Tim J Aitman. 2011. “*FCGR3B* Copy Number Variation Is Associated with Systemic Lupus Erythematosus Risk in Afro-Caribbeans.” *Rheumatology* 50 (7): 1206–10.

Moore, K L, K D Patel, R E Bruehl, F Li, D a Johnson, H S Lichenstein, R D Cummings, D F Bainton, and R P McEver. 1995. “P-Selectin Glycoprotein Ligand-1 Mediates Rolling of Human Neutrophils on P-Selectin.” *The Journal of Cell Biology* 128 (4): 661–71.

Morris, David L, Amy L Roberts, Abigail S Witherden, Ruth Tarzi, Paula Barros, John C Whittaker, Terence H Cook, Timothy J Aitman, and Timothy J Vyse. 2010. “Evidence for Both Copy Number and Allelic (NA1/NA2) Risk at the *FCGR3B* Locus in Systemic Lupus Erythematosus.” *European Journal of Human Genetics : EJHG* 18 (9): 1027–31.

Moser, K L, J a Kelly, C J Lessard, and J B Harley. 2009. “Recent Insights into the Genetic Basis of Systemic Lupus Erythematosus.” *Genes and Immunity* 10 (5): 373–79.

Mueller, Michael, Paula Barros, Abigail S Witherden, Amy L Roberts, Zhou Zhang, Helmut Schaschl, Chack-Yung Yu, et al. 2013. “Genomic Pathology of SLE-Associated Copy-Number Variation at the *FCGR2C/FCGR3B/FCGR2B* Locus.” *American Journal of Human Genetics* 92 (1): 28–40.

Murphy, Kenneth. 2012. *Janeway’s Immunobiology, 8th Edition*.

Nakahira, M., M. Tomura, M. Iwasaki, H.-J. Ahn, Y. Bian, T. Hamaoka, T. Ohta, M. Kurimoto, and H. Fujiwara. 2001. “An Absolute Requirement for STAT4 and a Role for IFN- as an Amplifying Factor in IL-12 Induction of the Functional IL-18 Receptor Complex.” *The Journal of Immunology* 167 (3): 1306–12.

Nath, Swapan K, Shizhong Han, Xana Kim-Howard, Jennifer a Kelly, Parvathi Viswanathan, Gary S Gilkeson, Wei Chen, et al. 2008. “A Nonsynonymous Functional Variant in Integrin-alpha(M) (encoded by *ITGAM*) Is Associated with Systemic Lupus Erythematosus.” *Nature Genetics* 40 (2): 152–54.

Need, Anna C, Joseph P McEvoy, Massimo Gennarelli, Erin L Heinzen, Dongliang Ge, Jessica M Maia, Kevin V Shianna, et al. 2012. “Exome Sequencing Followed by Large-Scale Genotyping Suggests a Limited Role for Moderately Rare Risk Factors of Strong Effect in Schizophrenia.” *American Journal of Human Genetics* 91 (2): 303–12.

Niederer, Heather A, Menna R Clatworthy, Lisa C Willcocks, and Kenneth G C Smith. 2010a. “FcγRIIB , FcγRIIIB , and Systemic Lupus Erythematosus.” *Annals of the New York Academy of Sciences* 1183: 69–88.

Niederer, Heather a, Lisa C Willcocks, Tim F Rayner, Wanling Yang, Yu Lung Lau, Thomas N Williams, J Anthony G Scott, et al. 2010b. “Copy Number, Linkage Disequilibrium and Disease Association in the *FCGR* Locus.” *Human Molecular Genetics* 19 (16): 3282–94.

Nold-Petry, Claudia a, Marcel F Nold, Jason W Nielsen, Alex Bustamante, Jarod a Zepp, Kathleen a Storm, Jae-Woo Hong, Soo-Hyun Kim, and Charles a Dinarello. 2009. “Increased Cytokine Production in Interleukin-18 Receptor Alpha-Deficient Cells Is Associated with Dysregulation of Suppressors of Cytokine Signaling.” *The Journal of Biological Chemistry* 284 (38): 25900–911.

Noubir, Sanaâ, Zakaria Hmama, and Neil E Reiner. 2004. “Dual Receptors and Distinct Pathways Mediate Interleukin-1 Receptor-Associated Kinase Degradation in Response to Lipopolysaccharide. Involvement of CD14/TLR4, CR3, and Phosphatidylinositol 3-Kinase.” *The Journal of Biological Chemistry* 279 (24): 25189–95.

O’Brien, Xian M, Katie E Heflin, Liz M Lavigne, Kebing Yu, Minsoo Kim, Arthur R Salomon, and Jonathan S Reichner. 2012. “Lectin Site Ligation of CR3 Induces Conformational Changes and Signaling.” *The Journal of Biological Chemistry* 287 (5): 3337–48.

O’Neill, Sean, and Ricard Cervera. 2010. “Systemic Lupus Erythematosus.” *Best Practice & Research. Clinical Rheumatology* 24 (6): 841–55.

Olsson, Lina M, and Rikard Holmdahl. 2012. “Copy Number Variation in Autoimmunity--Importance Hidden in Complexity?” *European Journal of Immunology* 42 (8): 1969–76.

Park, Yong-Wook, Seung-Jung Kee, Young-Nan Cho, Eun-Hee Lee, Hwa-Youn Lee, Eun-Mi Kim, Min-Ho Shin, et al. 2009. “Impaired Differentiation and Cytotoxicity of Natural Killer Cells in Systemic Lupus Erythematosus.” *Arthritis and Rheumatism* 60 (6): 1753–63.

Paunovic, V, H P Carroll, K Vandenbroeck, and M Gadina. 2008. “Signalling, Inflammation and Arthritis: Crossed Signals: The Role of Interleukin (IL)-12, -17, -23 and -27 in Autoimmunity.” *Rheumatology* 47 (6): 771–76.

Phipps-Green, Amanda J, Ruth K G Topless, Marilyn E Merriman, Nicola Dalbeth, Peter J Gow, Andrew a Harrison, John Highton, et al. 2009. “No Evidence for Association of the Systemic Lupus Erythematosus-Associated *ITGAM* Variant, R77H, with Rheumatoid Arthritis in the Caucasian Population.” *Rheumatology* 48 (12): 1614–15.

Pittoni, Valerio, and Guido Valesini. 2002. “The Clearance of Apoptotic Cells: Implications for Autoimmunity.” *Autoimmunity Reviews* 1 (3): 154–61.

Price, Alkes L, Gregory V Kryukov, Paul I W de Bakker, Shaun M Purcell, Jeff Staples, Lee-Jen Wei, and Shamil R Sunyaev. 2010. “Pooled Association Tests for Rare Variants in Exon-Resequencing Studies.” *American Journal of Human Genetics* 86 (6): 832–38..

Pritchard, J K. 2001. “Are Rare Variants Responsible for Susceptibility to Complex Diseases?” *American Journal of Human Genetics* 69 (1): 124–37.

Pritchard, Jonathan K, and Nancy J Cox. 2002. “The Allelic Architecture of Human Disease Genes: Common Disease-Common Variant...or Not?” *Human Molecular Genetics* 11 (20): 2417–23.

Quinlan, Aaron R, Donald A Stewart, and T Marth. 2008. “Pyrobayes: An Improved Base Caller for SNP Discovery in Pyrosequences.” *Nature Methods* 5 (2): 454–56.

Rahman, A. 2004. “Autoantibodies, Lupus and the Science of Sabotage.” *Rheumatology* 43 (11): 1326–36.

Ramos, Paula S, Lindsey a Criswell, Kathy L Moser, Mary E Comeau, Adrienne H Williams, Nicholas M Pajewski, Sharon a Chung, et al. 2011. “A Comprehensive Analysis of Shared Loci between Systemic Lupus Erythematosus (SLE) and Sixteen Autoimmune Diseases Reveals Limited Genetic Overlap.” *PLoS Genetics* 7 (12): e1002406.

Reed, Joanne H, Manish Jain, Kristen Lee, Ekambar R Kandimalla, Mohd Hafeez Faridi, Jill P Buyon, Vineet Gupta, and Robert M Clancy. 2013. “Complement Receptor 3 Influences Toll-like Receptor 7/8-Dependent Inflammation: Implications for Autoimmune Diseases Characterized by Antibody Reactivity to Ribonucleoproteins.” *The Journal of Biological Chemistry* 288 (13): 9077–83.

Reich, D E, and E S Lander. 2001. “On the Allelic Spectrum of Human Disease.” *Trends in Genetics* 17 (9): 502–10.

Rezzonico, R. 2001. “Ligation of CD11b and CD11c beta2 Integrins by Antibodies or Soluble CD23 Induces Macrophage Inflammatory Protein 1alpha (MIP-1alpha) and MIP-1beta Production in Primary Human Monocytes through a Pathway Dependent on Nuclear Factor-kappaB.” *Blood* 97 (10): 2932–40.

Rezzonico, Roger, Rachel Chicheportiche, Veronique Imbert, and Jean-michel Dayer. 2000. “Engagement of CD11b and CD11c β2 Integrin by Antibodies or Soluble CD23 Induces IL-1β Production on Primary Human Monocytes through Mitogen-Activated Protein Kinase – Dependent Pathways.” *Blood* 95 (12): 3868–77.

Rhodes, B, and T J Vyse. 2008. “The Genetics of SLE: An Update in the Light of Genome-Wide Association Studies.” *Rheumatology* 47 (11): 1603–11.

Rhodes, Benjamin, Barbara G Fürnrohr, Amy L Roberts, George Tzircotis, Georg Schett, Tim D Spector, and Timothy J Vyse. 2012. “The rs1143679 (R77H) Lupus Associated Variant of *ITGAM* (CD11b) Impairs Complement Receptor 3 Mediated Functions in Human Monocytes.” *Annals of the Rheumatic Diseases* 71 (12): 2028–34.

Ricardo-Carter, C, M Favila, R E Polando, R N Cotton, K Bogard Horner, D Condon, W Ballhorn, et al. 2013. “Leishmania Major Inhibits IL-12 in Macrophages by Signalling through CR3

(CD11b/CD18) and down-Regulation of ETS-Mediated Transcription." *Parasite Immunology* 35 (12): 409–20.

Rice, Gillian I, Yoandris Del Toro Duany, Emma M Jenkinson, Gabriella M a Forte, Beverley H Anderson, Giada Ariaudo, Brigitte Bader-Meunier, et al. 2014. "Gain-of-Function Mutations in *IFIH1* Cause a Spectrum of Human Disease Phenotypes Associated with Upregulated Type I Interferon Signaling." *Nature Genetics* 46 (5): 503–9.

Rivas, Manuel a, Mélissa Beaudoin, Agnes Gardet, Christine Stevens, Yashoda Sharma, Clarence K Zhang, Gabrielle Boucher, et al. 2011. "Deep Resequencing of GWAS Loci Identifies Independent Rare Variants Associated with Inflammatory Bowel Disease." *Nature Genetics* 43 (11): 1066–73.

Robinson, Talin, Silvia N Kariuki, Beverly S Franek, Marissa Kumabe, Akaash a Kumar, Maria Badaracco, Rachel a Mikolaitis, et al. 2011. "Autoimmune Disease Risk Variant of *IFIH1* Is Associated with Increased Sensitivity to IFN-A and Serologic Autoimmunity in Lupus Patients." *Journal of Immunology* 187 (3): 1298–1303.

Ross, G D, and V Větvicka. 1993. "CR3 (CD11b, CD18): A Phagocyte and NK Cell Membrane Receptor with Multiple Ligand Specificities and Functions." *Clinical and Experimental Immunology* 92 (2): 181–84.

Salmon, J E, J C Edberg, and R P Kimberly. 1990. "Fc Gamma Receptor III on Human Neutrophils. Allelic Variants Have Functionally Distinct Capacities." *The Journal of Clinical Investigation* 85 (4): 1287–95.

Sareneva, T., I. Julkunen, and S. Matikainen. 2000. "IFN-A and IL-12 Induce IL-18 Receptor Gene Expression in Human NK and T Cells." *The Journal of Immunology* 165 (4): 1933–38.

Sato Y, Miyata M, Sato Y, Nishimaki T, Kochi H, Kasukawa R. 1999. "CpG Motif-Containing DNA Fragments from Sera of Patients with Systemic Lupus Erythematosus Proliferate Mononuclear Cells in Vitro." *Journal of Rheumatology* 26 (2): 294–301.

Schaschl, H, T J Aitman, and T J Vyse. 2009. "Copy Number Variation in the Human Genome and Its Implication in Autoimmunity." *Clinical and Experimental Immunology* 156 (1): 12–16.

Schleinitz, Nicolas, Frédéric Vély, Jean-Robert Harlé, and Eric Vivier. 2010. "Natural Killer Cells in Human Autoimmune Diseases." *Immunology* 131 (4): 451–58.

Scofield, R Hal, Gail R Bruner, Bahram Namjou, Robert P Kimberly, Rosalind Ramsey-Goldman, Michelle Petri, John D Reveille, et al. 2008. "Klinefelter's Syndrome (47,XXY) in Male Systemic Lupus Erythematosus Patients: Support for the Notion of a Gene-Dose Effect from the X Chromosome." *Arthritis and Rheumatism* 58 (8): 2511–17.

Shapira, Yinon, Nancy Agmon-Levin, and Yehuda Shoenfeld. 2010. "Geoepidemiology of Autoimmune Rheumatic Diseases." *Nature Reviews. Rheumatology* 6 (8): 468–76.

Shaw, J M, a Al-Shamkhani, L a Boxer, C D Buckley, a W Dodds, N Klein, S M Nolan, et al. 2001. "Characterization of Four CD18 Mutants in Leucocyte Adhesion Deficient (LAD) Patients with Differential Capacities to Support Expression and Function of the CD11/CD18 Integrins LFA-1, Mac-1 and p150,95." *Clinical and Experimental Immunology* 126 (2): 311–18.

Silva, Anabel, Daniel M Andrews, Andrew G Brooks, Mark J Smyth, and Yoshihiro Hayakawa. 2008. "Application of CD27 as a Marker for Distinguishing Human NK Cell Subsets." *International Immunology* 20 (4): 625–30.

Siriboonrit, U, N Tsuchiya, M Sirikong, C Kyogoku, S Bejrachandra, P Suthipinittharm, K Luangtrakool, et al. 2003. "Association of Fcgamma Receptor IIb and IIIb Polymorphisms with Susceptibility to Systemic Lupus Erythematosus in Thais." *Tissue Antigens* 61 (5): 374–83.

Smith, Paul P, and Caroline Gordon. 2010. "Systemic Lupus Erythematosus: Clinical Presentations." *Autoimmunity Reviews* 10 (1): 43–45.

So, Hon-Cheong, Allen H S Gui, Stacey S Cherny, and Pak C Sham. 2011. "Evaluating the Heritability Explained by Known Susceptibility Variants: A Survey of Ten Complex Diseases." *Genetic Epidemiology* 35 (5): 310–17.

Springer, Timothy A. 1995. "Traffic Signals on Endothelium for Lymphocyte Recirculation and Leukocyte Emigration." *Annu Rev Physiol* 57: 827–72.

Stahl N, Farruggella TJ, Boulton TG, Zhong Z, Darnell JE Jr, Yancopoulos GD. 1995. "Choice of STATs and Other Substrates Specified by Modular Tyrosine-Based Motifs in Cytokine Receptors." *Science* 3 (267): 1349–52.

Stockl, Johannes, Otto Majdic, Winfried F Pickl, Alexander Rosenkranz, Elisabeth Prager, Elisabeth Gschwantler, and Walter Knapp. 1995. "Granulocyte Activation Via a Binding Site near the C-Terminal Region of Complement Receptor Type 3 a-Chain (CDll B) Potentially Involved in Lntramembrane Complex Formation With Glycosylphosphatidylinositol-Anchored FcyRlllB (CD16) Molecules." *Journal of Immunology* (154): 5452–63.

Strengell, Mari, Sampsa Matikainen, Jukka Sirén, Anne Lehtonen, Don Foster, Ilkka Julkunen, and Timo Sareneva. 2003. "IL-21 in Synergy with IL-15 or IL-18 Enhances IFN-Gamma Production in Human NK and T Cells." *Journal of Immunology* 170 (11): 5464–69.

Sun, Yan V, and Sharon L R Kardia. 2010. "Identification of Epistatic Effects Using a Protein-Protein Interaction Database." *Human Molecular Genetics* 19 (22): 4345–52.

Sutcliffe, N, a E Clarke, C Gordon, V Farewell, and D a Isenberg. 1999. "The Association of Socio-Economic Status, Race, Psychosocial Factors and Outcome in Patients with Systemic Lupus Erythematosus." *Rheumatology* 38 (11): 1130–37.

Suzuki, N., N.-J. Chen, D. G. Millar, S. Suzuki, T. Horacek, H. Hara, D. Bouchard, et al. 2003. "IL-1 Receptor-Associated Kinase 4 Is Essential for IL-18-Mediated NK and Th1 Cell Responses." *The Journal of Immunology* 170 (8): 4031–35.

Tan EM, Cohen AS, Fries JF, Masi AT, McShane DJ, Rothfield NF, Schaller JG, Talal N, Winchester RJ. 1982. "The 1982 Revised Criteria for the Classification of Systemic Lupus Erythematosus." *Arthritis and Rheumatism* 25 (11): 1271–77.

Ter Borg EJ, Horst G, Hummel EJ, Limburg PC, Kallenberg CG. 1990. "Measurement of Increases in Anti-Double-Stranded DNA Antibody Levels as a Predictor of Disease Exacerbation in Systemic Lupus Erythematosus. A Long-Term, Prospective Study." *Arthritis and Rheumatism* (33): 634–43.

Thornton, Brian P, Vhclav Vi, Mark Pitman, Robert C Goldman, and Gordon D Ross. 1996. “Analysis of the Sugar Specificity and Molecular Location of the β-Glucan-Binding Lectin Site.” *Journal of Immunology* 3 (156): 1236–46.

Torgerson, Dara G, Daniel Capurso, Rasika a Mathias, Penelope E Graves, Ryan D Hernandez, Terri H Beaty, Eugene R Bleecker, et al. 2012. “Resequencing Candidate Genes Implicates Rare Variants in Asthma Susceptibility.” *American Journal of Human Genetics* 90 (2): 273–81.

V. Magnusson. 2004. “Polymorphisms of the Fc Receptor Type IIB Gene Are Not Associated with Systemic Lupus Erythematosus in the Swedish Population.” *Arthritis and Rheumatism* 50 (4): 1344–47.

Van der Heijden, Joris, Willemijn B Breunis, Judy Geissler, Martin de Boer, Timo K van den Berg, and Taco W Kuijpers. 2012. “Phenotypic Variation in IgG Receptors by Nonclassical *FCGR2C* Alleles.” *Journal of Immunology* 188 (3): 1318–24.

Van Lookeren Campagne, Menno, Christian Wiesmann, and Eric J Brown. 2007. “Macrophage Complement Receptors and Pathogen Clearance.” *Cellular Microbiology* 9 (9): 2095–2102.

Varker, Kimberly, Sri Vidya Kondadasula, Michael R Go, Gregory B Lesinski, Rupa Ghosh-Berkebile, Amy Lehman, J Paul Monk, Thomas Olencki, Kari Kendra, and William E Carson. 2006. “Multiparametric Flow Cytometric Analysis of Signal Transducer and Activator of Transcription 5 Phosphorylation in Immune Cell Subsets in Vitro and Following Interleukin-2 Immunotherapy.” *Clinical Cancer Research* 12 (19): 5850–58.

Větvicka, V, M Hanikýrová, J Větvicková, and G D Ross. 1999. “Regulation of CR3 (CD11b/CD18)-Dependent Natural Killer (NK) Cell Cytotoxicity by Tumour Target Cell MHC Class I Molecules.” *Clinical and Experimental Immunology* 115 (2): 229–35.

Vetvicka, V, B P Thornton, and G D Ross. 1996. “Soluble Beta-Glucan Polysaccharide Binding to the Lectin Site of Neutrophil or Natural Killer Cell Complement Receptor Type 3 (CD11b/CD18) Generates a Primed State of the Receptor Capable of Mediating Cytotoxicity of iC3b-Opsonized Target Cells.” *The Journal of Clinical Investigation* 98 (1): 50–61.

Vivier, Eric, Elena Tomasello, Myriam Baratin, Thierry Walzer, and Sophie Ugolini. 2008. “Functions of Natural Killer Cells.” *Nature Immunology* 9 (5): 503–10.

Walker, Susan, Somwang Janyakhantikul, and John a L Armour. 2009. “Multiplex Paralogue Ratio Tests for Accurate Measurement of Multiallelic CNVs.” *Genomics* 93 (1): 98–103.

Walzog, B, P Weinmann, F Jeblonski, K Scharffetter-Kochanek, K Bommert, and P Gaehtgens. 1999. “A Role for beta(2) Integrins (CD11/CD18) in the Regulation of Cytokine Gene Expression of Polymorphonuclear Neutrophils during the Inflammatory Response.” *FASEB Journal* 13 (13): 1855–65.

Wandstrat, a, and E Wakeland. 2001. “The Genetics of Complex Autoimmune Diseases: Non-MHC Susceptibility Genes.” *Nature Immunology* 2 (9): 802–9.

Wang, Lu, Rachael a Gordon, Linda Huynh, Xiaodi Su, Kyung-Hyun Park Min, Jiahuai Han, J Simon Arthur, George D Kalliolias, and Lionel B Ivashkiv. 2010. “Indirect Inhibition of Toll-like Receptor

and Type I Interferon Responses by ITAM-Coupled Receptors and Integrins." *Immunity* 32 (4): 518–30.

Wen, Z K, W Xu, L Xu, Q H Cao, Y Wang, Y W Chu, and S D Xiong. 2007. "DNA Hypomethylation Is Crucial for Apoptotic DNA to Induce Systemic Lupus Erythematosus-like Autoimmune Disease in SLE-Non-Susceptible Mice." *Rheumatology* 46 (12): 1796–1803.

Willcocks, Lisa C, Edward J Carr, Heather a Niederer, Tim F Rayner, Thomas N Williams, Wanling Yang, J Anthony G Scott, et al. 2010. "A Defunctioning Polymorphism in *FCGR2B* Is Associated with Protection against Malaria but Susceptibility to Systemic Lupus Erythematosus." *Proceedings of the National Academy of Sciences of the United States of America* 107 (17): 7881–85.

Willcocks, Lisa C, Paul a Lyons, Menna R Clatworthy, James I Robinson, Wanling Yang, Stephen a Newland, Vincent Plagnol, et al. 2008. "Copy Number of *FCGR3B*, Which Is Associated with Systemic Lupus Erythematosus, Correlates with Protein Expression and Immune Complex Uptake." *The Journal of Experimental Medicine* 205 (7): 1573–82.

Witte, T, F L Dumoulin, J E Gessner, J Schubert, O Götze, C Neumann, R F Todd, H Deicher, and R E Schmidt. 1993. "Defect of a Complement Receptor 3 Epitope in a Patient with Systemic Lupus Erythematosus." *The Journal of Clinical Investigation* 92 (3): 1181–87.

Wright, S D, and B C Meyer. 1986. "Phorbol Esters Cause Sequential Activation and Deactivation of Complement Receptors on Polymorphonuclear Leukocytes." *Journal of Immunology* 136 (5): 1759–64.

Wu, C., P. Sakorafas, R. Miller, D. McCarthy, S. Scesney, R. Dixon, and T. Ghayur. 2003. "IL-18 Receptor Beta -Induced Changes in the Presentation of IL-18 Binding Sites Affect Ligand Binding and Signal Transduction." *The Journal of Immunology* 170 (11): 5571–77.

Xia, Yu, Václav Vetvicka, Jun Yan, Margareta Hanikýrová, Tanya Mayadas, and Gordon D Ross. 1999. "The B-Glucan-Binding Lectin Site of Mouse CR3 (CD11b/CD18) and Its Function in Generating a Primed State of the Receptor That Mediates Cytotoxic Activation in Response to iC3b-Opsonized Target Cells." *Journal of Immunology* 162: 2281–90.

Yabuhara A, Yang FC, Nakazawa T, Iwasaki Y, Mori T, Koike K, Kawai H, Komiyama A. 1996. "A Killing Defect of Natural Killer Cells as an Underlying Immunologic Abnormality in Childhood Systemic Lupus Erythematosus." *Journal Rheumatology* 23 (1): 171–77.

Yakubenko, Valentin P, Linda C Hsi, Martha K Cathcart, and Ashish Bhattacharjee. 2013. "From Macrophage Interleukin-13 Receptor to Foam Cell Formation: Mechanisms for αMβ2 Integrin Interference." *The Journal of Biological Chemistry* 288 (4): 2778–88.

Yang, Wanling, Minghui Zhao, Nattiya Hirankarn, Chak Sing Lau, Chi Chiu Mok, Tak Mao Chan, Raymond W S Wong, et al. 2009. "*ITGAM* Is Associated with Disease Susceptibility and Renal Nephritis of Systemic Lupus Erythematosus in Hong Kong Chinese and Thai." *Human Molecular Genetics* 18 (11): 2063–70.

Yang, Xiang-ping, Kamran Ghoreschi, Scott M Steward-tharp, Jaime Rodriguez-, Jinfang Zhu, John R Grainger, Kiyoshi Hirahara, et al. 2011. "Opposing Regulation of the IL-17 Locus through Direct, Reciprocal Actions of STAT3 and STAT5." *Nature Immunology* 12 (3): 247–54.

Yoshida, Y, K Kang, M Berger, G Chen, a C Gilliam, A Moser, L Wu, C Hammerberg, and K D Cooper. 1998. “Monocyte Induction of IL-10 and down-Regulation of IL-12 by iC3b Deposited in Ultraviolet-Exposed Human Skin.” *Journal of Immunology* 161 (11): 5873–79.

Yuan, Hui, Hai-Feng Pan, Lian-Hong Li, Jin-Bao Feng, Wen-Xian Li, Xiang-Pei Li, and Dong-Qing Ye. 2009. “Meta Analysis on the Association between FcgammaRIIa-R/H131 Polymorphisms and Systemic Lupus Erythematosus.” *Molecular Biology Reports* 36 (5): 1053–58.

Zenewicz, Lauren a, Clara Abraham, Richard a Flavell, and Judy H Cho. 2010. “Unraveling the Genetics of Autoimmunity.” *Cell* 140 (6): 791–97.

Zhou, Mo, Lian-Hong Li, Hui Peng, Rui Li, Chen-Chen Feng, Wang-Dong Xu, Rui-Xue Leng, Hai-Feng Pan, and Dong-Qing Ye. 2013. “Decreased *ITGAM* and FcγRIIIA mRNA Expression Levels in Peripheral Blood Mononuclear Cells from Patients with Systemic Lupus Erythematosus.” *Clinical and Experimental Medicine*, 14(3):269-74.

Zhou, Ping, Raymond L Comenzo, Adam B Olshen, Ezio Bonvini, Scott Koenig, Peter G Maslak, Martin Fleisher, et al. 2008. “CD32B Is Highly Expressed on Clonal Plasma Cells from Patients with Systemic Light-Chain Amyloidosis and Provides a Target for Monoclonal Antibody-Based Therapy.” *Blood* 111 (7): 3403–6.

Zhou, Xu-Jie, Fa-Juan Cheng, Ji-Cheng Lv, Huan Luo, Feng Yu, Min Chen, Ming-Hui Zhao, and Hong Zhang. 2012. “Higher *DEFB4* Genomic Copy Number in SLE and ANCA-Associated Small Vasculitis.” *Rheumatology* 51 (6): 992–95.

Zhou, Xu-jie, Xiao-lan Lu, Swapan K Nath, Ji-cheng Lv, Sai-nan Zhu, Hai-zhen Yang, Lian-xiang Qin, et al. 2012. “Gene-Gene Interaction of *BLK, TNFSF4, TRAF1, TNFAIP3*, and *REL* in Systemic Lupus Erythematosus.” *Arthritis and Rheumatism* 64 (1): 222–31.

Zhou, Yebin, Jianming Wu, Dennis F Kucik, Nathan B White, David T Redden, Alexander J Szalai, Daniel C Bullard, and Jeffrey C Edberg. 2013. “Multiple Lupus-Associated *ITGAM* Variants Alter Mac-1 Functions on Neutrophils.” *Arthritis and Rheumatism* 65 (11): 2907–16.

Zuk, Or, Eliana Hechter, Shamil R. Sunyaev, and Eric S. Lander. 2012. “The Mystery of Missing Heritability: Genetic Interactions Create Phantom Heritability.” *Proceedings of the National Academy of Sciences of the United States of America* 109 (4): 1193–98.

Zuo, Xian-Bo, Yu-Jun Sheng, Su-Juan Hu, Jin-Ping Gao, Yang Li, Hua-Yang Tang, Xian-Fa Tang, et al. 2014. “Variants in *TNFSF4, TNFAIP3, TNIP1, BLK, SLC15A4* and *UBE2L3* Interact to Confer Risk of Systemic Lupus Erythematosus in Chinese Population.” *Rheumatology International* 34 (4): 459–64.

Appendix A: PCR Reaction Compositions and Calculations

Qiagen PCR Buffer and Promega dNTPs were used in all reactions, unless otherwise stated

1 *ITGAM* promoter sequencing

Reagent	Concentration (various)	Volume (µl)	Final concentration
PCR Buffer	10X	1.0	0.5X
dNTPs	2.5mM	1.0	0.25mM
Forward Primer 5'- CACCATGCCCAGCTAATTAAA	10µM	0.5	0.5µM
Reverse Primer 5'- CTCCTCCCCACCCAGAGT	10µM	0.5	0.5µM
Hot Star *Taq* Polymerase	5U/µl	0.1	0.5U
ddH_2O	-	4.9	-
DNA	20ng/µl	2.0	2.0ng/µl
Total	**-**	**10.0**	**-**

2. *ITGAM* Novel Variant Confirmation PCR

Reagent	Concentration (various)	Volume (µl)	Final concentration
PCR Buffer	10X	2.0	1X
dNTPs	2.5mM	2.0	0.25mM
Forward Primer*	10µM	1.0	0.5µM
Reverse Primer*	10µM	1.0	0.5µM
Hot Star *Taq* Polymerase	5U/µl	0.2	1.0U
ddH_2O	-	4.9	-
DNA	10ng/µl	3.0	1.5ng/µl
Total	**-**	**20.0**	**-**

*See Table 2.1 for primer sequences

3. SSP-PCR F941V

Reagent	Concentration (various)	Volume (µl)	Final concentration
PCR Buffer	10X	1.0	1X
dNTPs	2.5mM	1.0	0.25mM
Outer Forward*	10µM	0.5	0.5µM
Outer Reverse*	10µM	0.5	0.5µM
Inner Forward*	10µM	0.5	0.5µM
Inner Reverse*	10µM	0.5	0.5µM
Hot Star *Taq* Polymerase	5U/µl	0.1	0.5U
ddH_2O	-	4.9	-
DNA	20ng/µl	1.0	2ng/µl
Total	**-**	**10.0**	**-**

*See Methods Table 2.2 for primer sequences

4. *ITGAM* Site-directed mutagenesis

4.1. Primer Calculations

4.1.1. Amount of primer in ρmoles needed for 125ng of primer:

$$125\text{ng primer (}\rho\text{moles)} = \frac{125\text{ng}}{330 \times \text{number of bases of primer}} \times 1000$$

4.1.2. Volume of primer needed for site-directed mutagenesis reaction:

$$\text{volume (µl)} = \frac{\rho\text{moles of primer}}{10\ \rho\text{moles/µl}}$$

4.2. Summary of used primers

Primer	Sequence 5' – 3'	Length (b)	Amount (ρm)	Volume (µl)
M441T F	gcagaacactggcacgtgggagtccaacg	29	13.06	1.31
M441T R	cgttggactcccacgtgccagtgttctgc	29	13.06	1.31
A858V F	ccgaagtgtctggggtcttgaagagcaccag	31	12.22	1.22
A858V R	ctggtgctcttcaagaccccagacacttcgg	31	12.22	1.22
F941V F	tctccactaaatatctcaacgtcacggcctcagagaat	38	10.00	1.00
F941V R	attctctgaggccgtgacgttgagatatttagtggaga	38	10.00	1.00
G1145S F	atgagtgaagggagtcccccgggggg	25	15.15	1.52
G1145S R	ccccccgggggactcccttcactcat	25	15.15	1.52

4.3. PCR reaction composition

Reagent	Concentration (various)	Volume (µl)	Final concentration
Reaction Buffer	10x	5.0	1x
pcDNA3.1-CD11b	10ng/µl	1.0	0.2ng/µl
Forward primer*	10ρmoles/µl	Various**	2.5ng/µl
Reverse primer*	10ρmoles/µl	Various**	2.5ng/µl
dNTP mix		1.0	
Quik Solution		3.0	
ddH_2O	-	Various***	-
***Pfu* Ultra High Fidelity Polymerase**		1µl	
Total	**-**	**50.0**	**-**

*See primer sequences in A4.2

**See equations A4.1.1 and A4.1.2

***Volume of ddH_2O = 50µl -11µl –(volume forward primer + volume reverse primer)

5. *FCGR2B* -I232T genotyping by SequalPrep™ Long-Range PCR (Invitrogen)

Reagent	Concentration (various)	Vol. (µl)	Final concentration
SequalPrep Reaction Buffer (with dNTPs)	10X	1.0	1X
Enhancer A	10X	0.5	0.5X
DMSO	-	0.2	-
Forward Primer 5'-CCTCACCTGGAGTTCCAGGAGGGAG	10µM	0.5	0.5µM
Reverse Primer 5'-GCTTGGGTGGCCCCTGGTTCTCA	10µM	0.5	0.5µM
SequalPrep Long Polymerase™	5U/µl	0.18	0.9U
ddH_2O	-	6.62	-
DNA	20ng/µl	0.5	2.4ng/µl
Total	**-**	**10.0**	**-**

6. *FCGR3* CNV

6.1. Paralogue Ratio Test (PRT)

PCR was run in duplicate; one with FAM labelled primer, and the other with HEX labelled primer

Reagent	Concentration (various)	Volume (µl)	Final concentration
low dNTPs PRT Mix*	10X	1.0	1X
Forward Primer 5'-ATGATCTGGCCCTGAAACTC	10µM	0.5	0.5µM
Reverse 5'-[HEX/FAM]TGAGTTCAAGAAAGCAGTTTGG	10µM	0.5	0.5µM
***Taq* Polymerase**	5U/µl	0.1	0.5U
ddH_2O	-	6.9	-
DNA	20ng/µl	1.0	2ng/µl
Total	**-**	**10.0**	**-**

*See Appendix C2

6.2. Restriction Enzyme Digest Variant Ratio (REDVR)

Reagent	Concentration (various)	Volume (µl)	Final concentration
low dNTPs PRT Mix*	10X	1.0	
A Forward 5'TTTTGCAGTGGACACAGGAC	10µM	0.5	0.5µM
A Reverse 5'-[VIC]GGGTTGCAAATCCAGAGAAA	10µM	0.5	0.5µM
***Taq* Polymerase**	5U/µl	0.1	0.5U
ddH2O	-	6.9	-
DNA	20ng/µl	1.0	2ng/µl
Total	**-**	**10.0**	**-**

*See Appendix C2

Appendix B: Thermocycler Conditions

1. *ITGAM* promoter sequencing

PCR Step	Temperature (°C)	Time (minutes)	
Enzyme Activation	95.0	15.0	
Denaturation	94.0	0.5	
Annealing	58.0	0.5	30 cycles
Extension	72.0	1.0	
Final Extension	72.0	10.0	

2. *ITGAM* Novel Variant Confirmation PCR

PCR Step	Temperature (°C)	Time (minutes)	
Enzyme Activation	95.0	15.0	
Denaturation	94.0	0.5	
Annealing	Various*	0.5	30 cycles
Extension	72.0	0.5	
Final Extension	72.0	10.0	

*See Methods table 2.1

3. SSP-PCR F941V

PCR Step	Temperature (°C)	Time (minutes)	
Enzyme Activation	95.0	15.0	
Denaturation	94.0	0.5	
Annealing	56.9	0.5	30 cycles
Extension	72.0	0.5	
Final Extension	72.0	10.0	

4. *ITGAM* Site-directed Mutagenesis

PCR Step	Temperature (°C)	Time (minutes)	
Enzyme Activation	95.0	1.0	
Denaturation	94.0	0.83	
Annealing	60.0	0.83	18 cycles
Extension	72.0	9.0	
Final Extension	68.0	7.0	

5. *FCGR2B*-I232T genotyping by LR PCR

PCR Step	Temperature (°C)	Time (seconds)	
Enzyme Activation	94.0	120	
Denaturation	94.0	10	
Annealing	66.0	30	10 cycles
Extension	68.0	180	
Denaturation	94.0	10	25 cycles
Annealing	66.0	30	
Extension	68	180 +20sec/cycle	
Final Extension	72.0	300	

6. *FCGR3* CNV

6.1. Paralogue Ratio Test

PCR Step	Temperature (°C)	Time (minutes)	
Denaturation	95.0	0.5	
Annealing	56.0	0.5	30 cycles
Extension	70.0	3.0	
Annealing	56.0	1.0	
Final Extension	70.0	20.0	

6.2. Restriction Enzyme Digest Variant Ratio (REDVR)

PCR Step	Temperature (°C)	Time (minutes)	
Denaturation	95.0	0.5	
Annealing	53.0	0.5	30 cycles
Extension	70.0	3.0	
Annealing	53.0	1.0	
Final Extension	70.0	20.0	

Appendix C: Recipes

1. Precipitation Buffer

Reagent	Stock Concentration	Volume Used (µl)
Sodium Acetate	3M (pH6)	75
H_2O	n/a	362.5
Ethanol	95%	1562.5
	Total	**2000**

2. Low dNTP 10x PCR Mix

Reagent	Stock Concentration	Volume Used (µL)	Final Concentration
TrisHCl pH8.8	2M	500	500mM
Ammonium Sulphate	1M	250	125mM
MgCl2	1M	28	14mM
2-mercaptoethanol	100%	10.5	75mM
dATP	100mM	40	2mM
dCTP	100mM	40	2mM
dGTP	100mM	40	2mM
dTTP	100mM	40	2mM
BSA	10mg/ml	250	1.25mg/ml
Water	n/a	800	n/a
	Total	**2000**	

Appendix D: Publications resulting from work presented in this thesis

Rhodes, Benjamin, Barbara G Fürnrohr, Amy L Roberts, George Tzircotis, Georg Schett, Tim D Spector, and Timothy J Vyse. 2012. "The rs1143679 (R77H) Lupus Associated Variant of *ITGAM* (CD11b) Impairs Complement Receptor 3 Mediated Functions in Human Monocytes." *Annals of the Rheumatic Diseases* 71 (12): 2028–34.

Roberts, Amy L, Ellen R A Thomas, Shriram Bhosle, Laurence Game, Olga Obraztsova, Timothy J Aitman, Timothy J Vyse, and Benjamin Rhodes. 2014. "Resequencing the Susceptibility Gene, *ITGAM*, Identifies Two Functionally Deleterious Rare Variants in Systemic Lupus Erythematosus Cases." *Arthritis Research & Therapy* 16 (3): R114.